Chapter 1: Introduction and Statement of Purpose

1.1 Introduction

The bioaccumulation of mercury (Hg) and methylmercury (MeHg) has led to fish advisory warnings in approximately 42 US states. Furthermore, large gaps remain in our understanding of the mercury sources involved and the atmospheric and biogeochemical processes that influence the bioaccumulation of Hg and MeHg (Burgess, Neil, 1998). MeHg is a methylated form of Hg that is easily bioaccumulated and biomagnifies through the food chain. Though Hg itself does not pose a substantial risk, MeHg represents a neurotoxin that can have strong negative impacts on an area's biota. Many studies have explored the impacts of elevated MeHg on wildlife (Evers, D. and Lane, 2000, Evers et al., 2003, Kenow et al., 2003). It is well known that Hg is introduced to hydrologic systems through air deposition as well as point sources. Other known causes of Hg contamination include the construction of dams as seen by increased Hg levels following the construction of several hydroelectric dams in Canada (Burgess, Neil, 1998). Several studies have shown that runoff can deliver substantially varied amounts of Hg and MeHg depending on the influence of impoundments, wetlands, agricultural lands, forest types, and urban areas (USGS, and Vermont DEC, 1998). For the purpose of this study, wetlands, agricultural lands, forest type, and other land cover classes will be used in an attempt to relate MeHg (methyl-mercury) in the Common Loon (*Gavia immer*) to various landscape factors.

In Maine, especially the Rangeley Lakes (study area), MeHg represents a serious risk. Currently, there are fish consumption warnings in almost all of Maine lakes due to MeHg levels that are higher than the national average (Evers et al., 2003). The Rangeley Lakes area also has a substantial amount of available data that has been collected by Biodiversity Research Institute (BRI) over the last several years and provides adequate sample coverage of the area. Lake Aziscohos, one of the reservoirs in the study area, has levels in some territories that greatly exceed the national average further defining the need to understand the processes that are contributing to the increased MeHg in the area.

The Common Loon is being used in this analysis for a variety of reasons. First, the territorial nature of the birds provides a unique method for segmenting the larger lakes and reservoirs into smaller units for analysis and abundant data are available. A mated pair of loons will typically return to the same territory year after year (Evers et al, 2003). This phenomenon provides scientists and biologists with a unique opportunity to collect Hg (mercury) data year after year for the same pair of loons as well as to gain an understanding of the variability that exists between adjacent territories and the variability between breeding seasons. It also allows for scientists to monitor yearly change in MeHg levels in the birds. Lake Umbagog, also a reservoir in the study area, has seen declines in the Common Loon population for a number of years leading to increased efforts by the Loon Preservation Committee (LPC) and Biodiversity Research Institute (BRI) to understand the why the declines are happening (Evers, D.C., 2002). Increased MeHg availability, a decrease in suitable nesting habitat, and other environmental stressors may contribute to the decline.

Second, due to the ways that Hg bioaccumulates, the collection of blood samples for analysis of MeHg levels provides insight into what is happening in each of the territories. As a loon feeds, MeHg accumulates in the blood. Because MeHg will process out of the blood and into the feathers over time, much of the MeHg that is found in the blood has been accumulated from the individual territory and has not been brought in during migration or over-wintering. Feather samples (not used in this analysis, but important nonetheless) provide a pseudo-historic perspective of MeHg bioaccumulation as they tend to receive much of the MeHg that gets processed out of the bird, and may lead to a greater understanding of the winter stresses that the birds are exposed to. The time at which the birds are captured is also a factor. The breeding season extends from around the first of May until the end of August. Consequently, this also relates to the time when MeHg availability is at its greatest. The collection of samples does not occur until the loon pair has hatched chicks. This allows several months for the MeHg from other sources to be processed out and the available MeHg from the territory to be accumulated in the blood.

The Common Loon is important in understanding not only the ways that MeHg bioaccumulates, but also the behavioral ramifications of increased MeHg in the bird. Studies by Evers et al (2003), have shown that there can be serious repercussions in the breeding success of the Common Loon due to increased MeHg. Activities such as diving and nest sitting are also negatively impacted leading to a potential increase in mortality among the chicks (Evers et al., 2003).

The location of the Common Loon high in the food chain also presents a unique opportunity to explore the effects of MeHg biomagnification. The Common Loon in many cases will consume the same types of fish (though smaller in size) that a human will consume. Data for the Common Loon are also readily available and in great abundance, especially in the North East where Hg levels are currently above the recommended safe amount. Piscivorous (fish-eating) birds such as the Common Loon are thought to be excellent indicators of aquatic health and have been used as ecological indicators in a variety of studies (Evers et al., 2003, Kenow et al., 2003).

1.2 Statement of Purpose

Over the past 30-40 years, levels of mercury (Hg) in aquatic and hydrologic systems have increased greatly within the United States and Canada. Associated with this has been the rise in the bioavailability of methylmercury (MeHG) to the extent that the current levels pose risks to both human and aquatic health (Evers et al, 2003.). Past studies indicate that environmental risk levels vary significantly in response to MeHg. Factors that influence MeHg and Hg bioavailabilty include the associated hydrology, biogeochemistry, habitat, topography, and relative proximity to airborne sources of Hg and MeHg (Evers et al, 2003).

The following questions exist regarding Hg in the environment: 1) Is there a correlation between Hg and MeHg in the Common Loon and land cover type? and 2) Can a model be developed that relates Hg and MeHg levels in an ecosystem to these factors such that levels can be accurately predicted by the analysis of geographic data? Once these factors are determined, resource managers may be better suited to predict potential "hotspots" of Hg bioaccumulation and the relative risk to the associated biota of an area, as well as explore potential methods for reducing the risk.

The objective of this thesis is to develop a GIS-based decision support framework that can identify areas in a watershed that represent the highest risk of mercury bioaccumulation to the common loon. This thesis will use multiple linear regression as the basis for the model development and will be discussed in further detail in the methodology in chapter 3. The large number of samples available and the diverse landscape of the Rangeley Lakes area should provide a unique opportunity to explore the relationships that exist between MeHg, Hg, and the associated land cover characteristics.

The model will be built on the ArcGIS framework and will incorporate the spatial analytical tools for which GIS is strongly suited. Three major hypotheses will be explored in this research and are outlined below:

1. Much of the current research addresses Hg bioaccumulation at the watershed scale. Substantial variability, however, can exist within a particular watershed. Examining the problem from a larger scale and analyzing the relationships that exist within individual loon territories should better explain Hg risk as a function of land cover characteristics.

2.If a reasonable model can be produced, will there be a marked drop-off in accuracy of the model as we move further from the territory boundary?

3.If a reasonable model can be produced, we should gain a clearer understanding of the impact of land cover types on the availability of Hg and the associated risk to hydrologic systems as a function of distance from the individual boundary.

Chapter 2: Literature Review

2.1 Introduction

The following chapter brings together three major points of interest in Hg risk. The first point briefly details the history of Hg in aquatic systems, human components of the overall problem we have today, and particular types of industries that are the culprits of adding additional Hg to the environment. I also present a background of Hg in the environment. The second point outlines the environmental phenomena that drive the dissemination of Hg, and the subsequent bioaccumulation of that Hg into the local ecosystem. The third point addresses the attempts being made at modeling and/or understanding the phenomena that drives Hg's availability to local ecosystems and biota.

2.2 History and Background

Naturally occurring mercury has been historically used in alchemy, chemistry, and manufacturing (Vermont Dept. of Env. Conservation, 1998). Of great significance in Hg research, and most certainly what prompted the initial interest in understanding the bioaccumulation and biomagnification of Hg, came about in the 1950's when aquatic discharge of wastewater that contained Hg resulted in over one hundred deaths in Minamata Bay, Japan (DTMC, 2002). MeHg (the methylated form of mercury) is more detrimental to an area's biota than Hg because it represents a neurotoxin that can be biomagnified through the food chain, ultimately posing a risk to humans if mercury contaminated fish are consumed. Mercury (Hg) is released naturally into the environment through a variety of weathering processes, such as the breakdown of cinnabar (HgS) from bedrock, diagenesis of sediments and wet soils, and release into oceans from deepwater crustal vents (Vermont Dept. of Env. Conservation, 1998). The bioaccumulation, biomagnification, and subsequent risk of Hg to the local environment has led to fish advisory warnings in over 40 states. Of those, many have issued statewide advisories warning against consumption. Recent research strongly suggests that activities since industrialization have resulted in significant increases in Hg and MeHg (USEPA, 1997). To date, the largest single anthropogenic source of Hg in the United States is from coal burning power plants, which are estimated to account for over 45% of the total available Hg in the environment (Air Quality Conference, 1999). Major point sources of Hg include coal wastes, medical wastes, and manufacturing (chlor-alkali facilities, cement, and pulp and paper) (Vermont Dept. of Env. Conservation, 1998). The Maine Department of Environmental Protection estimates that in Maine the expected loading rate for Hg from pulp and paper mills is approximately 3.1 lb/year, or an average concentration of 13 parts per trillion (ppt). Another potential source of Hg contamination can be found in Publicly Owned Treatment Works (POTWs), used for treatment of wastewater (US EPA, 2001). A report published in 1999 suggested that the average Hg concentrations found in POTW effluents was around 7.25 ppt. (US EPA, 2001). Larger regional sources of Hg in Maine may include cities such as Bangor and Portland (Vermont Dept. of Env. Conservation, 1998), however much of the available Hg in Maine is deposited through atmospheric deposition (Peckanham et al., 2002). Other known causes of mercury contamination include the construction of dams as evidenced by increased mercury levels following the construction of several hydroelectric dams in Canada (Burgess, Neil, 1998).

2.3 Environmental Factors

There are many environmental factors that contribute to the availability of Hg and MeHg in hydrologic systems. Atmospheric deposition as mentioned above, has been considered one of the driving forces of increased MeHg and Hg in the northeastern United States. Considering one of the standard paths of the jet stream, which dips into the rust belt before driving north again into New Hampshire and Maine, and then slamming into the White mountains it is not surprising that we see elevated levels of contaminants in that region. The contaminants are delivered by the dominant winds and then deposited when the air is forced over the mountains.

Many non-commercial fish, throughout the United States, have been measured for Hg levels (Figure 2.1) by the United States Environmental Protection Agency (USEPA). Many of these fish have Hg levels that should be of concern to those consuming them. In addition, many commercial fish such as tuna also exhibit levels that are higher than current health standards allow.

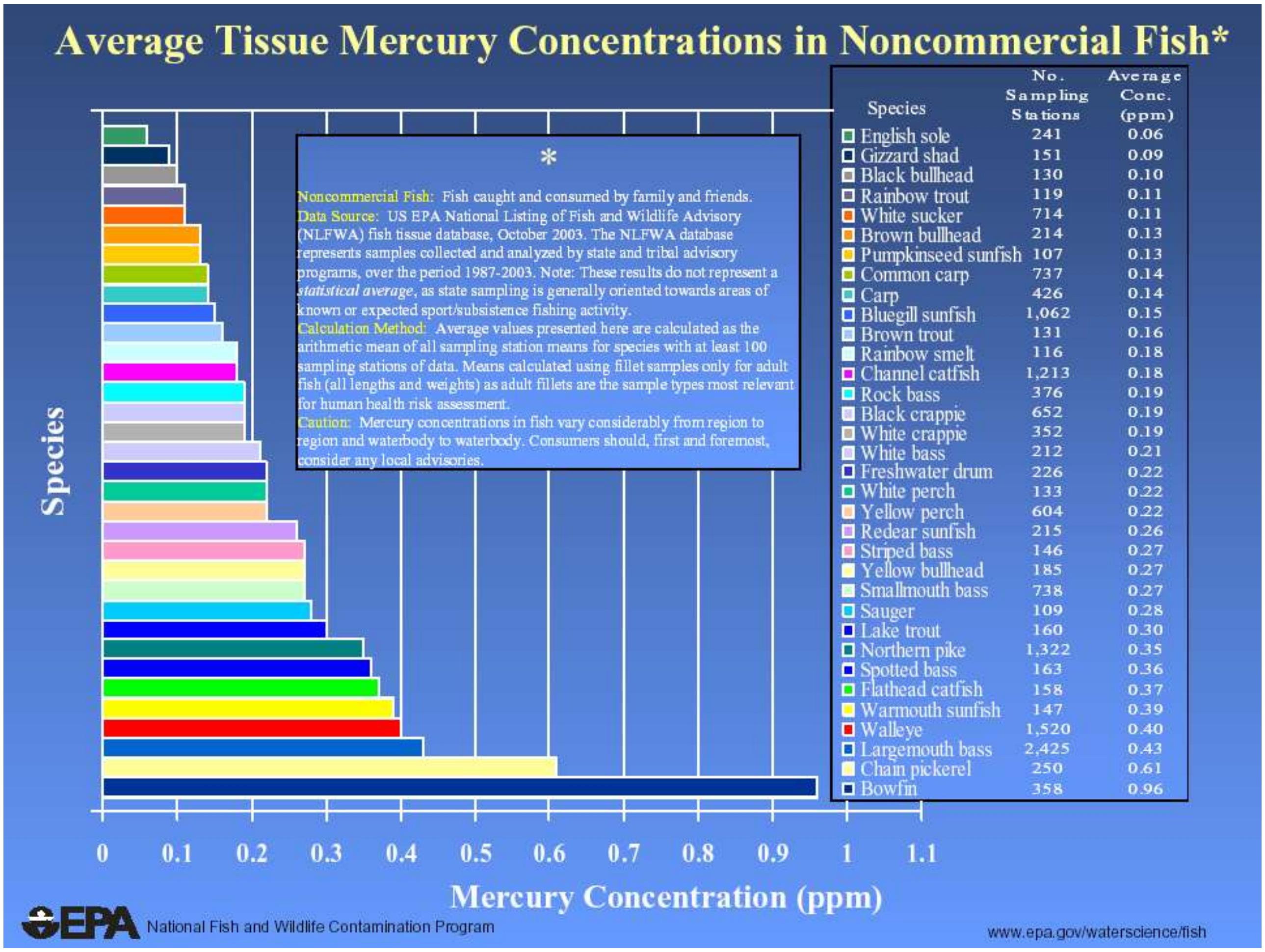

Figure 2.1
Mercury Levels in non-commercial fish (e.g. sport fish)
Source: US EPA (http://www.epa.gov/waterscience/fish)

Research has shown a strong positive correlation between the total levels of Hg and MeHg and the total amount of dissolved organic carbon in an ecosystem (Peckenham et al., 2002, Lee et al., 1998, Bishop et al., 1995, and Evers et al., 2003). Therefore one reason we may see elevated levels in and around dams is that they collect organic matter. Slower moving bodies of water such as wetlands and lakes also collect organic matter and may be important in understanding Hg and MeHg bioaccumulation and bioavailability. As stated by the Mississippi Department of Environmental Quality in the June 26, 2000 version of the Escatawpa River Phase One Total Maximum Daily Load for Mercury:

> The presence of sediments along with a ready source of biodegradable organic carbon resulting from plant production, may explain why wetlands are a major locale for production of MMHg (another form of MeHg, short for mono-methyl mercury). Circulation with surface waters may make wetland MMHg available for uptake. Emerging insects may then substantially increase transfer of MMHg produced in wetlands to predatory fish. (Mississippi Department of Environmental Quality, 2000. pg. 9).

Other studies have shown that MeHg increases in watersheds with proportionally greater areas in forest or wetlands, possibly due to the increased amount of dissolved organic carbon and organic matter available. In undisturbed watersheds, total mercury was commonly associated with the filtered phase, the point at which elements become absorbed by suspended sediment particles, but became closely associated with particulate matter in agricultural watersheds (Vermont Dept. of Env. Conservation 1998, and Kamman and Engstrom, 2001). In general, the literature suggests that the presence of wetlands is one of the most important variables affecting the availability of MeHg and Hg in hydrologic systems. The presence of agricultural lands has also been found to related to Hg and MeHg. However, the presence of this land cover type exhibits a negative influence on Hg and MeHg availability.

Hg and MeHg accumulation appears to peak during midsummer when water temperature biological growth rates, those times that growth occurs in hydrologic systems, are high. This is also the time period when the common loon is breeding on Maine lakes. Other factors that may influence bioavailability of Hg and MeHg and total levels include spring snowmelt runoff and summer storms, implying that the best times to collect data on Hg and MeHg levels occur during the summer months (Vermont Dept. of Env. Conservation 1998). Several researchers have found recently that the amount of Hg introduced to a system can vary widely due to individual storm events (Peckenham et al., 2002). This suggests that local phenomena such as adjacent wetlands that become flooded may contribute to increased levels in some places.

In Canada, as well as in the state of Maine, particular bedrock geology types have been correlated to Hg in the aquatic systems (Vaidya and Howell, 2001, and Peckenham et al., 2002). The breakdown of some types of bedrock can lead to increased Hg availability; Hg is known to exist in shale, granite, and limestone (Vaidya and Howell, 2001, and Faust and Aly, 1981). Some of the chemicals compounds found to be related to Hg include aluminum, zinc, copper and lead.

Bacteria also contribute to the methylation process (the conversion of Hg to MeHg). Some studies have shown that sulfate-processing bacteria take up Hg and convert it through metabolic processes into MeHg (USGS Fact Sheet FS-216-95, 1995). Many of these bacteria reside in wetland environments further emphasizing the role that wetlands play in Hg and MeHg availability.

Figure 2.2 presents a representation of the mechanisms that drive the dissemination and subsequent uptake of Hg in aquatic systems. As can be seen from Figure 2.2, the processes that drive the bioaccumulation and biomagnification of Hg are quite complex. Many factors contribute to the input, transfer, and subsequent bioaccumulation and biomagnification of Hg in aquatic systems.

Within the state of Maine, Hg levels in water appear to vary spatially as a function of longitude and latitude, with concentrations rising as you move north and west (Peckenham et al., 2002), depending on the flow state. This tendency in suggests that using a geographically weighted regression may be useful in Maine. Interestingly, eastern Canada (extending north from the Great Lakes and east to the Atlantic Ocean) has not exhibited a similar pattern.

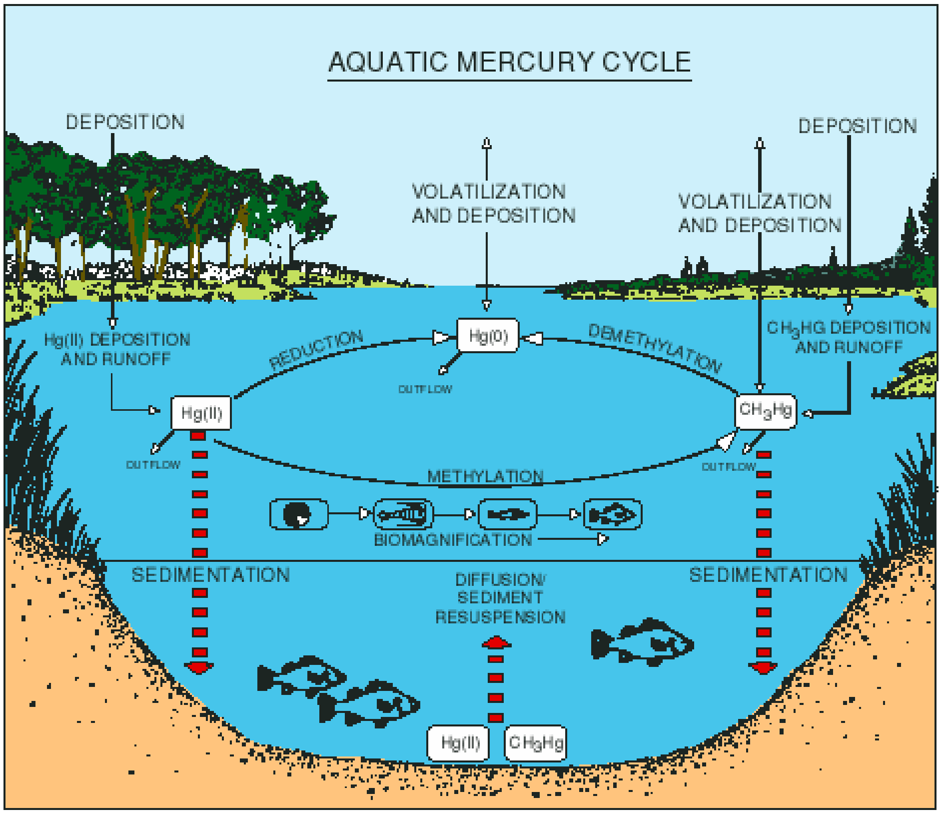

Figure 2.2
Mercury cycle in aquatic environment: from deposition and volatilization, to transport and diffusion, to bioaccumulation and biomagnification.
Source: USGS (http://wi.water.usgs.gov/pubs/FS-216-95/f6.gif)

Research Efforts

In an effort to understand the fate and transport of Hg in aquatic systems much research has focused on understanding the mechanisms that contribute to the bioaccumulation and biomagnification of Hg. Attempts to date have addressed the issue through the use of various fate and transport algorithms, mass balance equations, and various geographical analyses (Vaidya and Howell, 2001, DTMC, 2002, and Rencz et al., 2002).

Some of the research discussed below comprises standard statistical/numerical models created using non-spatial data, while others include the use of Geographic Information Systems (GIS) in an attempt to bring in the spatial component. Many of the research efforts have also focused on using various piscivorous birds as indicators of aquatic health, however most of the GIS-based models make attempts at explaining the MeHg variation in either fish tissue or in water and not in piscivorous birds. The use of piscivorous birds as indicators is not an uncommon practice and has been used extensively in attempts to explain the variability of MeHg in aquatic systems as well as in attempts to evaluate the overall health of an aquatic ecosystem (Evers et al., 2001, Thompson, 1996, and Wolfe et al., 1998).

Spatial Models/Research

This section will briefly address some of the spatial models that have been developed in an effort to understand the bioaccumulation and biomagnification of Hg. Substantial effort has been undertaken by many state agencies as well as federal agencies to provide a means of understanding the variability of Hg in hydrologic systems, to create total maximum daily loads (TMDL's), and to assess potential risk.

The mercury maps project developed by the United States Environmental Protection Agency made an attempt to quantify the spatial relationships between air deposition and fish tissue Hg concentrations. Previous modeling efforts conducted by the United States Environmental Protection Agency made attempts to describe the fate and transport of Hg in both the watershed and the aquatic ecosystem (U.S. EPA, 1997). One of the previous models included the Mercury Cycling Model (MCM) and is documented in the Mercury Study Report to Congress (MSRC) (U.S. EPA, 1997). The main assumption of the Mercury Maps model states "that a ratio reduction in air dispersion watershed loads will produce an equivalent ratio reduction in average fish tissue concentration in that watershed, at steady state" (U.S. EPA, 1997).

The USGS has developed the SPARROW model (Spatially Referenced Regressions on Watershed Attributes). The SPARROW model was developed in an effort to relate nutrient stream concentrations to pollutants and various watershed characteristics, however its applicability to understanding Hg is now being investigated. In New England, the SPARROW model has been applied regionally in collaboration between the U.S. EPA and the New England Interstate Water Pollution Control Commission (NEIWPCC) to assess nutrient loading in New England Watersheds. The SPARROW model has also been applied to the development of regional TMDLs and various nutrient criteria studies. Efforts are currently underway to apply SPARROW to Hg concentrations though its applicability is still unclear.

In the Pascagoula Basin in Jackson and George counties of Mississippi, Hg TMDLs were developed for the Escatawpa River. The study addresses water body identification, land use disruption, fish tissue data, and potential point source inputs of Hg (Mississippi Department of Environmental Quality, 2000). From the executive summary:

> The fresh water portions of the Escatawpa River are impaired by mercury. Largemouth bass and catfish caught in these segments have been sampled and the data show a definite impairment due to levels of mercury in the fish flesh, which exceed the FDA Action level. (Mississippi Department of Environmental Quality, 2000. pg. viii).

The use of fish samples, as mentioned above, tends to be the way in which organizations address Hg contamination. The Escatawpa river study is no different in that the main objective is to address Hg levels in fish tissue. As of the date of the publication, the model addresses only point source contributions to the water body (Mississippi Department of Environmental Quality, 2000). As reported in the document,

> One of the major components of a TMDL is the establishment of instream numeric endpoints, which are used to evaluate the attainment of acceptable water quality. Instream numeric endpoints, therefore, represent the water quality goals specified in the TMDL. (Mississippi Department of Environmental Quality, 2000. pg. 8).

The Sacramento River Watershed Program (SRWP) has been working on the development of a model to address the fate and transport of Hg in the Sacramento River Watershed (SRW). An initial conceptual model was developed and detailed in Appendix 2 of the original document. This portion of the literature review addresses Appendix 4, the Mercury Models Report. The report specifies a series of four linkages needed to develop a mercury model in the SRW. The first link addresses the atmospheric transport and deposition to water bodies, the second addresses the transport and transfer in waterbodies, the third addresses the cycling of Hg to MeHg, and finally the bioaccumulation in fish tissue (DTMC, 2002).

The following paragraphs address individual analyses or studies, not necessarily models, which have been completed utilizing GIS techniques. These include using GIS to randomly select study sites and to evaluate adjacent physical properties of the lakes.

Kamman et al. (2004) recently published research that assesses the mercury distribution of sediments, water, and biota in Vermont and New Hampshire using a geographically randomized design. Results of the study showed varying concentrations of Hg in water across the states and varying concentrations of Hg in sediments that are in agreement with other studies conducted within the state (Kamman et al., 2004). Within the area of biota, fish tissue levels were analyzed in comparison with other water quality variables in an attempt to develop a set of linear discriminant functions, per lake type, to predict and evaluate Hg levels in yellow perch. An average age of 4.6 years was used in the analysis. These linear discriminant functions are to be applied to lakes that fall outside of the study area (Kamman et al., 2004). Yellow perch have been used frequently in previous studies both to evaluate lake condition as well as to develop fish consumption advisories (Kamman et al., 2004). The yellow perch also cover several trophic levels depending on size.

A fairly recent study in Canada completed by Vaidya and Howell (2001) attempted to explain Hg concentrations of lakes in Kejimkujik National Park using GIS and Statistics. A combination of principle components analysis and stepwise multiple regression was used in attempt to explain the MeHg concentrations in the lakes (Vaidya and Howell, 2001). The results from their study found positive correlations between mean annual mercury levels in the lakes and lake surface area, lake basin area, lake basin area to lake surface area ratio, granite bedrock, and negatively with greywhacke bedrock geology. They further show that mercury in the study area originates within the watershed (Vaidya and Howell, 2001).

In all cases, the models have attempted to relate the bioaccumulation of mercury to fish tissue or water and have neglected the higher trophic level species such as the Common Loon or other piscivorous wildlife. At this point I am not aware of a model implemented in, either partially or fully, the framework of a GIS system that addresses higher trophic level biota. All the models discussed above addressed the issue at a watershed level as well, averaging the concentrations across a lake. This methodology does not lend itself to understanding the variability within lakes and the subsequent risk it poses to higher trophic level species due to that variability.

Non-Spatial Models/Research

Non-spatial numerical/statistical models have attempted to explain MeHg levels in higher trophic level biota. There are current efforts underway by BRI to develop a wildlife criterion value for the common loon in an effort to assess the impacts of MeHg on piscivorous wildlife (Evers et al., 2003). Researchers at BRI are also analyzing MeHg concentrations in cavity nesting ducks, in particular the golden eye (*Bucephala clangula*), the common merganser (*Mergus merganser*), the wood duck (*Aix sponsa*), and the hooded merganser (*Lophodytes cucullatus*), and assessing the impacts of MeHg to mink and river otter.

Substantial efforts have also been directed toward understanding MeHg variation in other species. Golet and Haines (2001) used snapping turtles as indicators of aquatic health. Snapping turtles, common in many fresh water ecosystems, also bioaccumulate Hg (Golet and Haines, 2001). Other research has shown that reptiles, such as American Alligators in Florida and northern water snakes in Michigan, bioaccumulate Hg.

Other efforts have examined Hg levels in the horseshoe crab. Burger (1997a) analyzed Hg levels in horseshoe crabs and found declining levels during the study period ranging from 1993-1995. Results showed that there were higher levels in the horseshoe crab eggs than in the adult female horseshoe crabs (Burger, 1997a). Burger (1997b) also analyzed heavy metal concentrations in Herring Gulls and found substantial variation among the groups studied. The study area ranged from eastern Long Island, New York to Virginia and significant concentrations of Hg were found to be randomly distributed throughout (Burger, 1997b). The study utilized bird feathers, which can make interpretation of Hg source difficult at best, particularly because the birds are migratory. In an effort to address that problem feathers from chicks were collected (Burger, 1997b).

The literature and research cited in this chapter is not comprehensive and is intended to give an overview of recent Hg studies in the U.S. and Canada. None of these studies attempted to explain the variability that can exist within a watershed. Most of the existing studies document the Hg and MeHg concentrations in fish and wildlife, and the mechanisms that contribute to those concentrations within the entire watershed. In the case of the common loon, where there may be multiple nesting pairs with significantly varying levels of MeHg, a watershed approach may be inappropriate to truly the explain the within lake variability. For example, instead of looking at the problem from a watershed level, it may be more appropriate to look at the problem as a function of distance from the lake or loon territory.

Chapter 3: Methods and Procedures

3.1 Location of Study

The area of interest is the Rangeley Lakes region located in western Maine and eastern New Hampshire (Figure 3.1). The study will examine the upper parts of the Kennebec and Androscoggin rivers as well as the entire watershed that flows into Lake Umbagog. The area is comprises thirty-four 7.5 minute USGS quadrangles that include the following major lakes/reservoirs: Umbagog, Richardson, Mooselookmeguntic, Rangeley, and Aziscohos. The study area was selected for several reasons. First it exhibits Hg levels that are higher than the national average (Evers et al., 2003). Second, significant amounts of Hg data are available for the area. The initial model will be based on the Rangeley Lakes area because the majority of the Biodiversity Research Institute's research has been conducted in that region making data available. Once the initial model was created, it was tested, cross-referenced with existing data, and validated against known Hg levels. This was necessary to determine the reliability of the model in predicting Hg levels and the associated risk those levels pose to the local biota. Within the study area, known point sources of Hg do not exist. Therefore, the main focus of this thesis will be based on the assumption that the predominant influx of Hg is through non-point sources, which include both dry and wet deposition.

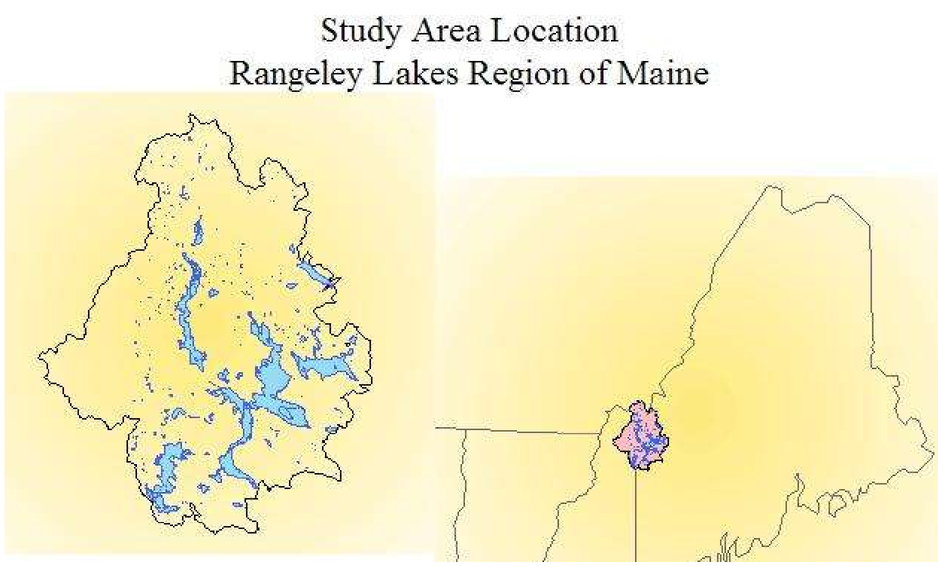

Figure 3.1
Study area located in northwestern Maine and northeastern New Hampshire.
Area covers approximately 246,372 hectares.

3.2 Hardware and Software

The hardware used for development of the GIS based model was a standard Pentium 4 computer. Software used included ArcGIS, ARC/INFO workstation, Statistix, and MiniTab. Additionally, new Hg collection software (HgTracker) based on the Palm operating system was tested and is described in the next section. Collection of loon sample locations was done using a Garmin12 GPS unit, Garmin ETrex GPS unit, or the Magellan GPS for the Handspring Visor handheld computer, all of which collect only autonomous GPS data (Figure 3.2). It should be noted that the Magellan Companion for the Visor was integrated into the HgTracker field collection software that will be discussed later in this chapter. Locations of water samples were collected in the same manner using autonomous GPS technology. A brief description of loon capture techniques can be found in the data collection section below.

Figure 3.2
GPS units used for data collection. From left to right: Garmin Etrex, Garmin 12, Magellan Companion for Handspring Visor

3.3 Field Data Collection (HgTracker)

Data collection in the field can introduce error into the spatial database. This error can arise for a number of reasons including human perception at the time of information gathering and variation in how the collected data are entered into the larger database. To facilitate the seamless integration of multiple data sources it is necessary to implement standards for how data are collected and managed. HgTracker is a software product originally developed for the palm operating system that provides for seamless collection and integration of Hg related data. The software was used during the summer of 2003 for collection of individual loon territory data in lieu of the traditional, and often less accurate pen and paper method. Data were collected during surveys of the area and information was recorded in regards to loon territory fidelity, nesting and breeding success, and general information in regards to behavior. Additional information about intruding loons were collected as well.

The software provides a platform that requires the user to enter information about loon age, band combination, nesting success, and territory fidelity in a manner that greatly reduces the possibility of user entry error from mistyped keystrokes, abbreviations, or just plain blunders. For example, in the existing database, collected by pen and paper method, an adult loon may be coded as "adult", "adlt", or "A". This inconsistency in data entry makes it difficult to query and analyze the database, therefore much of the attribute information in the HgTracker software was made available through drop down menus, checkboxes, or radio buttons in an effort to assure consistency. The HgTracker software also provides a method for capturing GPS locations of nest bowls for individual loon territories, which can be useful in locating the nests the following year, as well as in facilitating implementation into a GIS system for additional spatial analysis. The basic procedure for collecting loon territory information and samples is described in section 3.5 below.

Lastly, the HgTracker software provides a seamless environment for integration of the data into a Microsoft access database. This allows for data, collected by several people or organizations, to be seamlessly integrated into one cohesive database with minimal chance of user error or inconsistency in data entry methods. This also facilitates a user friendly environment for data sharing among collaborating organizations and agencies.

3.4 Digital Data Collection and Preparation

Data were collected from a variety of sources. Table 3.2 provides a list of the data, the data type, and the source of the data. The two main data sources were the Maine Office of GIS and Biodiversity Research Institute. Other data sources included the Prism website for collection of precipitation data and the New Hampshire GRANITE site for collection of data that fell outside the state of Maine. The Hg sample sites were provided by the BioDiversity Research Institute (BRI) located in Falmouth, Maine under the direction of Dr. David Evers. Sample locations have been collected over the last several years and are well distributed within the study area.

Initial geo-referenced data were collected in a variety of projections, however, the predominant referencing scheme was based on latitude and longitude coordinate locations. Scales varied depending on the source of the data and that information is included in Table 3.1. Data layers that were collected at 1:24000 scale were downloaded from either the Maine Office of GIS website or the New Hampshire GRANITE website, then cleaned and built for topology using ARC/INFO workstation. The data were then merged and dissolved using ARC/INFO workstation in order to provide seamless data sets within the study area. Once the data sets were complete (e.g. merged and cleaned) they were projected into the Maine Stateplane West coordinate system for the North American Datum of 1983. All data used and the associated spatial analysis was done using that coordinate system, the parameters of which are shown in Table 3.2. All data that were in the ARC/INFO coverage format were converted to the ESRI shapefile format to facilitate use of the model and data among those agencies that do not have full ARC/INFO capabilities as well as to meet requirements set for by the Northeastern Ecosystem Research Cooperative (NERC), which has requested that all spatial data be delivered in ESRI shapefile format to facilitate data sharing among collaborative organizations and to minimize a disparate number of data formats.

Tabular data (shown in Table 3.1) that included latitude and longitude information were added as event themes in ArcGIS and then converted into shapefile format using ArcGIS. The new shapefiles were then exported into the Maine Stateplane West coordinate system for the North American Datum of 1983. This insured that all spatially referenced layers used in the analysis were in the same projection within the GIS.

Table 3.1
Data sets used in model. Data were collected from a variety of sources and represent various scales. Data included both vector and raster data types.

Data Sets	Data Type	Data Scale	Source
Precipitation Rates	**Raster**	**1:250,000**	**PRISM website**
Wetland Type	**Raster**	**30m Raster Resolution**	**Maine Office of GIS/ GRANITE**
Forest Cover	**Raster**	**30m Raster Resolution**	**USGS**
Land Use	**Polygon**	**30m Raster Resolution**	**USGS**
Slope/Topography	**Raster**	**30m Raster Resolution**	**USGS**
Hydrography	**Line**	**1:24000**	**Maine Office of GIS/ GRANITE**
Hydrography	**Polygon**	**1:24000**	**Maine Office of GIS/ GRANITE**
Loon Samples	**Point/Tabular**	**Autonomous GPS**	**Biodiversity Research Institute**
Territory	**Point/Tabular**	**Autonomous GPS**	**Biodiversity Research Institute**

Table 3.2
Projection parameters used in model. All data sets were projected to the above coordinate system.

NAD 1983 UTM Zone 19N	Transverse Mercator
False Easting:	500000.000000
False Northing:	0.000000
Central Meridian:	-69.000000
Scale Factor:	0.999600
Latitude Of Origin:	0.000000

3.5 Territory Surveys and Loon Sample Collection

Currently there are 199 loon mercury samples within the study area. However, of the 199 samples, only 61 represented adult male loon samples. An explanation of why only the adult male loon samples were used is provided later in this chapter. Figure 3.3 shows the spatial distribution of male loon samples currently collected by either BRI or one of their collaborators. Loon samples in general were collected using a method developed by the Biodiversity Research Institute and represent a continuous sampling methodology. Surveys were conducted during the breeding season (May – August) to determine territory fidelity and to monitor and record information in regards to the number of nesting loon pairs on each lake. The HgTracker software was used to gather the survey information and seamlessly integrate it into a Microsoft Access database. The basic method for collecting survey information is described below:

1. Loon territories were assigned to individuals at the start of the breeding season, generally during the first two weeks of May.
2. Surveys were conducted every 7 to 10 days and information collected on territory fidelity, nest locations, intruder information, and nesting success (when appropriate), as well as the general activities of the pair such as fishing or preening.
3. The Hg Tracker software was used to collect the above information and the integrated GPS unit was used to record the location of the nest bowls, hummock, man-made rafts, or scrapes.

   Bowl: Nest approximately ½ meter in diameter and 12 cm in height. The bowl is typically located on shore and is made of grasses and mosses.

   Hummock: Very similar to the traditional bowl however it is located in marshy areas on tufts of grasses sitting just above the water.

Man-made raft: A raft is constructed of cedar posts and anchored just offshore. This allows for the loons to build a nest that will fluctuate with variations in water level allowing for increased nesting success and increased protection from potential predators.

Scrape: As described by BRI, a scrape is the "lazy" loon's nest generally consisting of only a small cleared area "scraped" out in the sand or gravel. If the loons are feeling particularly energetic they may place a few small sticks around the scrape in an effort to delineate the nest from the surrounding area.

4. Finally, if a pair was successful in their breeding attempt, the birds were captured and samples collected for analysis of both blood Hg and feather Hg levels. For consistency sake, blood was always drawn from the caudal tibial vein in the leg located medially over the tarsal joint, and the second secondary feather was clipped. Clipping of the second secondary insures consistency in the data collection and does not inhibit flight.
5. Each adult bird was banded with an United States Fish and Wildlife (USFWS) band and 3 colored bands representing an unique combination. Juveniles were banded in the same manner however single color bands were used if the tarsus was to small to accommodate two bands on each leg.
6. Once samples were collected, they were labeled and sent out for analysis using Cold Vapor Atomic Fluorescence Spectrophotometry (CVAFS) technology.

Capturing the birds required a number of steps. Once the pair was found, a combination of bright lights, electronic calls, careful maneuvering of the boat, and a whole lot of luck was used to bring the loons in close enough to net. Collection of samples was accomplished in a non-lethal manner. Information from the collected samples were then entered into the model at the capture location.

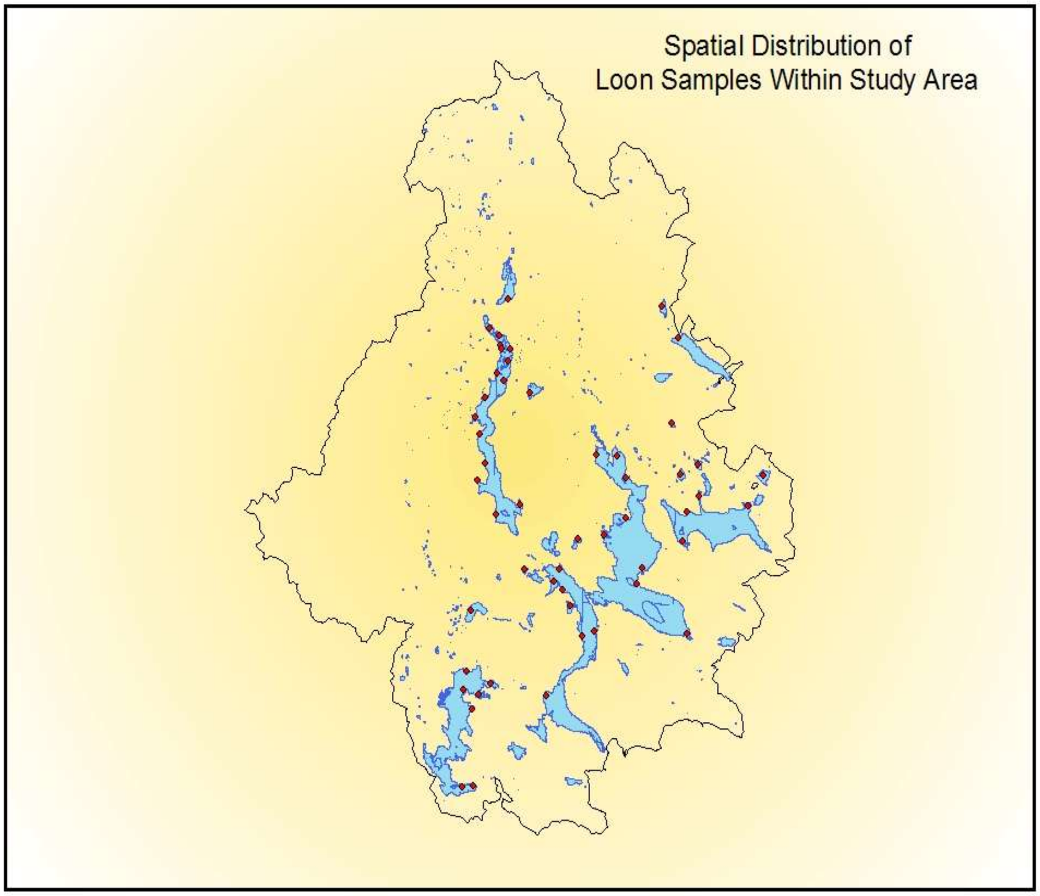

Figure 3.3
Spatial distribution of Male Loon samples within study area. The sample data was either currently existing and supplied by Biodiversity Research Institute or collected during the summer of 2003 by this researcher.

3.6 Model Development

Once the necessary data were collected, the conceptual framework for the model (Figure 3.4) was developed. The creation of the framework involved a detailed project schematic that outlined the individual steps needed to complete the project. Once the steps were defined and the data collected, the flow model was put together to aid in implementation of the individual steps of the process.

There were five major steps involved in preparing the data necessary for statistical analysis. Those steps are listed below and then defined in the following paragraphs.

1. Created Thiessan polygons from point samples to form “loon territories" necessary to begin the analysis.
2. Buffered the polygons at 3 intervals (150m, 300m, 600m). This step provided the areas within each of the 3 intervals needed to collect the land cover information.
3. Reclassified the NLCD (National Land Cover Database) data into individual land cover classes. This step provided the individual land cover classes necessary to obtain percentages within the territories. These were based on existing categories in the dataset.
4. Used a Zonal Statistics function to obtain percent of each land cover type.
5. Exported the resulting data to a dbase (*.dbf) file for import into MiniTab for statistical analysis.

The individual point locations for the loon territories were converted into thiessan polygons. A thiessan polygon can be described as a polygon developed in such a manner that no location within that polygon is closer to any other sample point than the sample point contained within the polygon. Thiessan polygons are also known as voronoi polygons or Dirichlet polygons (Burrough, 2000). Because delineations of the polygons are completely dependent upon the location of the sample points if a point was collected near the edge of a loon territory the resulting polygon may not accurately depict the true geographic area of the actual territory. In theory it should include most of the area. Thiessan polygons were used to delineate loon territories within the GIS because spatially referenced and delineated territories were currently not available. This method also allowed for segmentation of the lakes in order to explain the variability of MeHg within each of the territories. If there were multiple samples in the same territory, the values were averaged. Multiple values can exist in a single territory because a particular bird may be captured year after year. This allows for a value to represent the average available MeHg in a particular location.

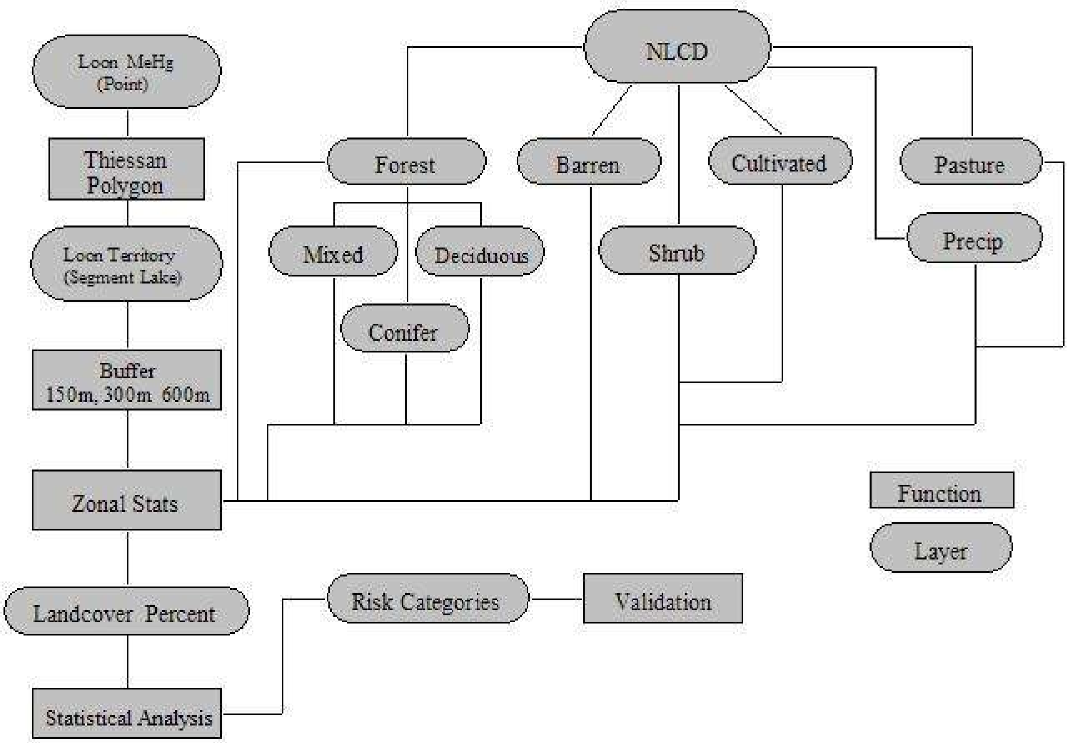

Figure 3.4
Conceptual flow chart of model methodology. Developed prior to model development to aid in implementation. The above chart represents the five major GIS operations used in the analysis.

Once the territories were created, a spatial join integrated the loon MeHg levels from the individual loon sample points into the thiessan polygons. Figure 3.5 shows the "territories" generated from the thiessan polygon procedure. Loon samples were subdivided into three categories: Male Adult, Female Adult, and Juvenile. For the purpose of this thesis the model was developed using the male loon samples. There are several reasons to use only the male samples:

1. Males tend to exhibit the highest Hg levels and levels are not affected by egg laying processes.
2. Females exhibit the next highest levels but may process out some the HG from the burden of laying eggs. This may lead to erroneous estimates in the regression model.

3. Juveniles exhibit the lowest levels. This is potentially due to the fact that the juvenile loons have not had the opportunity to bioaccumulate as much Hg as their adult counterparts (Evers et al., 2003).

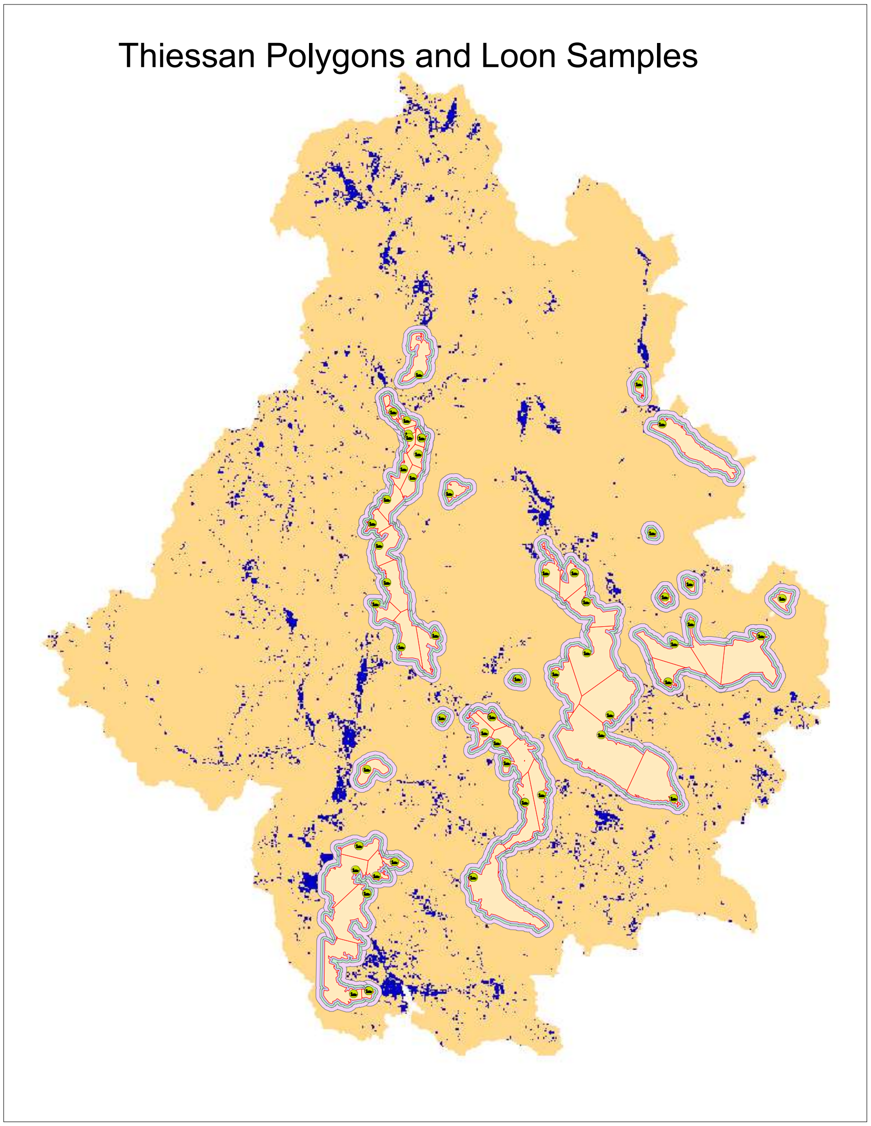

Figure 3.5
Thiessan polygons developed to act as "Loon Territories" in the model. These polygons were also used to obtain the buffered areas needed in the land cover analysis. The buffered area around each of the territories is also included.

There were a total of 61 samples used in the analysis that accounted for 30.5% of the total number of samples and 65.5% percent of the territories. The samples were then randomly subset in ArcGIS using Geostatistical Analyst into a test data set and a training data set allowing for 35 - 41 samples in each set. This process was repeated 30 times in an effort to assess the sensitivity of the model.

Once the thiessan polygons were generated and the sample MeHg levels incorporated, the individual territories were buffered at 3 intervals: 150m, 300m, and 600m. Individual land cover characteristics from each of the buffered zones were then incorporated into the initial territory shapefile. As mentioned in the literature review, wetlands have been determined to be a major contributor to the available MeHg in an area. That being the case, it seems logical to assume that, if there is a larger percentage of wetlands within a particular proximity to a territory, then the available MeHg will be greater. By analyzing the land cover variability within certain proximities of the individual territories we should be able to more accurately explain the variability of MeHg within the common loon. Figure 3.5 also represents the buffered areas around each of the individual loon territories.

For each of the three distances, the percent landcover of each class was recorded and spatially joined into the territory table using a zonal statistics function. This table was then exported from ArcMap as a dbase file and then imported into Minitab for statistical analysis. A basic Pearson Product Moment correlation test was run to determine the relationship between the independent variables (landscape factors) and the dependent variable (loon MeHg level). This was initially run on the entire sample set. Once the individual relationships were determined, ordinary least squares regression was used to create the regression equation based on the training data set. Upon completion of the regression equation the resulting residuals were analyzed to insure that the assumptions of ordinary least squares regression were met. This process was repeated for all three of the buffered areas surrounding the loon territories.

Once the regression equations were created and the residuals analyzed the regression equation was implemented in ArcGIS using the Raster Calculator. In order to restrict the raster calculator results to the extent of the thiessan polygons the percent value of each land cover class was converted into its own raster layer. This allowed for 8 different sets of raster layers based on the extent of the thiessan polygons to be input into the regression equation. Once this was completed, the variations between the new Hg values calculated from the equation and the original measured Hg levels was assessed.

In an effort to address the sensitivity of the model, the R^2 values from all thirty iterations were recorded and a 95% confidence interval calculated to determine the number of iterations that fell within that confidence interval. This was again completed for all distance classes. The residual plots were then examined for all thirty iterations in an effort to determine if any one iteration did not meet the assumptions of ordinary least squares regression. The range of R^2 values was also analyzed for each distance class in an attempt to explain the variation between each of the regressions.

Chapter 4: Results and Discussion of Statistical Analysis

4.1 Introduction

This chapter will present and discuss the statistical results from the analysis. They will be presented in the order of the distance class from least to greatest. The last section will address overall conclusions and the final results from the statistical analysis of this thesis. This thesis utilized least squares regression and extensive effort was taken to analyze and understand the residual distributions from the model. In order to meet the normality requirements of least squares regression the dependent variable was log-transformed (Figure 4.1).

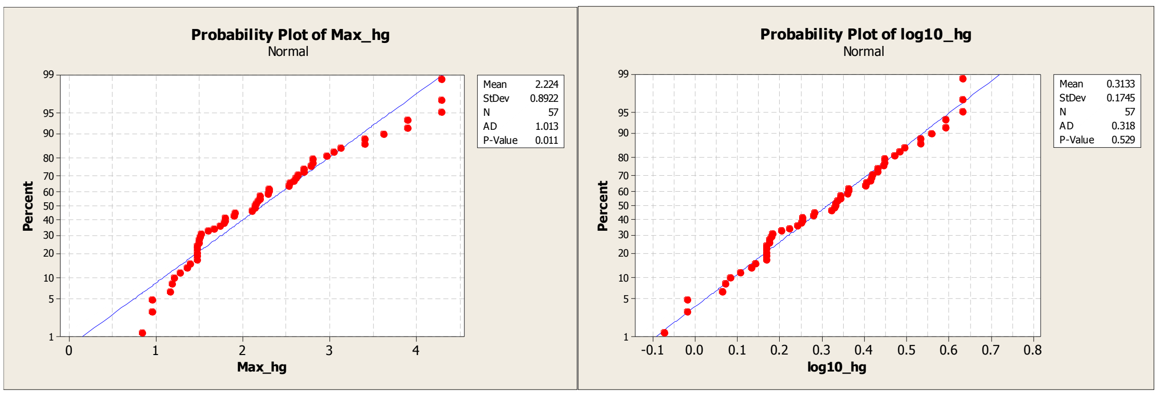

Figure 4.1: Example of log-transformation used on the dependent variable (Hg). In order to meet the normality requirements of ordinary least squares regression the transformation was necessary. The left graph represents the measured Hg levels and the right graph represents the log-transformed values. The p-value greater than 0.05 indicates significance (right graph).

4.2 Basic Statistics: 150 meter Distance Class

Three variables were significantly correlated ($p < 0.05$) with Hg levels in the Common Loon (Table 4.1) based on Pearson's Product Moment Correlation Coefficient. Three variables were also found to be significant in the regression model and the fourth (wetlands) was included because it was found to be significant in Pearson's test and exhibits a p-value only slightly above 0.05 (Table 4.2). The ANOVA indicates that the regression model is significant ($p < 0.05$) however some of the variables were not significant and do little to explain the variance of Hg in the Common Loon (Table 4.3). The variables used in this model ($n = 8$) explain 53.3% of the Hg variance ($R^2 = 53.3$). The residual plots meet the assumptions of normality and are randomly distributed when compared with the fitted values (Figure 4.2). The Durbin-Watson statistic (1.23901) indicates that the residuals do not exhibit autocorrelation and further suggest the model is adequate at this distance class.

Table 4.1
Pearson's correlation coefficients from 150 meter distance class (n = 57). Significant correlations are shown in bold. Cell contents show Pearson's correlation coefficient (top) and the p-value (bottom). Shrub = Shrub land, Mixed = mixed forest, Decid = deciduous forest, Cult = cultivated land, Barren = Barren land, Precip = average precipitation.

	Wetland	Shrub	Mixed	Decid	Cult	Conif	Barren	Precip
Hg_Log10	**0.492**	**0.550**	0.115	0.018	**-0.300**	0.200	0.164	0.155
	0.000	**0.000**	0.392	0.891	**0.023**	0.135	0.223	0.250

Table 4.2
Regression coefficients, T-value, and P-values from 150 meter distance class (n = 57). Significant p-values are shown in bold.

Predictor	Coef	SE Coef	T	P
Constant	0.1033	0.3658	0.28	0.779
Wetland	2.031	1.018	1.99	**0.052**
Shrub	52.05	11.36	4.58	**0.000**
Mixed	0.3208	0.4379	0.73	0.467
Decid	-0.4124	0.6447	-0.64	0.525
Cult	-8.245	3.558	-2.32	**0.025**
Conif	-0.1494	0.2732	-0.55	0.587
Barren	-3.035	1.08	-2.81	**0.007**
Precip	0.004872	0.009557	0.51	0.613

Table 4.3
ANOVA table from 150 meter distance class. The P-value of 0.000 indicates that at this level the model is adequate in predicting Hg in the Common Loon.

Analysis of Variance					
Source	DF	SS	MS	F	P
Regression	8	0.90952	0.11369	6.85	**0.000**
Residual Error	48	0.79637	0.01659		
Total	56	1.70589			

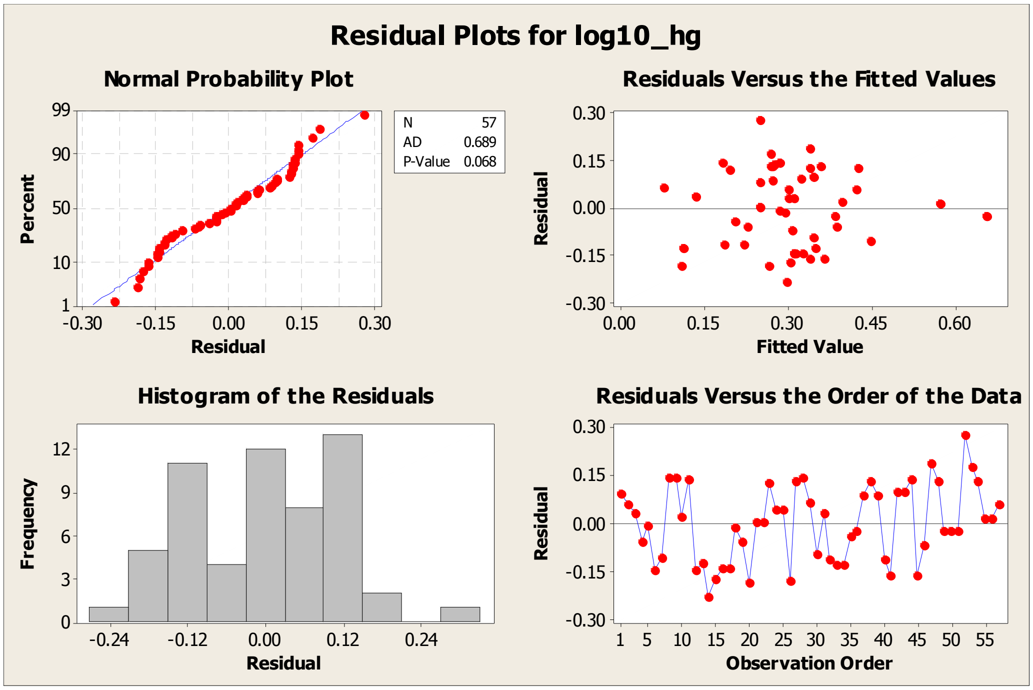

Figure 4.2
Residual plots for the 150 meter distance class (n = 57). The residuals meet the requirements of least squares regression as can be seen in the plots.

4.2.1 150 Meter Buffer: Subset

The following sections detail the results from the 150 meter buffered area. The results presented are for the initial subset of the data (n = 41). Hg levels were again log-transformed.

Within the subset data (n = 41) only two independent variables were found to be significant to Hg levels in the Common Loon based on Pearson's Correlation Coefficient (Table 4.4). Three variables were found to be significant in the regression (Table 4.5). The ANOVA indicates that the regression model is significant ($p < 0.05$), however, similar to using all samples, some of the variables were not significant and do little to explain the variance of Hg in the Common Loon (Table 4.6). The variables used in this model (n = 8) explain 57.4% of the Hg variance ($R^2 = 57.4$). The residual plots meet the assumptions of normality and are randomly distributed when compared with the fitted values (Figure 4.2). The Durbin-Watson statistic (1.54323) indicates that the residuals do not exhibit autocorrelation and further suggest the model is adequate at this distance class.

Table 4.4
Correlation coefficients from 150 meter distance class (n = 41).

	Wetland	Shrub	Mixed	Decid	Cult	Conif	Barren
Hg_Log10	**0.571**	**0.433**	0.011	-0.112	-0.259	0.247	0.086
	0.000	**0.005**	0.945	0.484	0.102	0.119	0.594

Table 4.5
Regression coefficients from 150 meter distance class (n = 41).

Predictor	Coef	SE Coef	T	P
Constant	0.5512	0.5003	1.1	0.279
Wetland	3.568	1.335	2.67	**0.012**
Shrub	46.67	12.89	3.62	**0.001**
Mixed	1.1616	0.6269	1.85	0.073
Decid	-1.2132	0.785	-1.55	0.132
Cult	-6.719	4.007	-1.68	0.103
Conif	-0.2068	0.2736	-0.76	0.455
Barren	-4.005	1.285	-3.12	**0.004**
Precip	-0.00785	0.013	-0.6	0.55

Table 4.6. ANOVA table from 150 meter subset (n = 41).

Analysis of Variance					
Source	DF	SS	MS	F	P
Regression	8	0.80077	0.1001	5.40	**0.000**
Residual Error	32	0.59325	0.01854		
Total	40	1.39402			

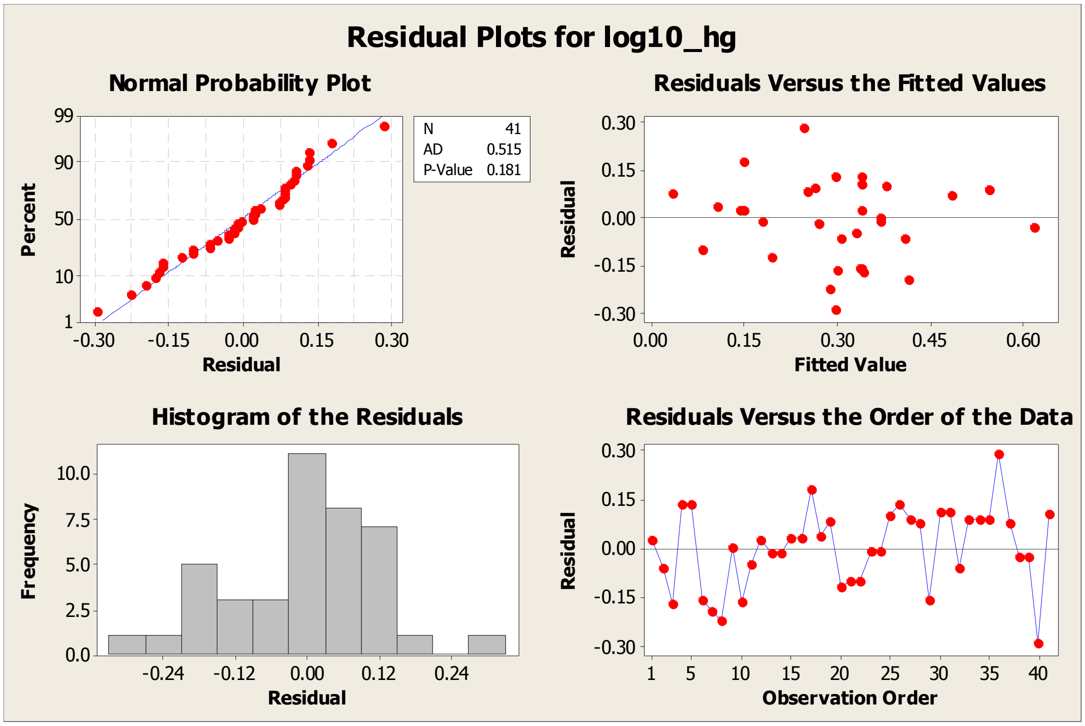

Figure 4.3
Residual plots for the 150 meter distance class subset (n = 41). Residuals are clearly randomly distributed, and meet the normality requirements for least squares regression.

Sensitivity

To insure that the sample was not biased, the Hg data were randomly subset thirty times using ArcGIS Geostatistical Analyst. Table 4.7 below lists the R^2 values for each of the thirty iterations within the 150 meter distance class. In all cases the Durbin-Watson statistic was significant indicating there is no autocorrelation in the residuals. The average R^2 value for the thirty iterations was 57.80. The standard deviation was 6.183. Of the thirty iterations, 22 fell within one standard deviation of the mean and all but one fell within two standard deviations of the mean.

Table 4.7
Results for the 150 meter distance class from thirty iterations of data subsets. Sample sizes varied based on how the subset was created and ranged from 34 samples to 43 samples.

Iteration	R^2	DurbWat
1	55.0	1.78945
2	45.9	1.52792
3	59.7	1.45408
4	59.3	1.24533
5	48.7	1.33189
6	60.6	1.56090
7	61.0	1.95494
8	55.4	1.32029
9	62.7	1.74647
10	63.2	2.06829
11	48.8	1.15306
12	54.3	1.58161
13	58.6	1.38379
14	57.3	1.07329
15	72.7	1.66701
16	48.0	1.78674
17	62.4	1.58605
18	61.3	1.52193
19	64.9	2.05954
20	59.2	1.64102
21	55.7	2.01813
22	47.2	1.33813
23	63.4	1.76334
24	53.8	1.68581
25	61.1	2.16634
26	58.4	1.63442
27	67.6	1.19515
28	58.1	1.63904
29	56.8	1.37262
30	53.0	1.47709

4.2.2 Discussion: 150 meter Distance Class

Correlation

There were several relationships found within the 150 meter distance class (n = 57). The positive relationship found between Hg and wetlands (0.492, p-value < 0.001), and the negative relationship with cropland (agricultural) (-0.3, p-value < 0.05) is supported by previous research done by Kamman et al. (2000). The strong positive relationship with shrub land (0.55, p-value < 0.001) has not been documented in the literature. Within the 150 meter distance class using the subset data (n = 41), we find a shift in the significant variables per their correlation coefficients and associated p-values. Using the subset data, wetlands (0.571, p-value < 0.001) and shrub land (0.433, p-value < 0.05) still exhibit significant relationships with Hg in the loon blood. We find using this subset of the data that cultivated lands still exhibit a negative relationship (-0.259, p-value > 0.05), however, it is not significant at the 95% confidence interval. Analysis of the thirty iterations of subset data show cropland as significant in a number of cases. Due to the relatively small amount of land used for agricultural purposes within the study area it is quite possible that samples from the subset data did not include territories where there was agricultural land within 150 meters.

Regression

The table of regression coefficients, t-values, and p-values indicates that there are four variables of significance within the model. Those variables: wetlands (p-value > 0.05), shrub land (p-value < 0.000), crop land (p-value < 0.05), and barren (p-value < 0.05), exhibit the strongest influence in the model when using all of the samples. The wetlands class was included (p-value = 0.052) because it was noted as a significant variable in the Pearson correlation matrix. When the subset data were used we found that three of the variables mentioned above were still significant (wetland, shrub land, and barren land) and depending on the subset analyzed, croplands still show up as significant, potentially due to the little amount of area actually being used for agricultural purposes.

Results from the analysis of variance table for both the entire set of data and the subset data show significance at the 95% confidence interval with p-values of < 0.001. The f-statistic for both models also shows significance suggesting at least one of the coefficients is different than zero. In both cases, the test for autocorrelation of residuals

(Durban-Watson Statistic) is significant, as in both cases it is found to be larger than the largest value in the dependent variable (DW = 1.239, and DW = 1.543) thus indicating that no autocorrelation exists.

Analysis of the residual distributions for each of the models at the 150 meter distance class further suggests that the model is significant, exhibiting normal distributions of residuals (p-value > 0.05). The residuals are also randomly scattered in regards to the fitted values, suggesting that the error that does exist is randomly distributed.

Sensitivity

Analysis from all thirty iterations also suggests the model is not overly sensitive to points selected, in regards to being well fit. It is sensitive, however, to point selection in regards to its predictive capability. Further analysis revealed that the model is adequate at predicting Hg levels in the Common Loon on larger reservoirs and subsequently decreases in accuracy, within the subset data, when a larger proportion of the samples come from smaller lakes (generally only one pair of nesting loons). When using all of the samples the model appears to provide reasonable estimates of Hg risk to the Common Loon. Residual plots from each of the iterations within the 150 meter distance class can be found in Appendix A.

Conclusion

Based on the results presented above, the regression models Hg risk in the Common Loon adequately. The assumptions of least squares regression have been met. Output from the model will be presented at the end of this chapter. The regression model was recalculated using only those variables found to be significant, and then implemented into the GIS using the Raster Calculator available in ArcGIS Spatial Analyst.

4.3 Basic Statistics: 300 meter Distance Class

Within this distance class three independent variables were found to be significant to Hg levels in the Common Loon based on Pearson’s Correlation Coefficient (Table 4.8). They are the same variables found to be significant in the 150 meter distance class. Three variables were found to be significant in the regression (Table 4.9). Cultivated land was included (the fourth variable included) because it was identified as having a relationship with loon Hg levels from Pearson's Correlation Coefficient. The ANOVA indicates that the regression model is significant ($p < 0.05$)(Table 4.10). The variables used in this model (n = 8) explain 41.5% of the Hg variance ($R^2 = 41.5$). The residual plots do not meet the assumptions of normality and are not randomly distributed when compared with the fitted values (Figure 4.). The Durbin-Watson statistic (1.25224) indicates that the residuals do not exhibit autocorrelation, however there should be some concern over the lack of normality in the residuals. There also appears to be a clustering around the fitted value of 0.3.

Table 4.8: Pearson's correlation coefficients. (n = 57). Significant variables are noted in bold.

	Wetland	Shrub	Mixed	Decid	Cult	Conif	Barren
Hg_Log10	**0.350**	**0.481**	-0.096	0.099	**-0.293**	0.110	0.179
	0.007	**0.000**	0.472	0.460	**0.026**	0.412	0.178

Table 4.9:
Regression coefficients, T-value, and P-values from 150 meter distance class (n = 57). Significant p-values are shown in bold.

Predictor	Coef	SE Coef	T	P
Constant	0.114	0.4186	0.27	0.786
Wetland	2.1102	0.8878	2.38	**0.021**
Shrub	15.004	3.664	4.10	**0.000**
Mixed	-0.3298	0.3228	-1.02	0.312
Deciduous	0.330	0.4812	0.69	0.496
Cultivated	-4.670	2.369	-1.97	**0.054**
Coniferous	-0.2082	0.2538	-0.82	0.416
Barren	-2.602	1.202	-2.17	**0.035**
Precipitation	0.00586	0.01105	0.53	0.598

Table 4.10:
Anova table from the 300 meter distance class.

Analysis of Variance					
Source	DF	SS	MS	F	P
Regression	8	0.79672	0.09959	5.04	**0.000**
Residual Error	49	0.96802	0.01976		
Total	57	1.76473			

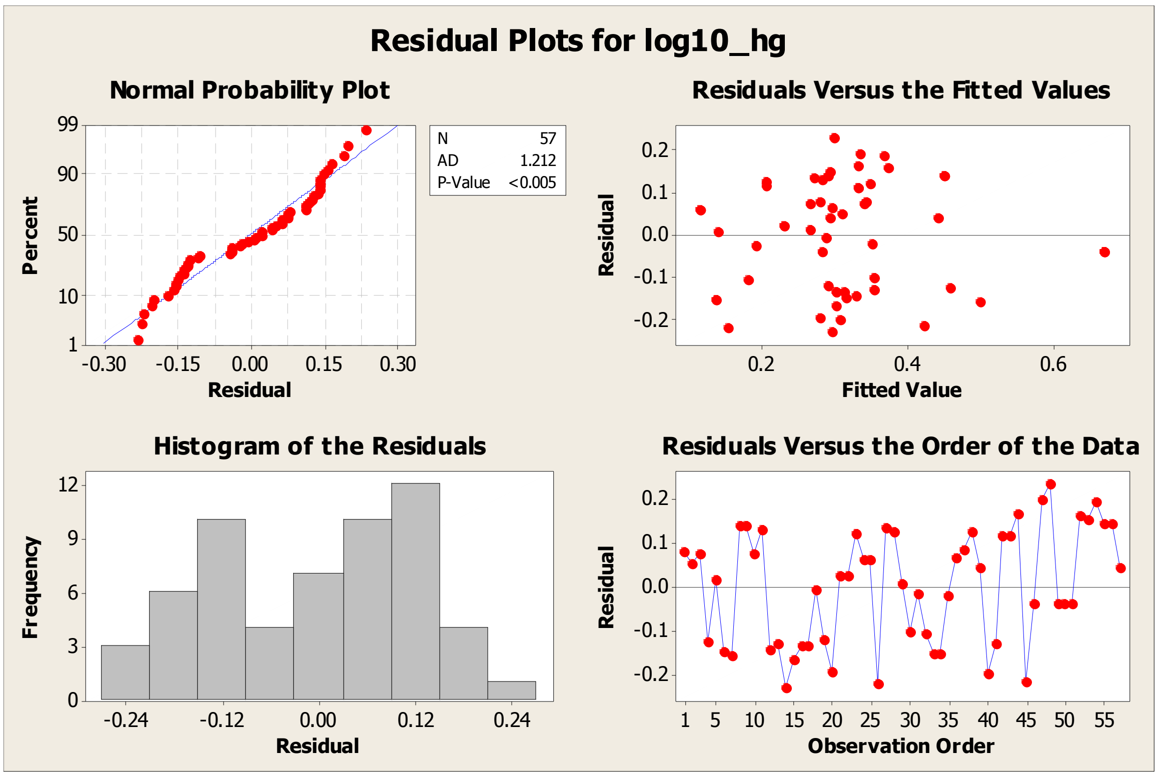

Figure 4.4
Residual plots for the 300 meter distance class (n = 57). The normal probability plot fails at p-value of less than 0.05

4.3.1 300 meter Buffer: Subset

The following section presents the results from the initial subset of the data (n = 41). This is the same subset used to generate the data from the 150 meter distance class.

Within the subset data (n = 41) three independent variables were found to be significant to Hg levels in the Common Loon based on Pearson's Correlation Coefficient (Table 4.11). Of the three variables, wetlands missed significance slighty (p-value =

0.08). Within the regression model for the subset data only shrub land was found to be significant (Table 4.12). Mixed forest was also identified (p-value = 0.055). The ANOVA indicates that the regression model is significant ($p < 0.05$) with at least one coefficient that is equal to zero (Table 4.13). The variables used in this model (n = 8) explain 49.6% of the Hg variance ($R^2 = 49.6$). The residual plots appear to meet the assumptions of normality and are randomly distributed when compared with the fitted values (Figure 4.5). The Durbin-Watson statistic (1.04063) indicates that the residuals do not exhibit autocorrelation.

Table 4.11
Correlation coefficients from 300 meter distance class (n = 41).

	Wetland	Shrub	Mixed	Decid	Cult	Conif	Barren
Hg_Log10	0.277	**0.558**	-0.245	0.035	**-0.310**	0.108	**0.350**
	0.080	**0.000**	0.123	0.827	**0.048**	0.501	**0.025**

Table 4.12
Regression coefficients from 300 meter distance class (n = 41).

Predictor	Coef	SE Coef	T	P
Constant	-0.5772	0.6311	-0.91	0.367
Wetland	2.032	1.361	1.49	0.145
Shrub	8.921	4.009	2.23	**0.033**
Mixed	-0.6873	0.3453	-1.99	0.055
Decid	0.1349	0.5456	0.25	0.806
Cult	-4.298	2.622	-1.64	0.111
Conif	-0.0739	0.2274	-0.32	0.747
Barren	-0.557	1.416	-0.39	0.696
Precip	0.02405	0.01666	1.44	0.158

Table 4.13
ANOVA Table for 300 meter distance class (n = 41).

Analysis of Variance					
Source	DF	SS	MS	F	P
Regression	8	0.64965	0.08121	3.94	**0.002**
Residual Error	32	0.65933	0.0206		
Total	40	1.30898			

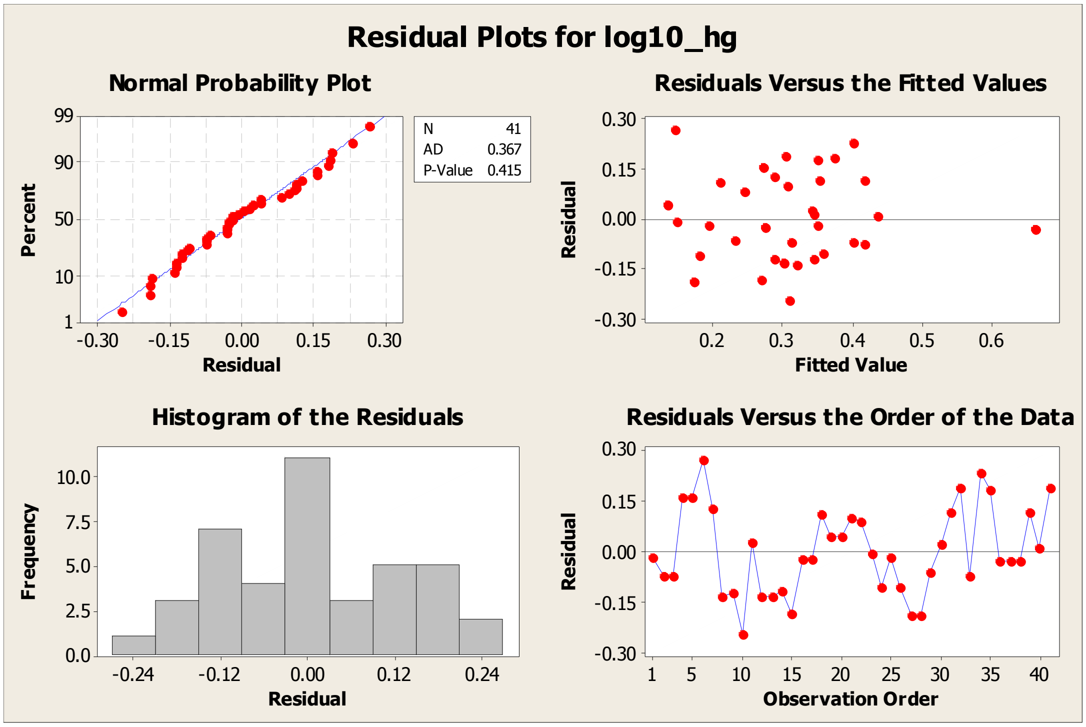

Figure 4.5
Residual plots for the 300 meter distance class (n = 41).

Sensitivity

In exactly the same manner as the 150 meter distance class, the Hg data were randomly subset thirty times using ArcGIS Geostatistical Analyst. The same subsets that were used to obtain the values for the 150 meter distance class were also used in the 300 meter distance class. This insured that each of the iterations used the same sample data and allowed for further interpretation among the results. The average R^2 value for the thirty iterations was 54.24, substantially higher than when computed using all the samples. The standard deviation was 5.87. Of the thirty iterations in this distance class, 21 fell within one standard deviation of the mean and all fell within two standard deviations of the mean. The model itself is again sensitive to the selection of samples included. Table 4.14 below lists the R^2 values for each of the thirty iterations within the 300 meter distance class.

Table 4.14
Results for the 300 meter distance class from thirty iterations of data subsets. Sample sizes varied based on how the subset was created but ranged from 34 samples to 43 samples.

Iteration	R^2	DurbWat
1	43.0	1.80184
2	46.4	1.58457
3	55.4	1.43169
4	61.9	1.17079
5	49.8	1.30445
6	58.8	1.66368
7	62.4	1.80967
8	46.4	1.24119
9	57.9	1.71295
10	61.4	2.06697
11	49.6	1.04063
12	50.9	1.49732
13	57.0	1.36699
14	57.9	1.32299
15	62.2	1.46731
16	44.1	1.88232
17	56.1	1.52613
18	57.7	1.53604
19	58.6	1.92490
20	49.8	1.79160
21	58.0	1.97752
22	50.6	1.64036
23	57.5	1.61672
24	48.6	1.70506
25	51.4	1.91612
26	56.4	1.65349
27	65.0	0.97059
28	52.4	1.51609
29	51.6	1.38767
30	48.4	1.35549

4.3.2 Discussion: 300 meter Distance Class

Correlation

At the 300 meter distance class (n = 57) I found significant relationships again with wetlands (0.35, p-value < 0.05), shrub land (0.481, p-value < 0.001), and cultivated land (0.293, p-value < 0.05). Within the 300 meter distance class using the subset data I found that wetlands were no longer considered significant (0.277, p-value > 0.05) at the 95% confidence interval. I still found a significant relationship with shrub land (0.558, p-value < 0.001), and cultivated land (-0.31, p-value < 0.05). Barren land also exhibits a significant relationship (0.35, p-value < 0.05). These results are similar to those found within the 150 meter distance class. Analysis of all thirty iterations continue to show some combination of these 4 variables as significant based on Pearson's Product Moment correlation.

Regression

Analysis of the regression model for the complete data set as well as all thirty iterations of the subset data show marked differences in their ability to accurately predict Hg in the Common Loon. The tables of regression coefficients, t-values, and p-values for the 300 meter distance class from chapter four show 3 variables that are significant to the model including wetlands (p-value < 0.05), shrub land (p-value < 0.001), and barren land (p-value < 0.05). Cultivated land is found not to be significant at the 95% confidence interval (p-value > 0.05), however, just barely misses the cut-off (p-value = 0.054). Within the subset data we no longer find wetlands to be significant, croplands to be significant, or barren land to be significant, which is contradictory to what was found in the 150 meter distance class, as well as what is found in the literature. This could potentially be attributed to a decrease in significance as a function of distance.

The analysis of variance tables still indicate that the models are significant at this point (p-value < 0.001 and p-value < 0.05). The f-statistic in both tables is still significant. The Durban-Watson statistic is still found to be significant, with all models exhibiting a value greater than the highest value of the dependent variable.

Analysis of the residuals suggests that this distance class may not be as appropriate as the 150 meter distance class. The initial model exhibited a random distribution of residuals, however, this assumption was not met by the subset data (p-value < 0.005). Similar problems were discovered when analyzing the residual plots from all thirty iterations of subset data (Appendix B).

Sensitivity

At this distance class the model is sensitive to both the data points selected in regards to being well fit, as well as to the selection of points in its predictive capability. In all cases, autocorrelation of the residuals did not exist. Because of the violation of the assumptions that the residuals are normally distributed and randomly distributed versus the fitted values, this distance class is not as accurate at making Hg predictions as the model based on the 150 meter distance class. In many cases, there was a clumping of the residuals in regards to the fitted values. We still find the same relationship with R^2 values in regards to territory size with the lower values corresponding to the smaller, single territory lakes.

Conclusion

The 300 meter distance class is far less robust, in many cases violating one or more of the assumptions of least squares regression, than the 150 meter distance class. It is more sensitive in point selection when using a subset of the samples, and in some cases, variables known to be significant per previous research are found not to be (wetlands, for example). This also supports the hypothesis that those variables considered to be significant per previous research as well as those found to be significant in this study exhibit a stronger influence if they are closer to the individual territory.

4.4 Basic Statistics: 600 meter Distance Class

The following section details the results from the final 600 meter distance class. This represents the furthest extent out from the loon territories at which this research looks. Within this distance class four independent variables were found to be significant to Hg levels in the Common Loon based on Pearson's Correlation Coefficient (Table 4.15). Three variables were found to be significant in the regression (Table 4.16). The ANOVA indicates that the regression model is significant ($p < 0.0001$) (Table 4.17). The variables used in this model ($n = 8$) explain 48.0% of the Hg variance ($R^2 = 48.0$). The residual plots do not meet the assumptions of normality and are not randomly distributed when compared with the fitted values (Figure 4.6). The Durbin-Watson statistic (1.34347) indicates that the residuals do not exhibit autocorrelation, however there should be some concern over the lack of normality in the residuals. There again appears to be a clustering of the residuals around the fitted value of 0.3.

Table 4.15
Correlation coefficients from 600 meter distance class (n = 57).

	Wetland	Shrub	Mixed	Decid	Cult	Conif	barren
Hg_Log10	**0.385**	**0.492**	-0.162	0.155	**-0.299**	-0.031	**0.263**
	0.003	**0.000**	0.228	0.248	**0.024**	0.819	**0.048**

Table 4.16
Regression coefficients and ANOVA table from 600 meter distance class (n = 41).

Predictor	Coef	SE Coef	T	P
Constant	0.0588	0.4133	0.14	0.888
Wetland	2.3518	0.887	2.65	**0.011**
Shrub	13.159	3.457	3.81	**0.000**
Mixed	-0.1361	0.317	-0.43	0.670
Decid	0.0846	0.364	0.23	0.817
Cult	-2.593	1.453	-1.78	0.081
Conif	-0.2052	0.2282	-0.90	0.373
Barren	-2.454	1.146	-2.14	**0.037**
Precip	0.00679	0.01123	0.60	0.548

Table 4.17
ANOVA table from 600 meter distance class (n = 57).

Analysis of Variance					
Source	DF	SS	MS	F	P
Regression	8	0.81884	0.10235	5.54	**0**
Residual Error	48	0.88705	0.01848		
Total	56	1.70589			

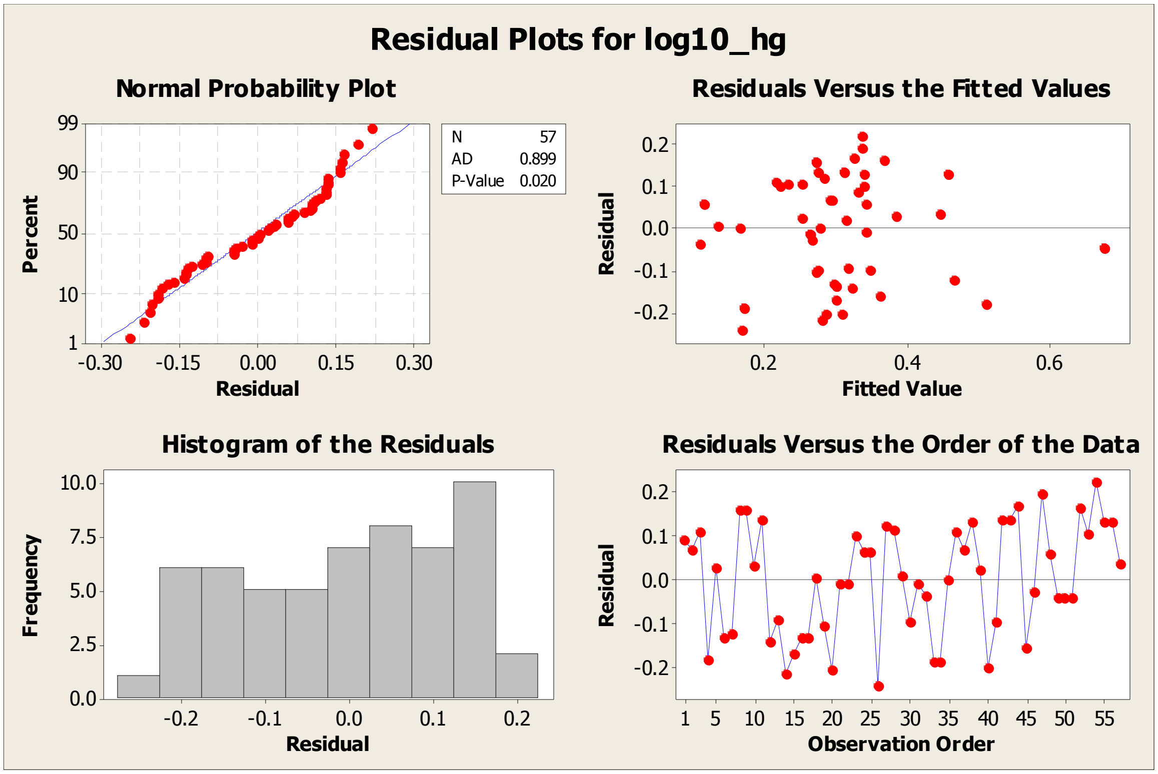

Figure 4.6
Residual plots for the 600 meter distance class (n = 57). The normal probability plot fails at p-value of less than 0.05

4.4.1 600 meter Distance Class: Subset Data

Within the subset of the 600 meter distance class four independent variables were found to be significant to Hg levels in the Common Loon based on Pearson's Correlation Coefficient (Table 4.18). Only one variable was found to be significant in the regression (Table 4.19). The variable identified was mixed forest, which has not shown up as significant in any other model. The ANOVA indicates that the regression model is significant ($p < 0.05$)(Table 4.20). The variables used in this model (n = 8) explain 54.9% of the Hg variance ($R^2 = 54.9$). The residual plots do meet the assumptions of normality and are randomly distributed when compared with the fitted values (Figure 4.7). The Durbin-Watson statistic (1.06631) indicates that the residuals do not exhibit autocorrelation.

Table 4.18
Correlation coefficients from 600 meter distance class (n = 41).

	Wetland	Shrub	Mixed	Decid	Cult	Conif	Barren
Hg_Log10	0.266	**0.578**	**-0.36**	0.14	**-0.311**	-0.036	**0.453**
	0.093	**0**	**0.021**	0.384	**0.048**	0.821	**0.003**

Table 4.19
Regression coefficients 600 meter distance class (n = 41).

Predictor	Coef	SE Coef	T	P
Constant	-0.3321	0.6043	-0.55	0.586
Wetland	2.131	1.151	1.85	0.073
Shrub	4.803	3.643	1.32	0.197
Mixed	-0.7849	0.3039	-2.58	**0.015**
Decid	0.3083	0.4245	0.73	0.473
Cult	-1.784	1.555	-1.15	0.26
Conif	-0.0793	0.2038	-0.39	0.7
Barren	0.422	1.296	0.33	0.747
Precip	0.01765	0.0161	1.09	0.283

Table 4.20
ANOVA table from 600 meter distance class (n = 41).

Analysis of Variance					
Source	DF	SS	MS	F	P
Regression	8	0.69724	0.08715	4.87	**0.001**
Residual Error	32	0.57215	0.01788		
Total	40	1.26938			

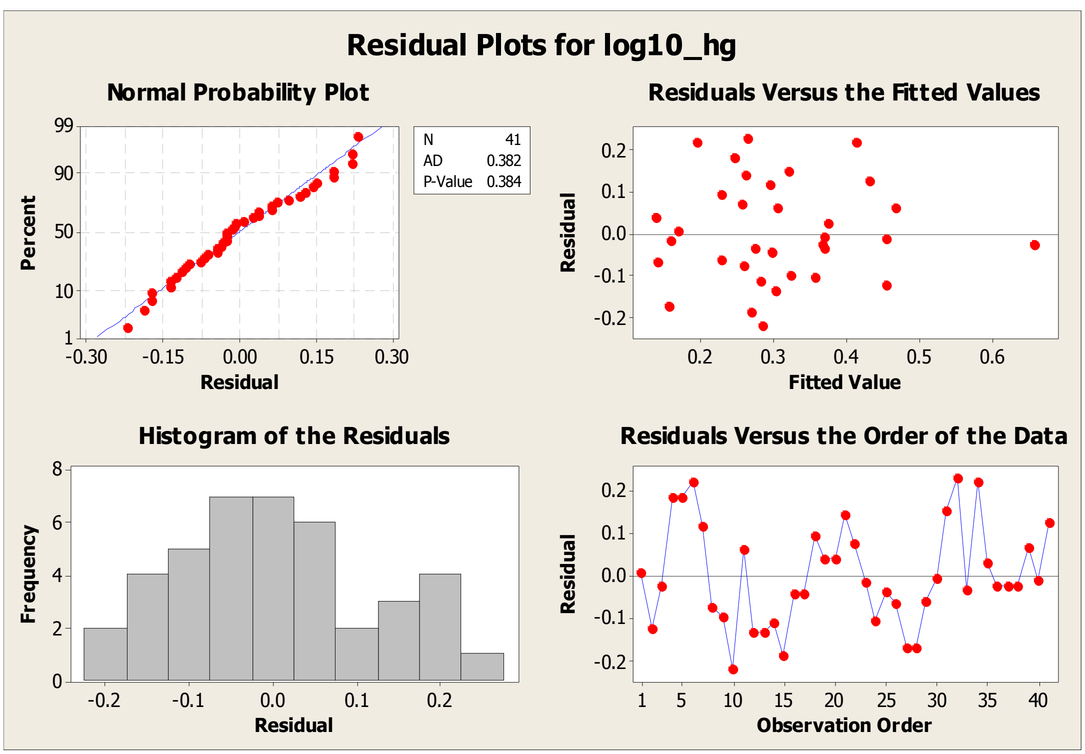

Figure 4.7
Residual plots for the 600 meter distance class (n = 41).

Sensitivity

As was done for the two previous distance classes, the data were subset thirty times in an effort to evaluate the sensitivity of the model in accurately predicting Hg levels in the common loon. The average R^2 for the thirty iterations within the 600 meter distance class was 54.12, which is lower than both the 150 meter and 300 meter distance classes. The standard deviation of the values was 5.76. Of the thirty iterations, 21 fell within 1 standard deviation, and all fell within two standard deviations. Table 4.21 displays the R^2values for the thirty iterations as well as some other supporting statistics.

Table 4.21
Results for the 600 meter distance class from thirty iterations of data subsets.

Iteration	R2	DurbWat
1	52.1	1.66278
2	46.4	1.59727
3	57.5	1.44636
4	63.8	1.37964
5	50.1	1.40566
6	61	1.77311
7	60.1	1.75133
8	43	1.17554
9	51.1	1.74053
10	56.3	2.02131
11	54.9	1.06631
12	58	1.69937
13	59.2	1.44741
14	53.8	1.4798
15	64.9	1.59661
16	46.8	1.9376
17	53	1.49428
18	56.5	1.50657
19	56.8	1.87189
20	49.3	1.58103
21	49	1.83264
22	44.4	1.49349
23	58.4	1.65445
24	49.2	1.67726
25	50	1.84092
26	53.3	1.60806
27	63.6	1.28122
28	49.5	1.63585
29	58.1	1.27587
30	53.4	1.56219

4.4.2 Discussion: 600 meter Distance Class

Correlation

Within the 600 meter distance class (n = 57) we find that all four of the variables noted as significant earlier, either in the correlation matrices, or in the regression equation are still significant. Wetlands (0.385, p-value < 0.05), shrub land (0.492, p-value < 0.001), cultivated land (-0.299, p-value < 0.05), and barren land (0.263, p-value < 0.05) exhibit similar relationships to those found in both the 300 meter and 150 meter distance classes. Within the subset data I found that wetlands are again not significant (0.266, p-value > 0.05). Cultivated land (0.311, p-value < 0.05), shrub land (0.578, p-value < 0.001), and barren land (0.453, p-value < 0.05) are found to be significant. Of interest is the negative relationship found with mixed forest (-0.36, p-value < 0.05) indicating that at this level mixed forest types exhibit an inverse relationship with Hg in Common Loon blood.

Regression

Similarly to the 300 meter distance class and the 150 meter distance class, the regression model developed for all the samples (n = 57) and the regression models developed for each of the thirty subsets were analyzed to determine if the assumptions of least squares regression were met, as well as to determine the ability of the model to predict Hg blood levels in the Common Loon. The tables of regression coefficients, t-values, and p-values from Chapter 4 show marked differences between those for the 150 meter distance class and the 300 meter distance class. When using all of the samples we find that wetland (p-value < 0.05), shrub land (p-value < 0.001), and barren land (p-value < 0.05) exhibit some level of significance. From the initial subset of the data I found that only one variable in the model exhibited a p-value less than the 0.05 confidence level. This variable was mixed forest. In both cases the p-value from the analysis of variance tables show significance, however, additional problems can be found upon further investigation.

Analysis of the residuals further suggests the model is not adequate. The residual plots generated from using all of the data show that the residuals are not normally distributed (p-value < 0.05), thus violating the assumption that residuals should exhibit a normal distribution. I also found that there is a clustering of the residuals versus the fitted values between the 0.2 and 0.4 range. Within the initial subset of the data I found that the residuals meet the normal distribution requirements (p-value > 0.05) and appear to be randomly distributed versus the fitted values. Because at least one of the two models shows robustness in the residuals all thirty were run. Marked differences exist in the individual iterations with regards to residual distribution and normality.

Sensitivity

At this distance class the model is again sensitive to both the selection of the points in regards to being well fit as well as in selection of the points in regards to its predictive capabilities. In all cases there was not a presence of autocorrelation in the residuals as noted by the Durbin-Watson statistics. In many cases, one or more of the assumptions of least squares regression were violated. This suggests that this distance class is inadequate at accurately predicting Hg levels in Common Loon blood as a function of land cover type. In many cases there was a clumping of the residuals versus the fitted values, or the normal distribution requirements of the residuals was not met.

Conclusions

This distance class is not suitable for predicting Hg levels in Common Loon blood. Many assumptions of least squares regression are violated when attempting to fit a model. It is much more sensitive in point selection when using a subset of the samples, and in some cases, variables known to be significant per previous research are found not to be (wetlands, for example), while others not known to be significant are identified as such (mixed forest). This further supports the hypothesis that those variables considered to be significant per previous research as well as those found to be significant in this study exhibit a stronger influence if they are closer to the individual territory.

4.5 Overall Conclusions: 150 meter, 300 meter, 600 meter

Marked differences exist between the 150 meter, 300 meter, and 600 meter distance classes. The differences found between the R^2 values, adjusted R^2 values, and predicted R^2 values for each of the distance classes when using all of the samples (n = 57) (Table 5.1) indicates that the 150 meter distance class more accurately models Hg in the Common Loon. If a model is well fit there should be little variation between the three R^2 values produced by the model. The increase in the R^2 value for the 600 meter distance class was slightly higher than the R^2 value for the 300 meter distance class. The slight increase n the R^2 value for the 600 meter distance class represents an increase in percentage of the positively correlated variables included in the model, potentially because the 600 meter buffers extend into another territories 150 meter buffer picking up significant variables that do not truly contribute to increased levels in the actual territory. In all cases there is not a substantial difference between the three, however, the model is more robust at the 150 meter distance class. In all cases the R^2 values were computed based on a revised model (Table 4.22) using only the four variables found to be significant throughout the analysis.

Table 4.22. R^2 Values for each distance class. The four variables used in the revised model were wetlands (positive relationship), shrub land (positive relationship), barren land (positive relationship), and cultivated land (negative relationship).

	150 meter	**300 meter**	**600 meter**
R^2	55.2	44.6	46
Adjusted R^2	51.7	40.3	41.7
Predicted R^2	49.51	36.33	36.83

The final regression equations used are presented below for each of the three distance classes.

At 150 meters the regression equation is:

$$HG\_Log = 0.290 + 1.89\ WT + 55.0\ SB - 7.05\ CT - 3.03\ BN$$

At 300 meters the regression equation is:

$$Hg\_Log = 0.284 + 2.39\ WT + 15.4\ SB - 3.99\ CT - 2.73\ BN$$

At 600 meters the regression equation is:

$$HG\_Log = 0.272 + 2.42\ WT + 13.9\ SB - 2.20\ CT - 2.56\ BN$$

where:

Hg_Log = the log-transformed mercury levels in the Common Loon blood samples.

WT = the percent of wetlands within the buffer

SB = the percent of shrub land within the buffer

CT = the percent of cultivated land within the buffer

BN = the percent of barren land within the buffer

In addition to the discrepancies found among the R^2 values there are other assumptions that need to be met. The issue of multicollinearity between pairs of independent variables should be addressed any time least squares regression is used. An idea of the significance of multicollinearity can be assessed through analysis of the variance inflation factors (VIF) for each of the three distance classes. In both the 150 meter and 300 meter distance classes the VIF's for each of the four variables was below three. MiniTab suggests that if the VIF's are greater than 5.0, the regression coefficients are poorly estimated. The 600 meter distance class exhibits higher VIF's (> 3) indicating that there is more likelihood that multicollinearity exists between two or more of the independent variables. In no case did MiniTab provide a warning that multicollinearity was an issue, because none of the individual VIF's for the independent variables was above the critical value of 5.0.

In order to determine if the estimated values were significantly different from the measured values, an F-test was used to determine whether equal variance existed around the means, an assumption of parametric tests. Once equal variance was determined, a two sample t-test was used to check whether the two sets of values were significantly different. At 150 meters the F-test was significant (Test statistic = 1.37, p-value > 0.05) since the p-value was above the confidence interval of 95%. The t-test showed that the two sets of values did not vary either, with a confidence interval that spans zero (-0.243867, 0.373320) and a test-statistic and p-value that were significant (t-value = 0.42, p-value > 0.05, DF = 112). At 300 meters the F-test was barely significant (Test statistic = 1.69, p-value = 0.053) at the 95% confidence interval. The resulting t-test showed that the two values did not vary, with a confidence interval that spans zero

(-0.214204, 0.386593) and a test-statistic and p-value that were significant (t-value = 0.57, p-value > 0.05, DF = 112). Due to the f-test results there should be some concern over the validity of the results. At 600 meters we find results that are dissimilar to those from the 300 meter distance class. The F-test was significant (Test statistic = 1.57, p-value > 0.05) and therefore meets the parametric assumptions of equal variance. Results from the two sample t-test were significant showing a confidence interval that spans zero (-0.219995, 0.379992) and acceptable values for the t-test (t-value = 0.53, p-value > 0.05, DF = 112).

Overall, the 150 meter distance class is more robust at predicting Hg levels in Common Loon blood when compared with the percentage of land cover classes within particular distances. This supports the hypothesis that those land cover types that are known to contribute to increased MeHg and Hg exhibit stronger influence if they are closer to the individual loon territory. This also supports research done by Zillioux et al. (1993) who suggested that only a small portion of the Hg deposited through atmospheric deposition actually makes it to the water body, thus much of the Hg available will be deposited either directly into the water, or in the immediate vicinity of the water.

4.6 GIS Implementation/Output

Incorporation of the resulting fitted values back into the GIS required several steps. This was completed using the model developed for all samples within the 150 meter distance class. First, in order to restrict the resulting raster layer to the extent of the lakes within the study area, the percentage of individual land cover types were calculated per loon territory. The resulting raster layers were then incorporated into the regression equation using the Raster Calculator available in ArcGIS Spatial Analyst. Results from the final output were anti-logged for display purposes and to allow for ranking based on risk levels, as specified by Evers et al., 2003. This also allows for assessment of the difference between the fitted values and the measured values (residuals) as a function of lake size. This allowed for further comparison to determine how well the fitted values estimate rank in regards to risk level and also allows for investigation into those lakes that the model may not perform as well in. Figures 5.1 and 5.2 show the resulting output from the Raster Calculator. Overall, at 150 meters the model appears to represent Hg levels in Common Loon blood with reasonable accuracy. As mentioned earlier, the largest variation in residuals was found on the smaller lakes. The largest residual was found on the northern end of Lake Aziscohos and is circled in Figures 5.1 and 5.2. It is thought that the high Common Loon blood Hg level associated with this territory is influenced by a contributing point source, and therefore not surprising that it represents the largest error.

Overall, the model presents a reasonable estimate of Hg levels in Common loon blood and fits even better when those levels are categorized based on risk level (0-1 = low, 1.1-3 = moderate, 3-4 = high, and >4 = extra high). Risk categories were developed by BRI and can be found in Evers et al. (2003). When incorrect, the model overestimated by one rank class in most cases. The largest error is again found in the northern end of Lake Aziscohos (Figure 5.2 C., circled in red) where the risk category was off by 2 classes. Again, this is an area believed to be influenced by a point source.

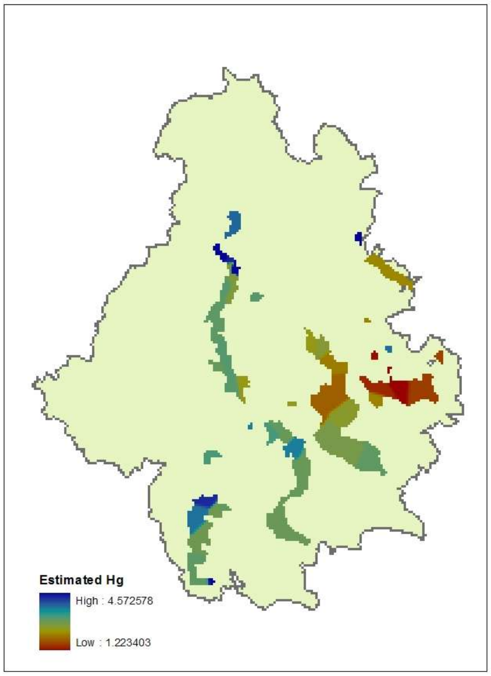

A.

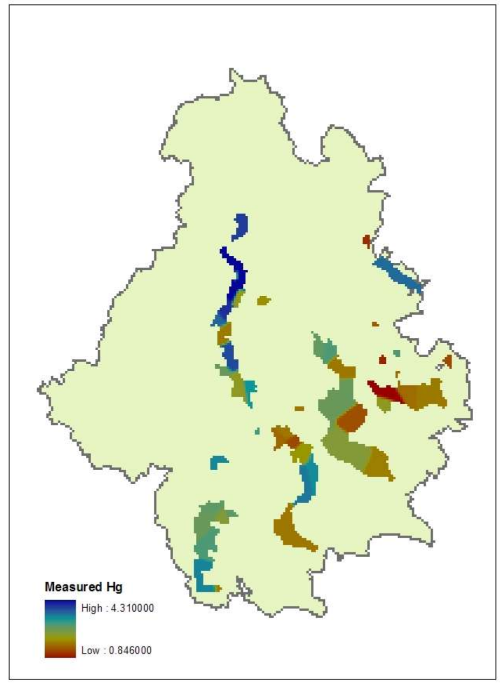

B.

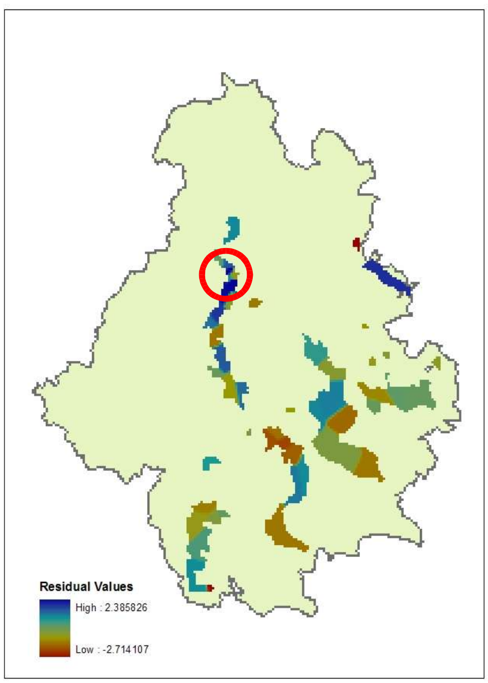

C.

Figure 4.8. Results implemented in the GIS. **A.** Estimated values based on the regression equation, implemented in the GIS, **B.** Measured values of Hg from the loon sample locations displayed as a function of territory, and **C.** Residuals from the analysis implemented to provide information on error variance.

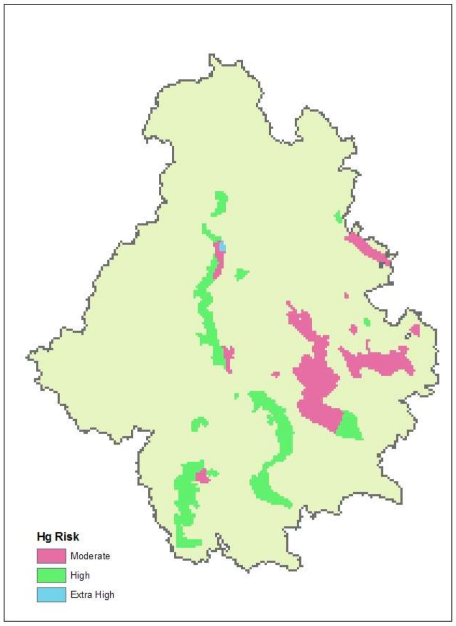

A.

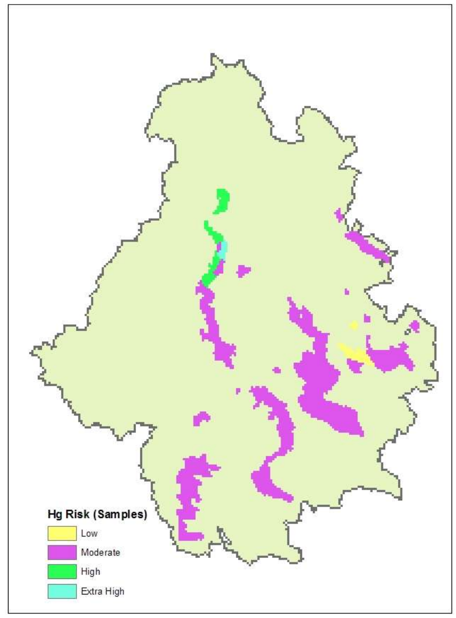

B.

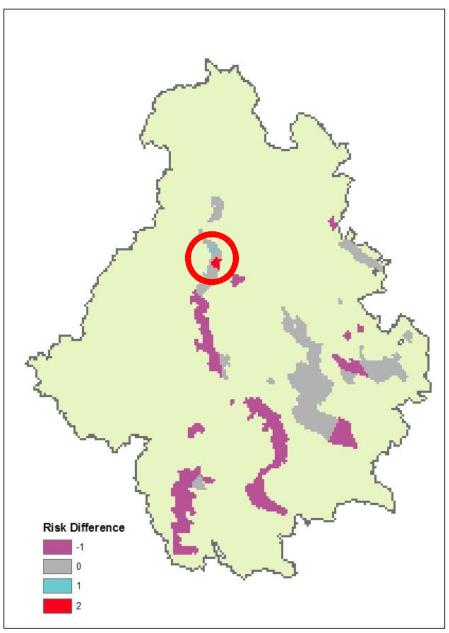

C.

Figure 4.9.
A. Estimated Risk based on the regression equation, implemented in the GIS, **B.** Risk categories calculated from the loon samples displayed as a function of territory, and **C.** the difference between the ranked groups. Note the red value in the upper center portion of the third map (circled in red). This represents the territory on Lake Aziscohos that may be influenced by a point source of Hg.

Chapter 5: Conclusions and Discussion

5.1 Conclusions

Chapter five will tie together the results of this thesis in the context of the previous research done and in regards to the hypotheses stated in chapter one. In many cases, the variables found to be significant in this study were also noted in previous research and will be discussed below. This work provides insight into some of the land cover types that contribute to increased Hg and MeHg and the spatial relationship they have with blood Hg levels in the Common Loon. The most notable find is that as the percentage of wetlands within close proximity to a loon territory increases there will likely be an increase in the Hg that is available to the loon in that territory and result in increased blood Hg levels. The three major hypotheses of this thesis are listed below.

1. Much of the current research addresses Hg bioaccumulation at a watershed level. Substantial variability, however, can exist within a particular watershed. This being the case, by looking at the problem from a larger scale and analyzing the relationships that exist within certain proximities of individual loon territories, we should be able to better explain Hg risk as a function of land cover characteristics.
2. If a reasonable model can be produced, we should see a marked drop-off in accuracy of the model as we move further from the territory boundary.
3. If a reasonable model can be produced, we should gain a clearer understanding of the impact certain land cover types can have on the availability of Hg and the associated risk to hydrologic systems as a function of distance from the individual boundary.

The model results indicate that the proximity of the contributing land cover types influence the rate at which Hg is available to the Common Loon, and that as you move further away from the loon territory these factors become less significant. This suggests that a smaller scale approach, such as a watershed scale, may not be as valid or as robust as analyzing the land cover at a larger scale, such as those areas immediately adjacent to the territory in question. Research by Zillioux et al. (1993) showed that not all of the Hg deposited in a watershed actually makes it into the water body. It would follow that the Hg deposited closer to a loon territory is more likely to become available to the loons within that territory. In the context of this research, there should be an increase in loon blood Hg as you increase the amount of wetlands and shrub land within 150 meters of the loon territory. Conversely, there should be a decrease in the available Hg if there are high concentrations of cultivated land or barren land within 150 meters.

Of the four independent variables used in the model, wetlands and cultivated land are documented in previous work as significant (Vermont Department of Environmental Conservation, 1998, Burgess, 1998, Kamman et al, 2004). Shrub land and barren land have not been previously documented as significant. Within the study area there is very little land cover that is either barren or shrub. In some cases these could be misclassified wetlands, or coincidental. These relationships should be explored further.

As expected, there was a decrease in both the robustness of the model and the validity of the model as you move further from the loon territories. The model based on the 150 meter buffer exhibited the strongest R^2 values and generally met the assumptions of least squares regression, indicating that wetlands, shrub lands, cultivated lands, and barren lands within 150 meters of the loon territory in question will have a far greater influence on the amount of available Hg than those that are located farther away.

At both the 300 meter distance class and the 600 meter distance class there is some concern that variables from the adjacent territories, significant at 150 meters, are being incorporated into the analysis. Overlap between the buffered areas, particularly within the 600 meter distance class has the capability of incorporating land cover types that are up to and possibly over a half of a kilometer away. For this reason, there should be concern over using this distance class for any detailed analysis of Hg in Common Loon blood, and further validates the notion that the closer the source of Hg the more likely it will make it into the hydrologic system.

This research provides a new method for analyzing the inter-lake variability of Hg that can exist in the Common Loon. It provides a sound method for segmenting lakes in an effort of understanding those factors that contribute to inter-lake loon Hg variability, and the relationships found through this research should be explored further.

5.2 Uncertainty

As with any research that addresses environmental phenomena, error in the analysis should be addressed. In the case of this study several aspects of uncertainty exist and should be discussed. The use of the NLCD data restricted the analysis of land cover to a 30 meter cell size resolution, covering approximately 900 square meters on the ground. In addition, the most recent NLCD data for the study area was from 1992, though not much has changed in the study area due to its location and accessibility. The starting point of 150 meters for the analysis was chosen in order to obtain a buffer that was at least five cells in depth.

In regards to loon territories, it was difficult to accurately delineate them. The use of thiessan polygons was chosen in an attempt to automate the delineation of loon territories and though they do not truly represent the actual territory boundary, they provide a reasonable estimate, from the scope of this thesis, of the contributing areas. It should again be noted that thiessan polygons do not truly reflect the spatial extent of the territories.

Due to the time and effort required to collect loon blood Hg samples, the samples used in this thesis span several years. This temporal difference in samples may not truly reflect the current amounts in the loons.

5.3 Future Work

Based on what was found in this study, the next step would be to incorporate water quality variables known to influence Hg availability such as dissolved organic carbon (DOC), total alkalinity, total phosphorous, and total nitrogen content. These variables should be collected per loon territory and used in conjunction with the land cover variables found to be significant within 150m of the individual territories. In addition, future work should attempt to delineate a more accurate and up to date land cover map utilizing a finer cell size resolution. This would allow for analysis within a closer distance of the loon territories. For example, start at 60 meters and work out to 150 meters. Additionally, the buffers could be extended up the contributing streams to account for the percentage of wetlands, croplands, shrub lands, and barren lands that are adjacent to the contributing streams. Further analysis of the impact of certain land use activities such as logging should also be considered as clear-cutting has the potential to increase over-land flow of water, and thus potentially increasing Hg, to and from the territories. It would also be prudent to check the validity of the methods against an adjacent set of lakes where samples are available such as the Flagstaff Lakes area of Maine. Application of these methods at a statewide level would also be another avenue to explore.

References

Air Quality Conference, Status of Mercury and Particulate Matter R&D, CATM Newsletter. Volume 5, Issue 1, 1999

Bishop, K., Lee, Y., Pettersson, C. and Allard, B. Methylmercury Output from the Svartberget Catchment in Northern Sweden During Spring Flood. Water, Air, Soil Pollution. Vol. 80, 445-454, 1995.

Burger, J. "Heavy metals in the eggs and muscle of horseshoe crabs (*Limulus polyphemus*) from Delaware Bay." Environmental Monitoring and Assessment 46, 279–287, 1997a

Burger, J. " Heavy Metals and Selenium in Herring Gulls (*LarusArgentatus*) Nesting in Colonies from Eastern Long Island to Virginia, Environmental Monitoring and Assessment 48**:** 285–296, 1997b

Burgess, Neil M., Mercury in Atlantic Canada: A Progress Report, 1998.

Burrough, Peter and McDonnell, Rachael. Principles of Geographic Information Systems, 2000, Oxford University Press Inc., New York, pg. 114.

Delta Tributaries Mercury Council.(DTMC), Strategic Plan for Mercury Risk in the Sacramento River Watershed., Appendix 4 Mercury Models Report, Oct 2002.

Driscoll, C. T., J. Holsapple, C. L. Schofield, and R. Munson. The Chemistry and Transport of Mercury in a Small Wetland in the Adirondack Region of New York, USA. Biogeochemistry 40: 137-146, 1998.

Evers, D.C., O.P. Lane, C. DeSorbo, L. Savoy. 2002. Assessing the impacts of methylmercury on picivorous wildlife using a wildlife criterion value based on the Common Loon, 1998 – 2001. Report BRI 2002-08 submitted to the Maine Department of Environmental Protection. BioDiversity Research Institute, Falmouth. Maine.

Evers, D.C., D. Yates, and L. Savoy. 2002. Developing a mercury exposure profile for mink and otter river in Maine. Report BRI 2002-10 submitted to the Maine Department of Environmental Protection and Maine Inland Fisheries and Wildlife. BioDiversity Research Institute, Falmouth. Maine.

Evers, Dave and O Lane. 2000. Assessing methylmercury availability in Maine's aquatic systems with the Belted Kingfisher, 1998-99. BRI Report submitted to Surface Water Ambient Toxic Monitoring Program. BioDiversity Research Institute, Falmouth. Maine.

Evers, D. 2002. Aspects of hydrological impacts on the Common Loon at Lake Umbagog. BRI Report 2002-09 submitted to U.S. Fish and Wildlife Service 1976 – 1999. BioDiversity Research Institute, Falmouth, Maine.

Faust, S.D. & Aly, O.M. Chemistry of Natural Waters. Ann Arbor, MI: Ann Arbor Science Publishers, Inc. pp 359–380, 1981.

Golet WJ, Haines TA. Snapping turtles (*Chelydra serpentina*) as monitors for mercury contamination of aquatic environments. Environmental Monitoring and Assessment 71:211-20, 2001.

Kamman, Neil C., Engstrom, Daniel R., Historical and present fluxes of mercury to Vermont and New Hampshire lakes inferred from ^{210}Pb dated sediment cores. Vermont Department of Environmental Conservation, November 2001.

Kamman, Neil C., Loray, P. M., Driscoll, C. T., Estabrook, R., Major, A., Pientka, B., Glasford, E. Assessment of Mercury in Waters, Sediments and Biota of New Hampshire and Vermont Lakes, USA, Sampled Using a Geographic Randomized Design. Environmental Toxicology and Chemistry, In Press, 2004.

Kenow, Kevin P., Gutreuter, S., Hines, R.K., Meyer, M.W., Fournier, F., Karasov, W.H. Effects of Methyl Mercury Exposure on the Growth of Juvenile Common Loons. Ecotoxicology, Vol. 12, pp. 171-182, 2003.

Krabbenhoft, D.P., J.M. Benoit, C.L. Babiarz, J.P. Hurley, and A.W. Andren. 1995. Mercury cycling in the Allequash Creek watershed, Northern Wisconsin. Water Air Soil Pollut. 80:425–433.

Lee, Y., Bishop, K., Munthe, J., Iverfeldt, A., Verta, M., Parkman, H. and Hultberg, H. An examination of current Hg deposition and export in Fenno-Scandian catchments. Biogeochem, Vol. 40, 125-235, 1998.

Mississippi Department of Environmental Quality, Escatawpa River Phase One Total Maximum Daily Load for Mercury, 2000.

Peckenham, J., S. Kahl, and B. Mower, Background Mercury Concentrations in River Water in Maine, U.S.A., Environmental Monitoring and Assessment. 89: 129 - 152, 2003

Rencz, A. N., N. J. O'Driscoll, G. E. M. Hall, T. Peron, K. Telmer, amd N. M. Burgess, Spatial Variation and Correlations of Mercury Levels in the Terrestrial and Aquatic Components of a Wetland Dominated Ecosystem: Kejimkujik Park, Nova Scotia, Canada. 143: 271 - 288, 2003.

Thompson, D.R., Mercury in Birds and Mammals, Environmental Contaminants in Wildlife: Interpreting Tissue Concentrations, pp. 341-356, 1996.

Tremblay, A., L. Cloutier, and M. Lucotte. 1998. Total mercury and methylmercury fluxes via emerging insects in recently flooded hydroelectric reservoirs and a natural lake. Sci. Total Environ. 219: 209-221.

USEPA., Mercury Study Report to Congress, Volume 1: Executive Summary. United States Environmental Protection Agency, Washington DC. More information available at:

http://www.epa.gov/oar/mercury.html, 1997.

USEPA, Mercury Maps: A Quantitative Spatial Link Between Air Deposition and Fish Tissue. 2001.

USGS, Mercury Contamination of Aquatic Ecosystems. Fact Sheet FS-216-95, 1995.

Vaidya, O. C. and G. D. Howell. Interpretation of Mercury Concentrations in Eight Headwater Lakes in Kejimkujik National Park, (Nova Scotia, Canada) By Use of a Geographic Information System and Statistical Techniques. Water, Air, and Soil Pollution 134: 165-188, 2002.

Vermont Department of Environmental Conservation, Inputs, Methylation, Transformation, and Historical Accretion of Mercury in Northern Freshwater Lakes. 1998.

Wolfe, M. F., Steven Schwarzbach, and Rini A. Sulaiman. Effects of mercury on wildlife: a comprehensive review. Environmental Toxicology and Chemistry 17(2), 146-160, 1998.

Zillioux, E. J., D. B. Porcella, J. B. Benoit. Mercury Cycling and Effects in Freshwater Wetland Ecosystems. Environ. Toxicol. Chem. 12:2245 - 2264, 1993.

Appendix A. Residuals Plots from Sensitivity Analysis

1.

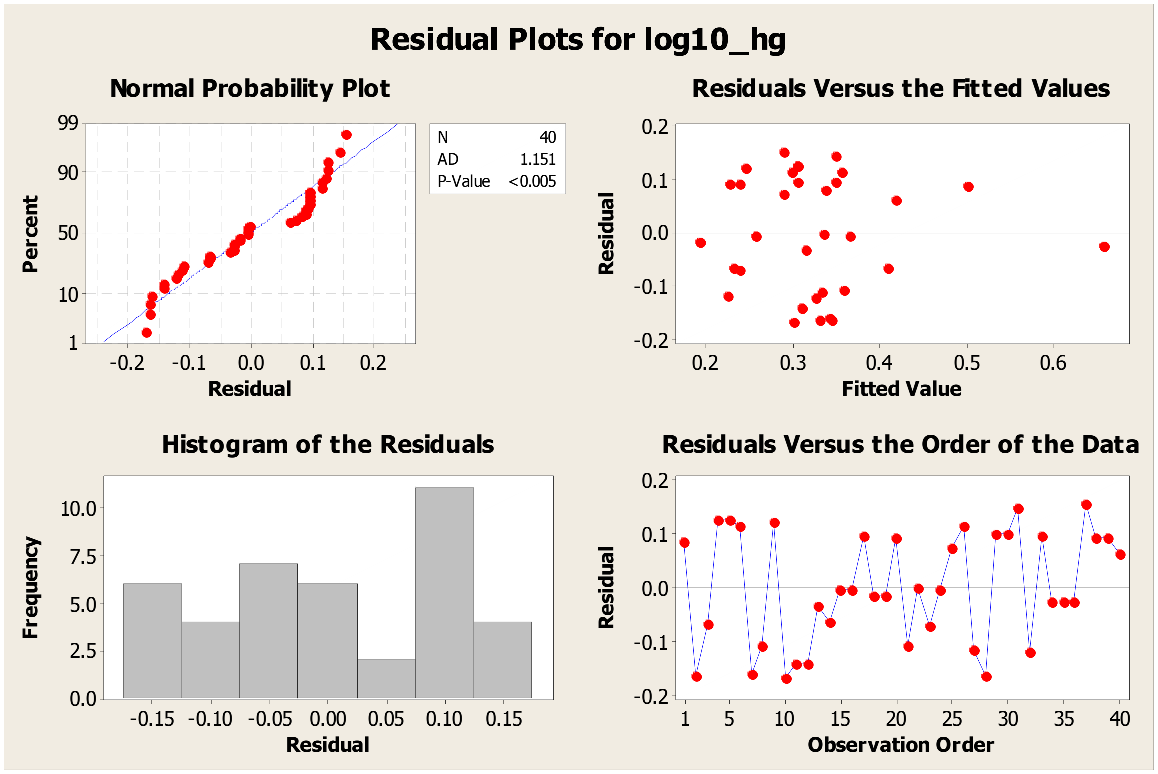

2.

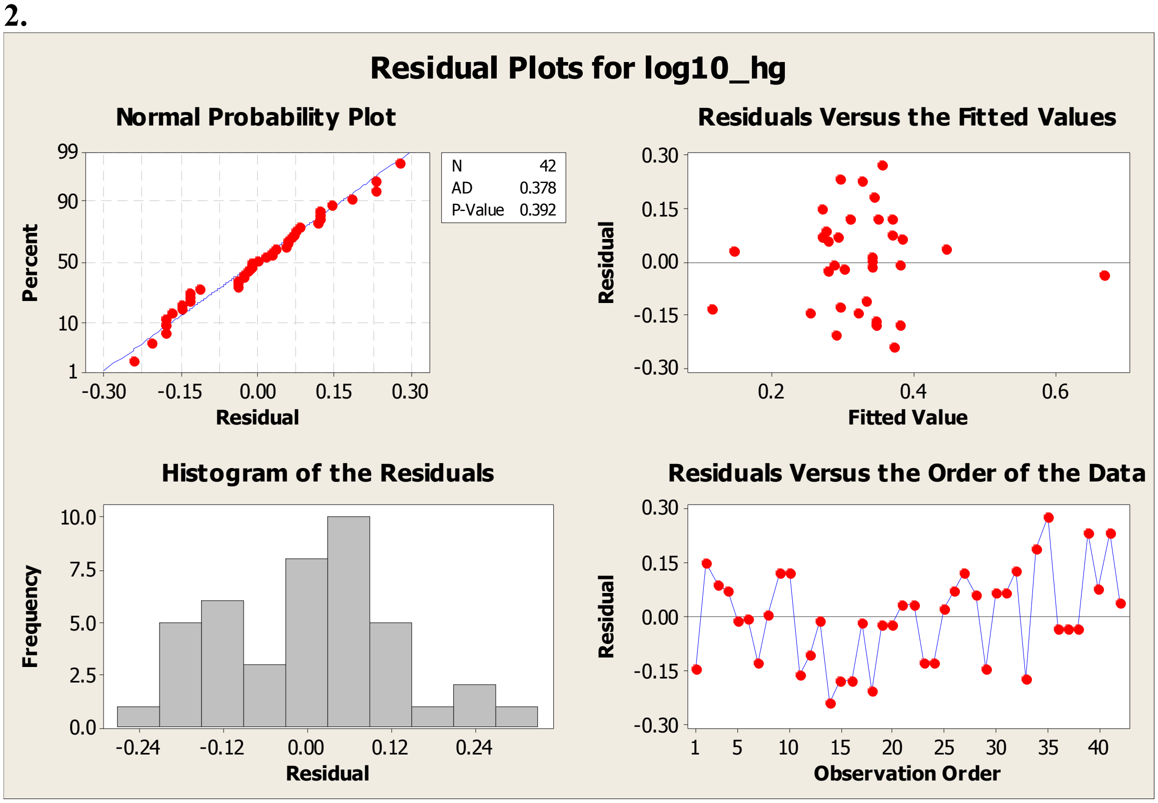

3.

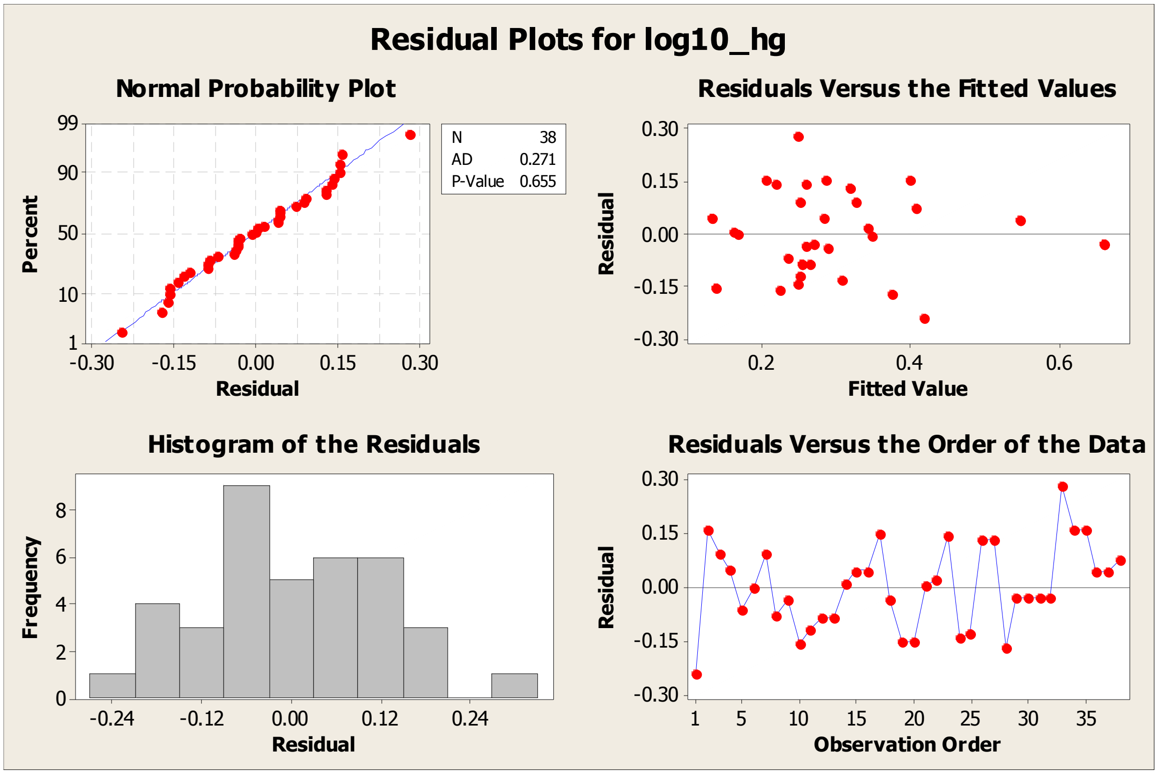

Residual Plots for log10_hg
Normal Probability Plot
Residuals Versus the Fitted Values
N 38
AD 0.271
P-Value 0.655
Percent
Residual
Fitted Value
Histogram of the Residuals
Residuals Versus the Order of the Data
Frequency
Observation Order

4.

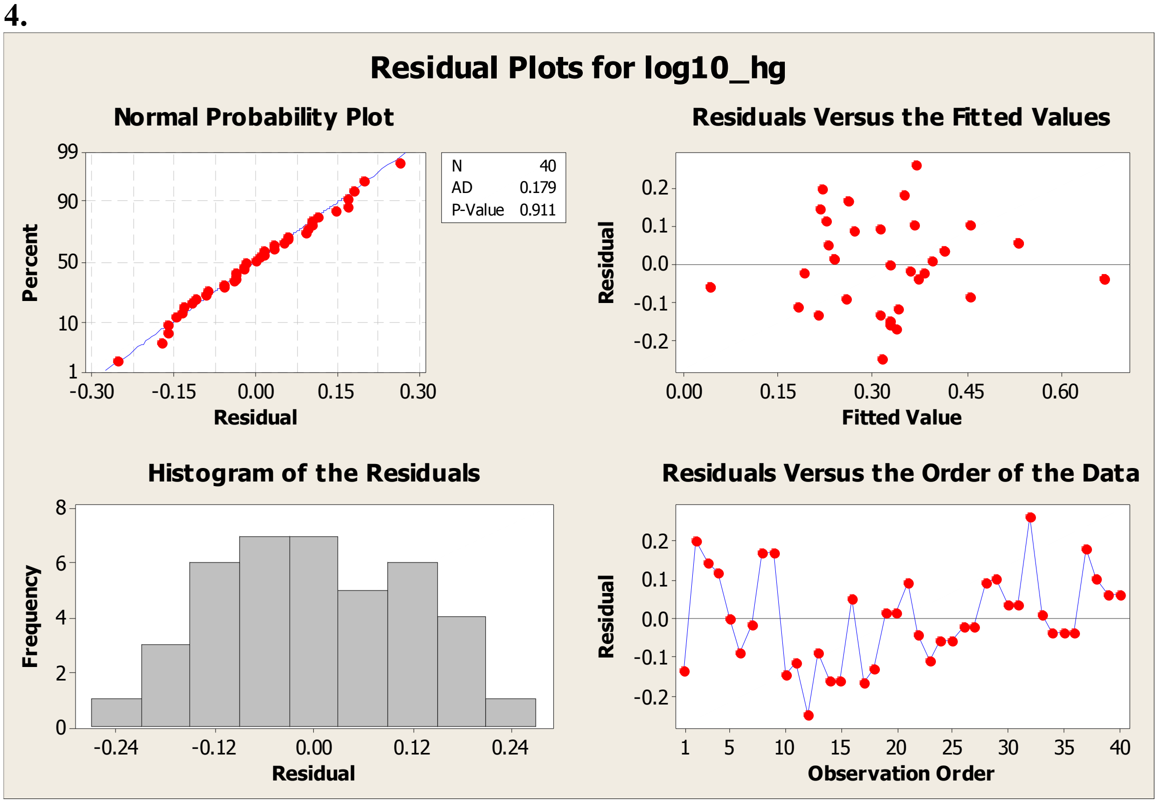

Residual Plots for log10_hg
Normal Probability Plot
Residuals Versus the Fitted Values
N 40
AD 0.179
P-Value 0.911
Percent
Residual
Fitted Value
Histogram of the Residuals
Residuals Versus the Order of the Data
Frequency
Observation Order

5.

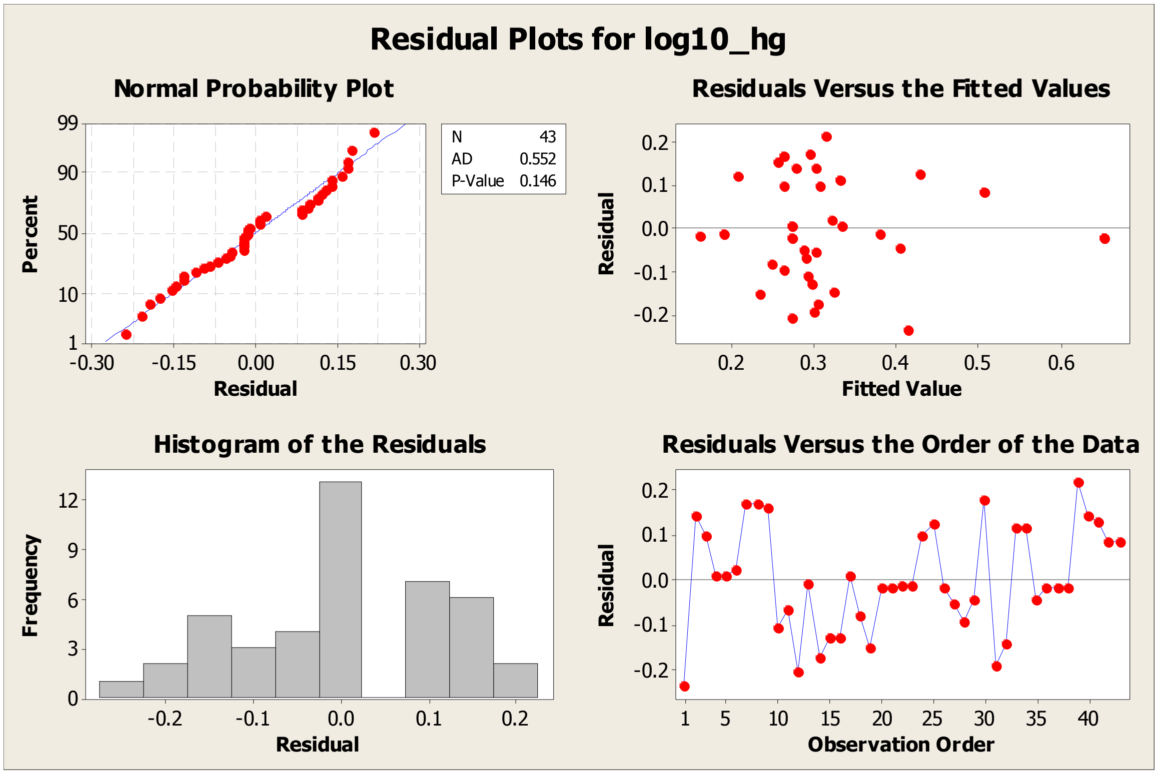
Residual Plots for log10_hg
Normal Probability Plot
Percent
Residual
N 43
AD 0.552
P-Value 0.146
Residuals Versus the Fitted Values
Residual
Fitted Value
Histogram of the Residuals
Frequency
Residual
Residuals Versus the Order of the Data
Residual
Observation Order

6.

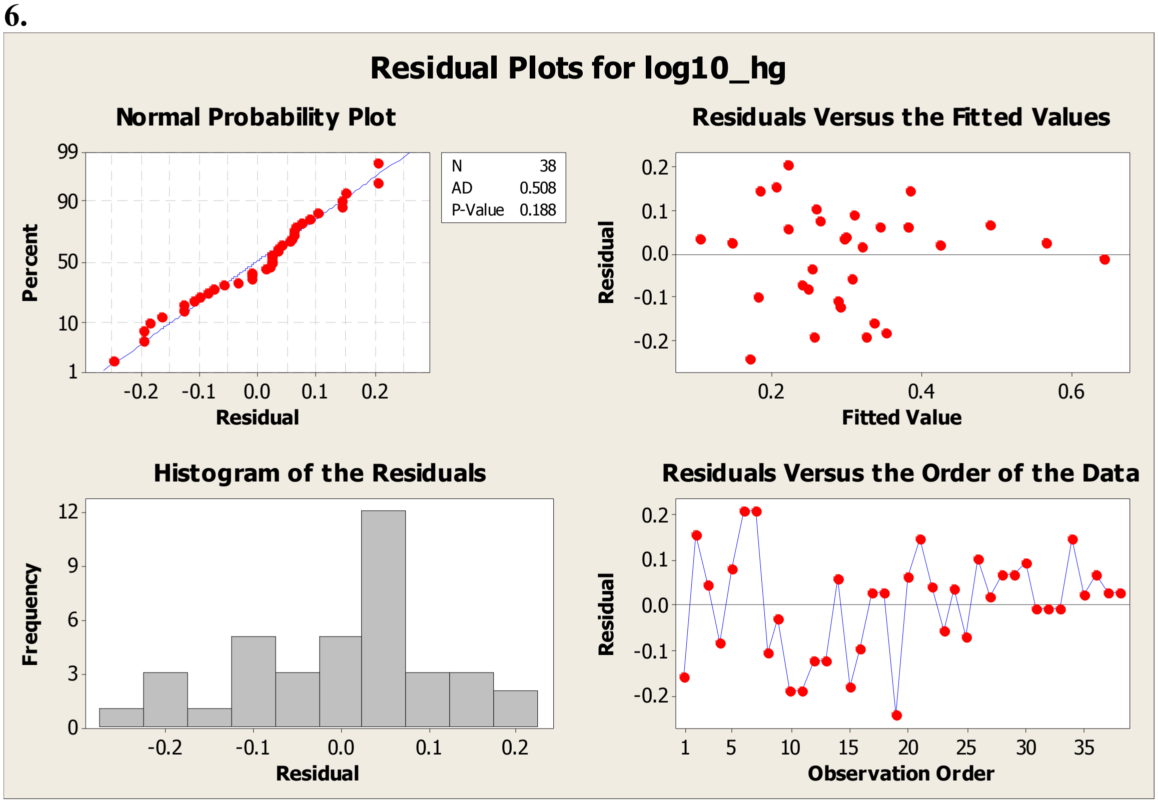
Residual Plots for log10_hg
Normal Probability Plot
Percent
Residual
N 38
AD 0.508
P-Value 0.188
Residuals Versus the Fitted Values
Residual
Fitted Value
Histogram of the Residuals
Frequency
Residual
Residuals Versus the Order of the Data
Residual
Observation Order

7.

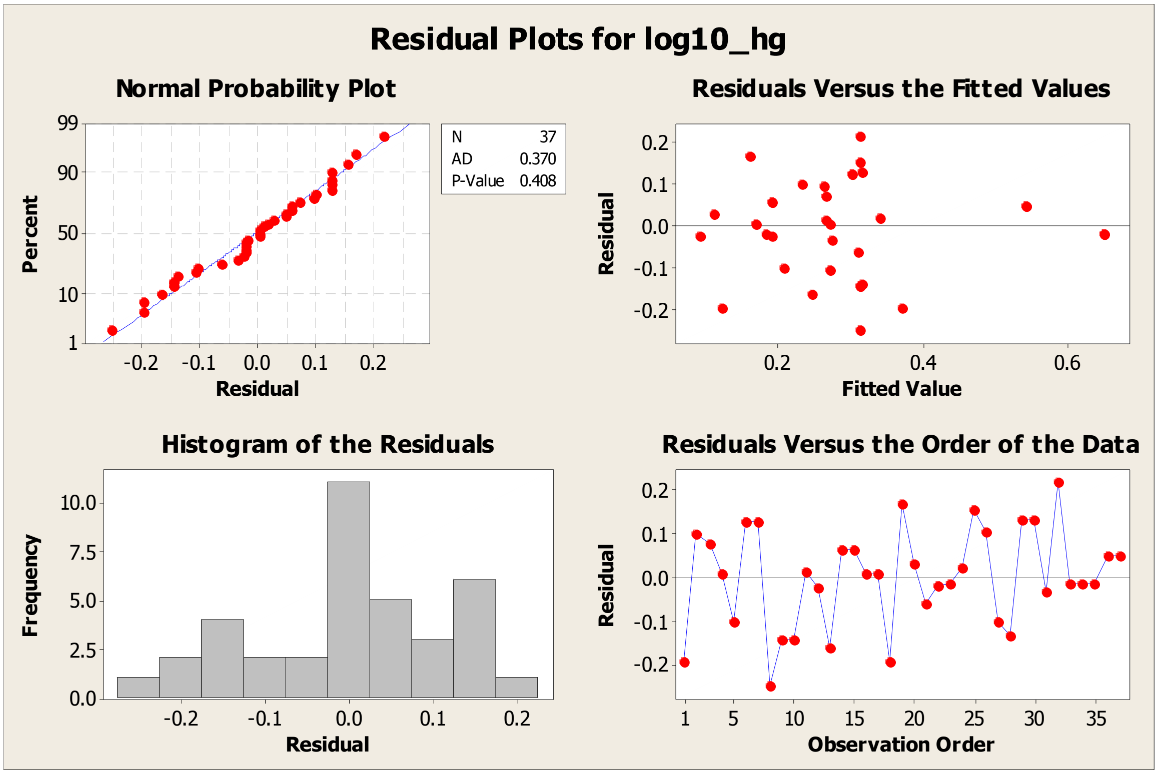
Residual Plots for log10_hg
Normal Probability Plot
Percent
Residual
N 37
AD 0.370
P-Value 0.408
Residuals Versus the Fitted Values
Residual
Fitted Value
Histogram of the Residuals
Frequency
Residual
Residuals Versus the Order of the Data
Residual
Observation Order

8.

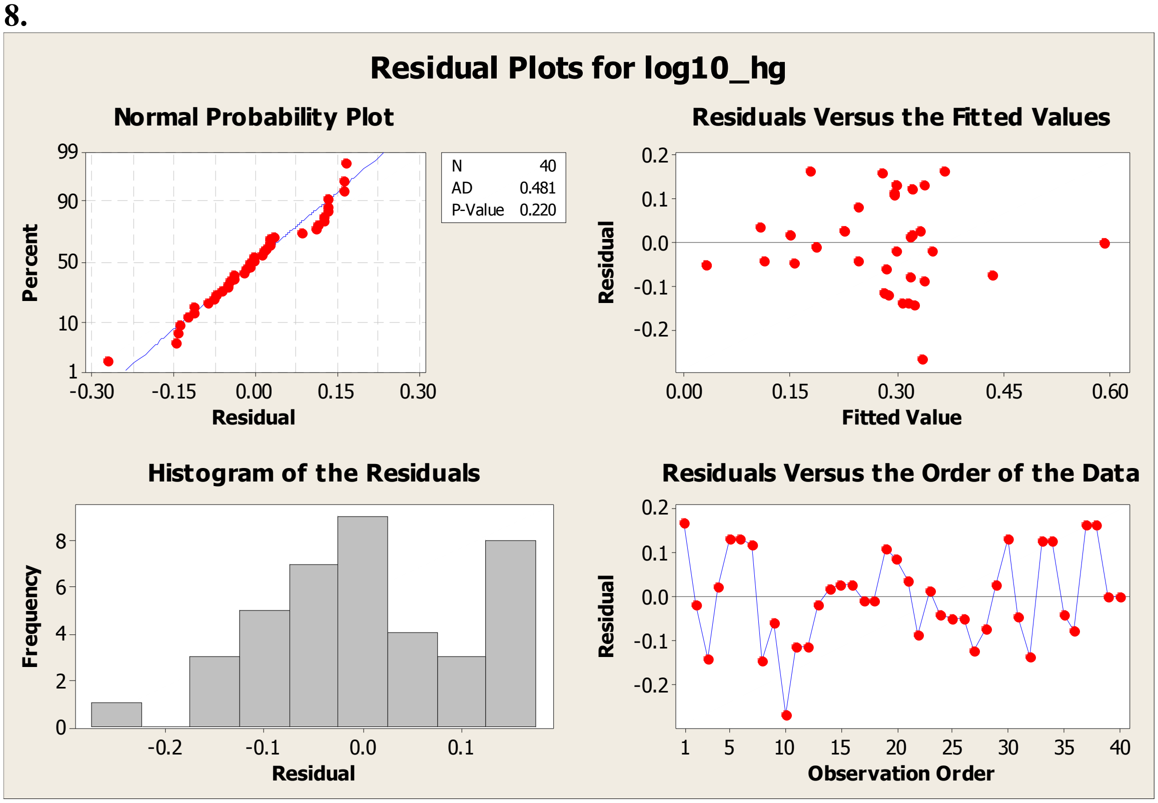
Residual Plots for log10_hg
Normal Probability Plot
Percent
Residual
N 40
AD 0.481
P-Value 0.220
Residuals Versus the Fitted Values
Residual
Fitted Value
Histogram of the Residuals
Frequency
Residual
Residuals Versus the Order of the Data
Residual
Observation Order

9.

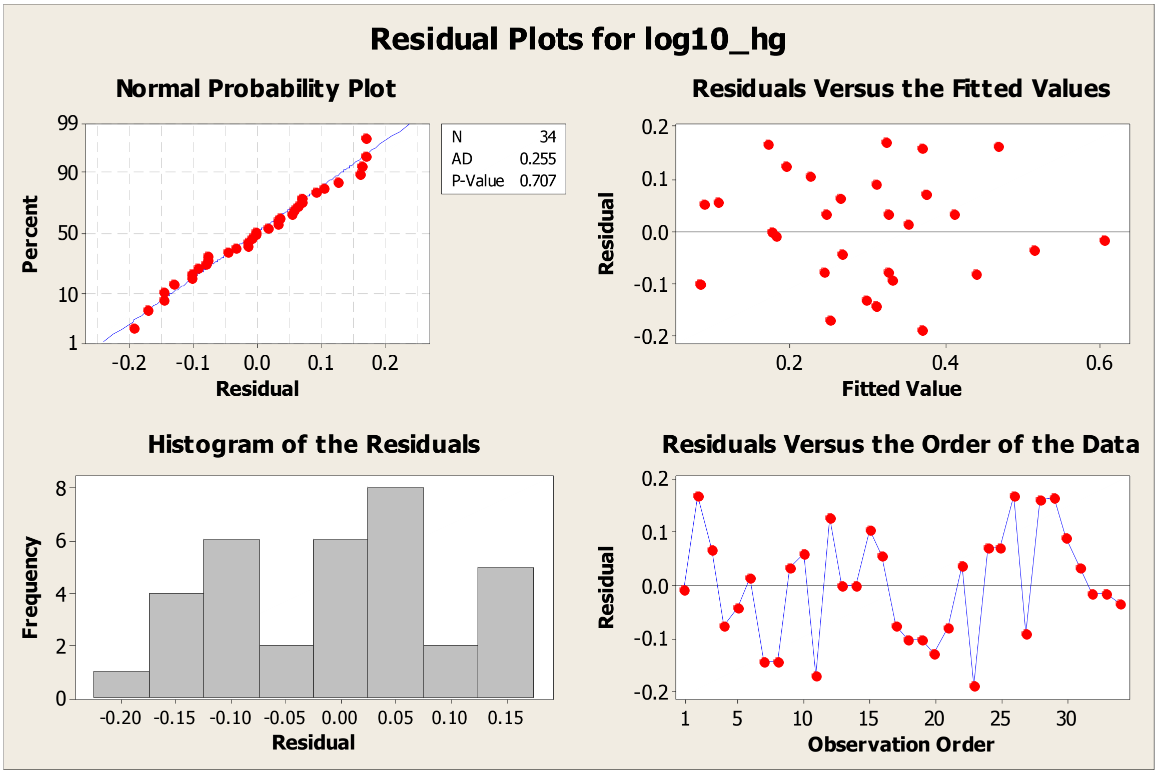
Residual Plots for log10_hg
Normal Probability Plot
Percent
Residual
N 34
AD 0.255
P-Value 0.707
Residuals Versus the Fitted Values
Residual
Fitted Value
Histogram of the Residuals
Frequency
Residual
Residuals Versus the Order of the Data
Residual
Observation Order

10.

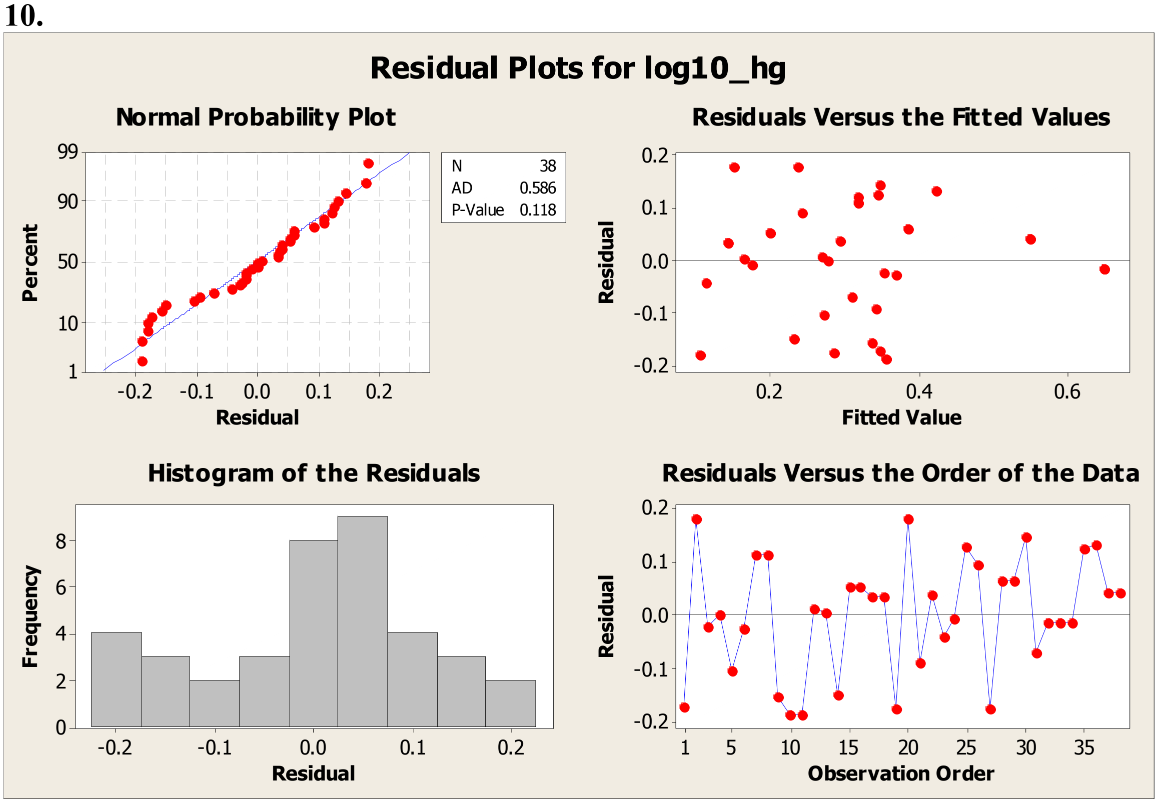
Residual Plots for log10_hg
Normal Probability Plot
Percent
Residual
N 38
AD 0.586
P-Value 0.118
Residuals Versus the Fitted Values
Residual
Fitted Value
Histogram of the Residuals
Frequency
Residual
Residuals Versus the Order of the Data
Residual
Observation Order

11.

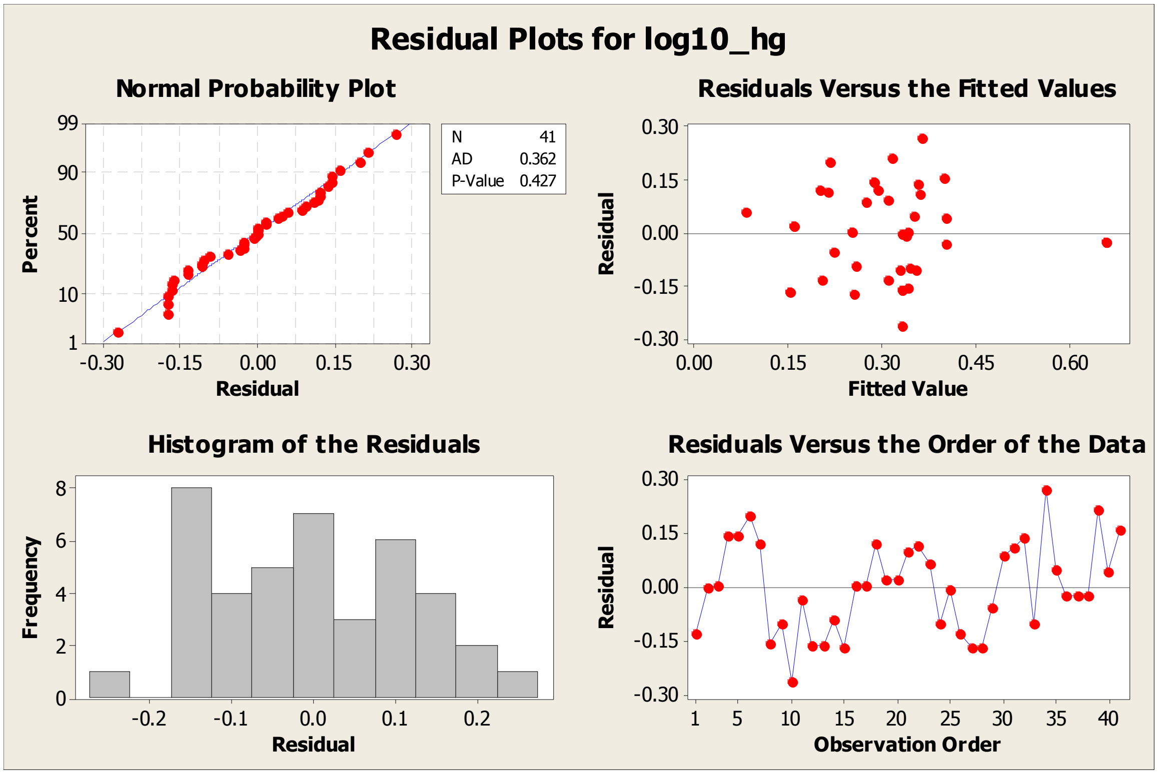
Residual Plots for log10_hg
Normal Probability Plot
Percent
Residual
N 41
AD 0.362
P-Value 0.427
Residuals Versus the Fitted Values
Residual
Fitted Value
Histogram of the Residuals
Frequency
Residual
Residuals Versus the Order of the Data
Residual
Observation Order

12.

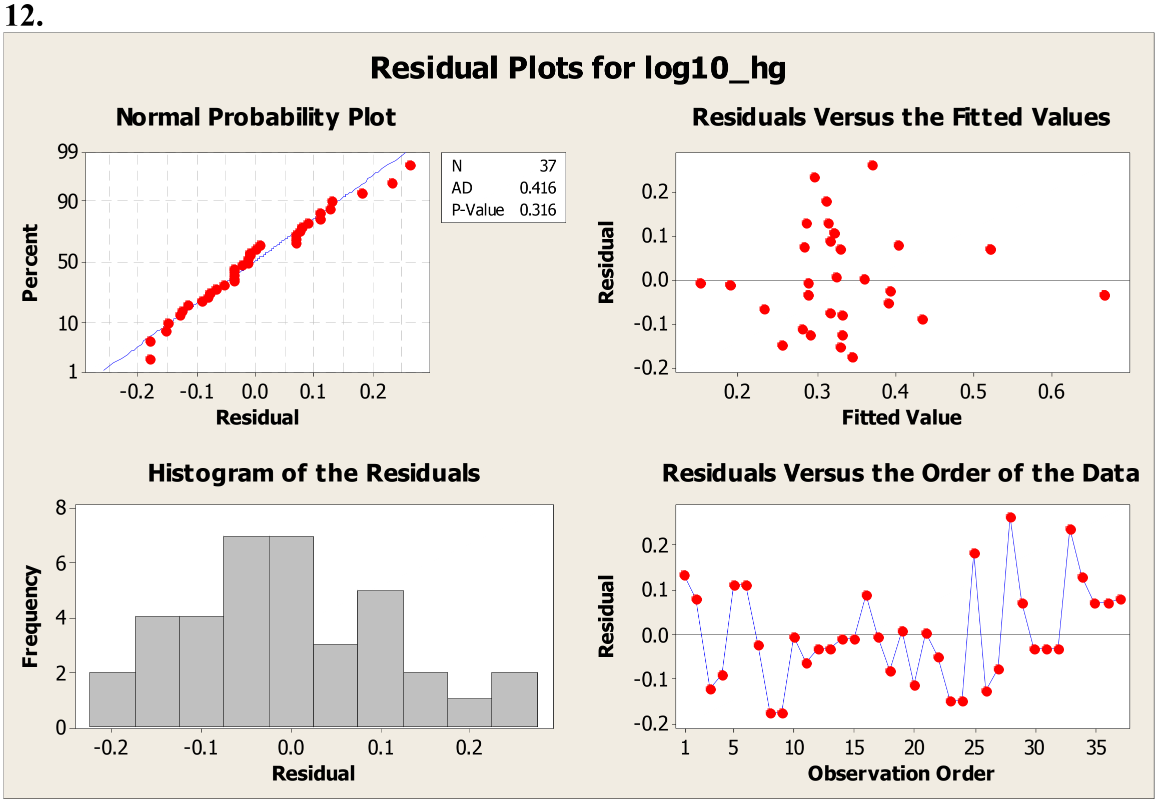
Residual Plots for log10_hg
Normal Probability Plot
Percent
Residual
N 37
AD 0.416
P-Value 0.316
Residuals Versus the Fitted Values
Residual
Fitted Value
Histogram of the Residuals
Frequency
Residual
Residuals Versus the Order of the Data
Residual
Observation Order

13.

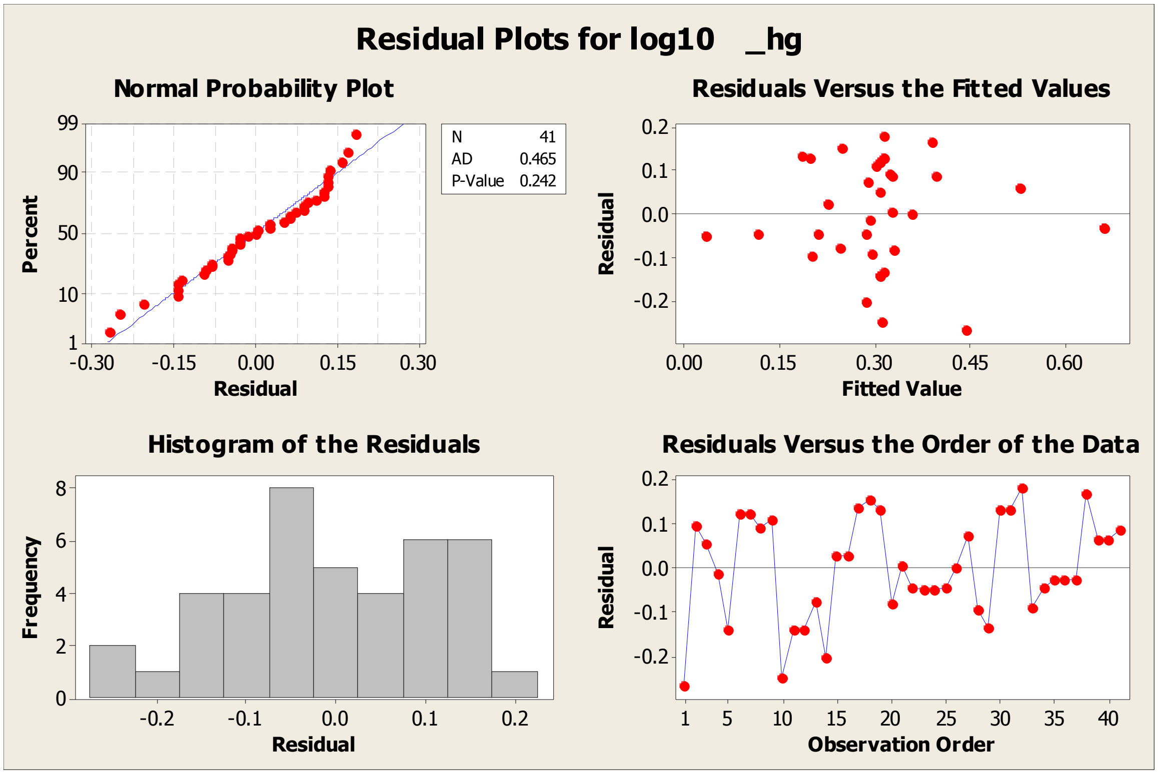

Residual Plots for log10 _hg
Normal Probability Plot
Percent
Residual
N 41
AD 0.465
P-Value 0.242
Residuals Versus the Fitted Values
Residual
Fitted Value
Histogram of the Residuals
Frequency
Residual
Residuals Versus the Order of the Data
Residual
Observation Order

14.

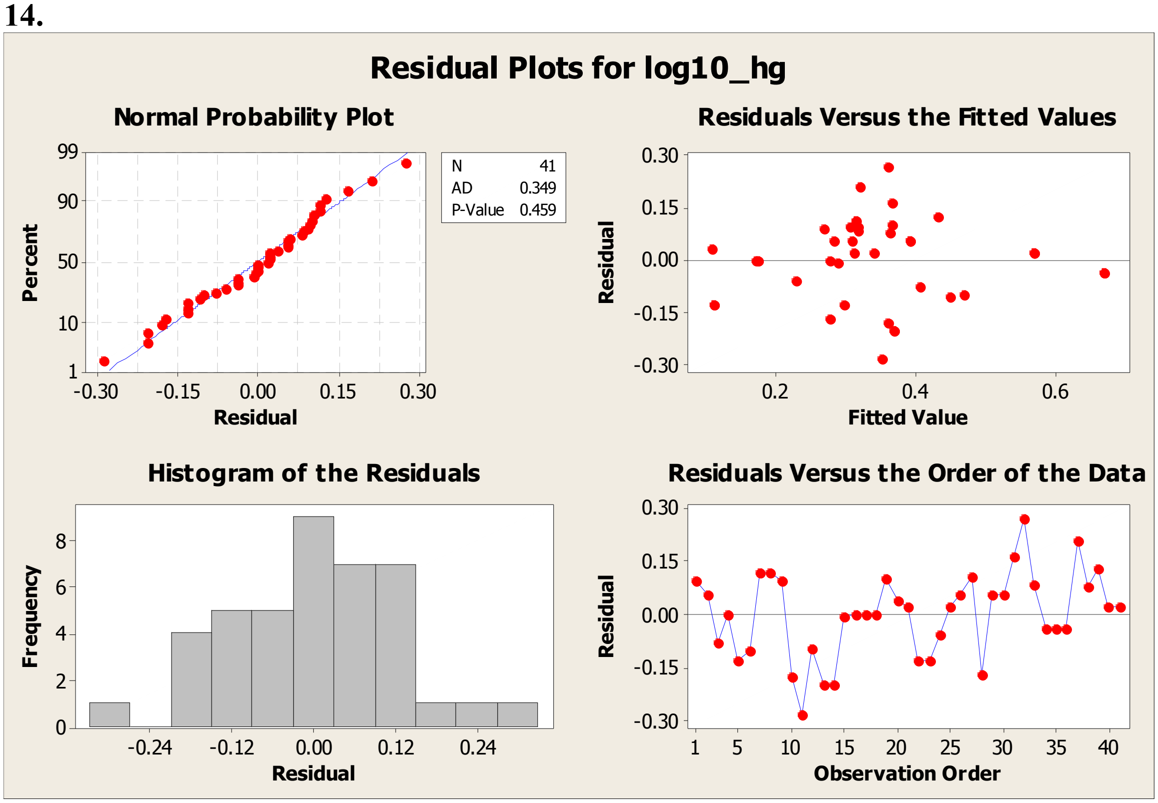

Residual Plots for log10_hg
Normal Probability Plot
Percent
Residual
N 41
AD 0.349
P-Value 0.459
Residuals Versus the Fitted Values
Residual
Fitted Value
Histogram of the Residuals
Frequency
Residual
Residuals Versus the Order of the Data
Residual
Observation Order

15.

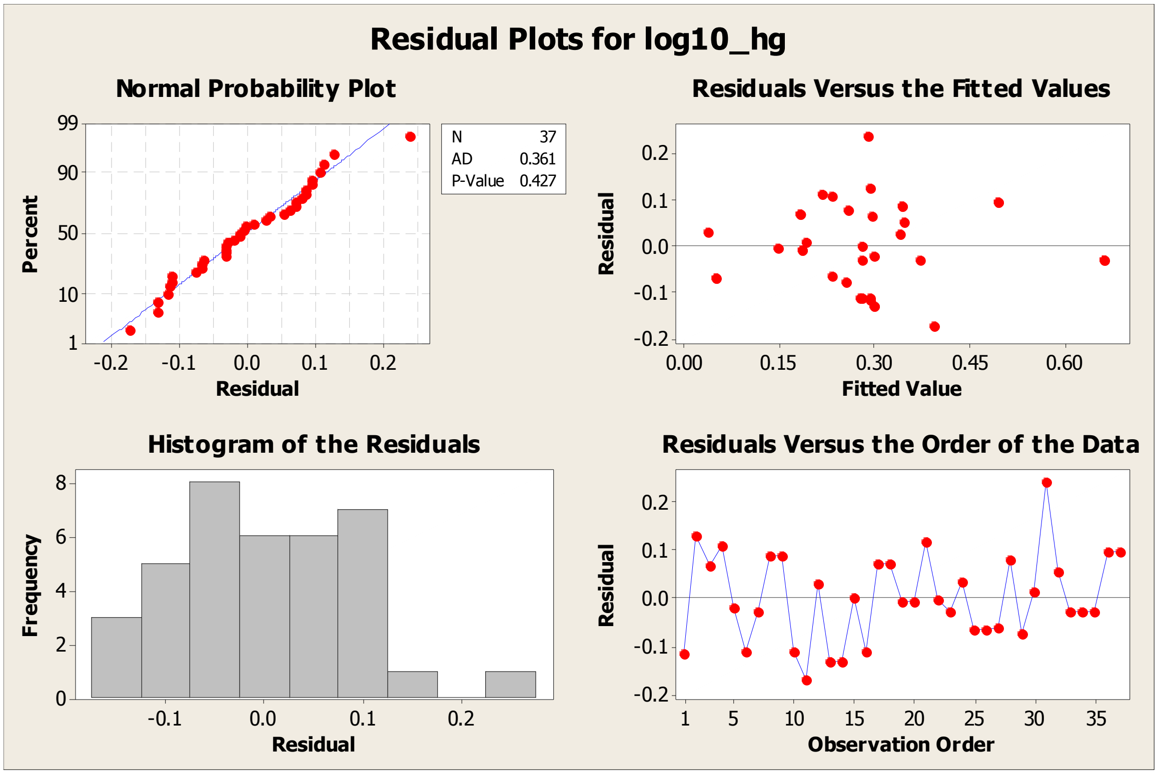

Residual Plots for log10_hg
Normal Probability Plot
Residuals Versus the Fitted Values
Percent
99
90
50
10
1
-0.2
-0.1
0.0
0.1
0.2
Residual
N 37
AD 0.361
P-Value 0.427
Residual
0.2
0.1
0.0
-0.1
-0.2
0.00
0.15
0.30
0.45
0.60
Fitted Value
Histogram of the Residuals
Residuals Versus the Order of the Data
Frequency
8
6
4
2
0
-0.1
0.0
0.1
0.2
Residual
Residual
0.2
0.1
0.0
-0.1
-0.2
1
5
10
15
20
25
30
35
Observation Order

16.

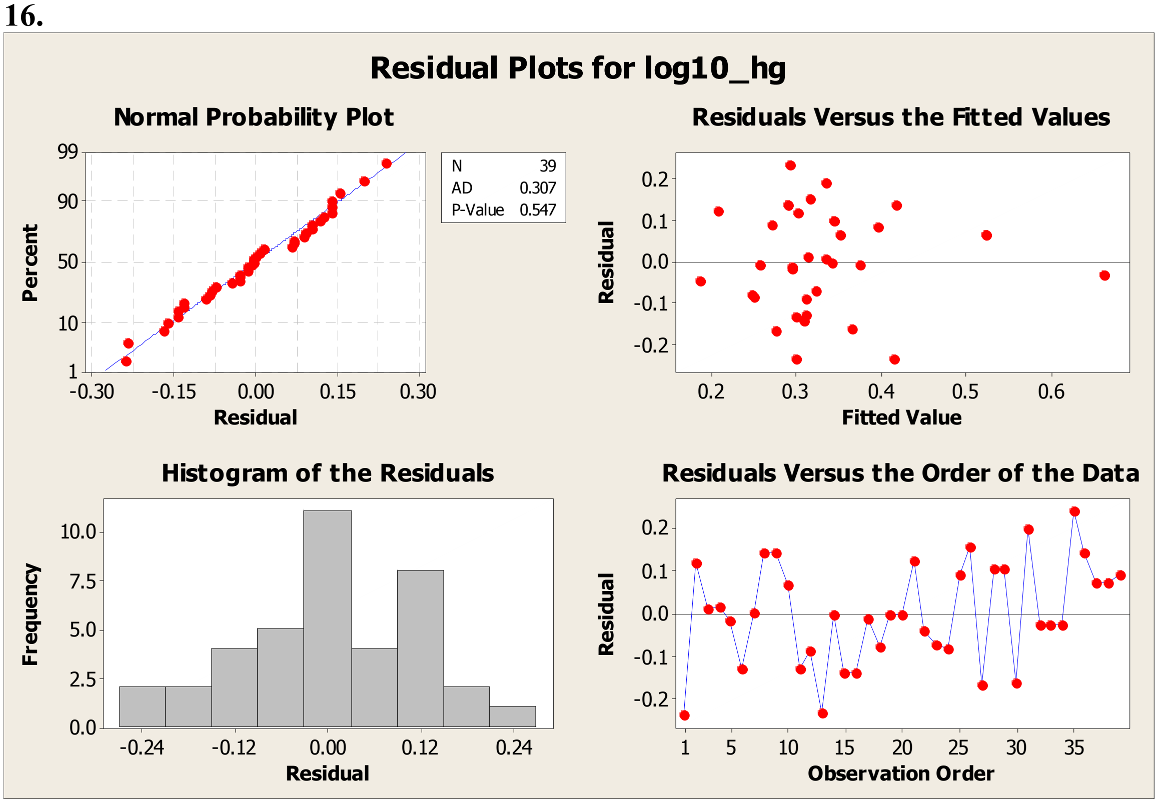

Residual Plots for log10_hg
Normal Probability Plot
Residuals Versus the Fitted Values
Percent
99
90
50
10
1
-0.30
-0.15
0.00
0.15
0.30
Residual
N 39
AD 0.307
P-Value 0.547
Residual
0.2
0.1
0.0
-0.1
-0.2
0.2
0.3
0.4
0.5
0.6
Fitted Value
Histogram of the Residuals
Residuals Versus the Order of the Data
Frequency
10.0
7.5
5.0
2.5
0.0
-0.24
-0.12
0.00
0.12
0.24
Residual
Residual
0.2
0.1
0.0
-0.1
-0.2
1
5
10
15
20
25
30
35
Observation Order

17.

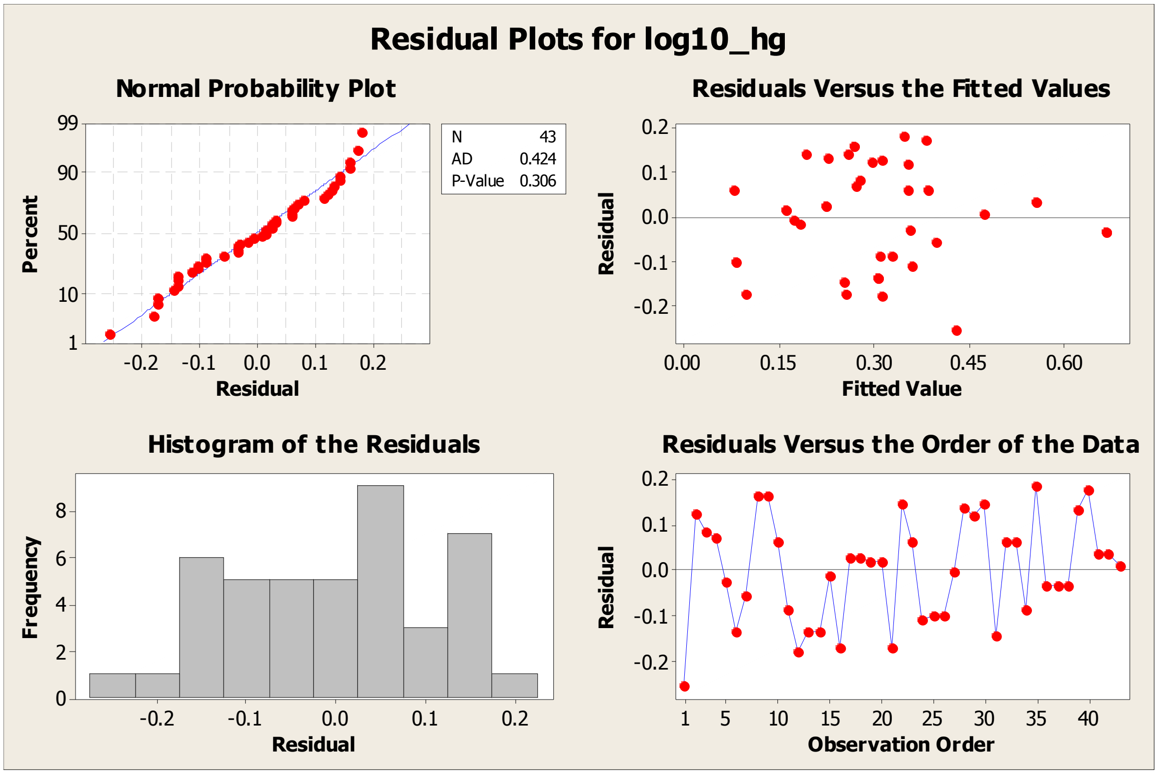
Residual Plots for log10_hg
Normal Probability Plot
Residuals Versus the Fitted Values
Histogram of the Residuals
Residuals Versus the Order of the Data
N 43
AD 0.424
P-Value 0.306
Percent
Residual
Fitted Value
Frequency
Observation Order

18.

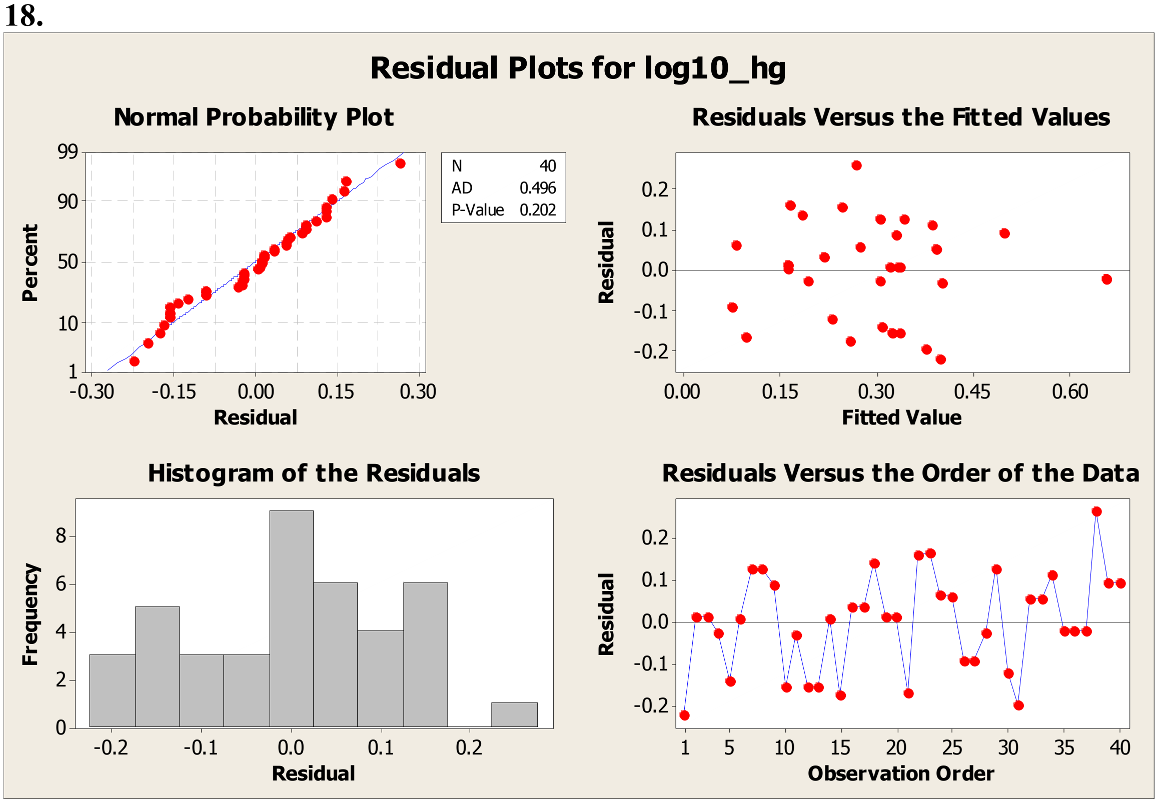
Residual Plots for log10_hg
Normal Probability Plot
Residuals Versus the Fitted Values
Histogram of the Residuals
Residuals Versus the Order of the Data
N 40
AD 0.496
P-Value 0.202
Percent
Residual
Fitted Value
Frequency
Observation Order

19.

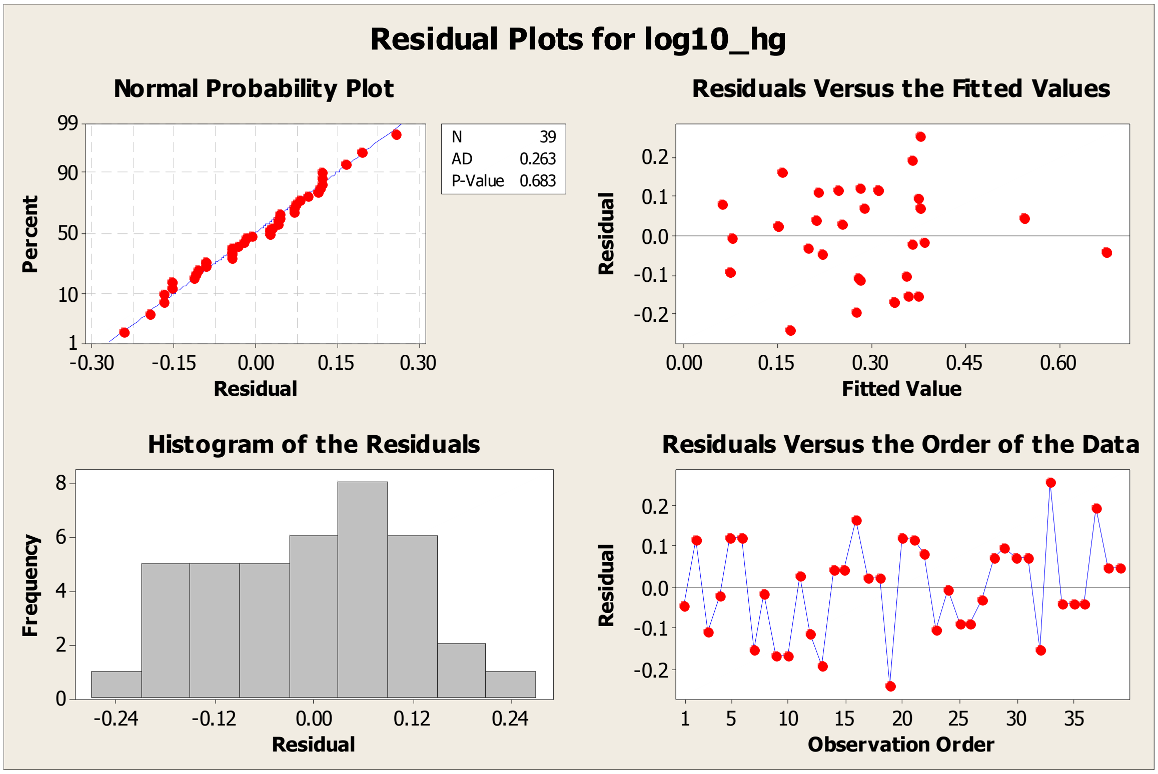
Residual Plots for log10_hg
Normal Probability Plot
Percent
Residual
N 39
AD 0.263
P-Value 0.683
Residuals Versus the Fitted Values
Residual
Fitted Value
Histogram of the Residuals
Frequency
Residual
Residuals Versus the Order of the Data
Residual
Observation Order

20.

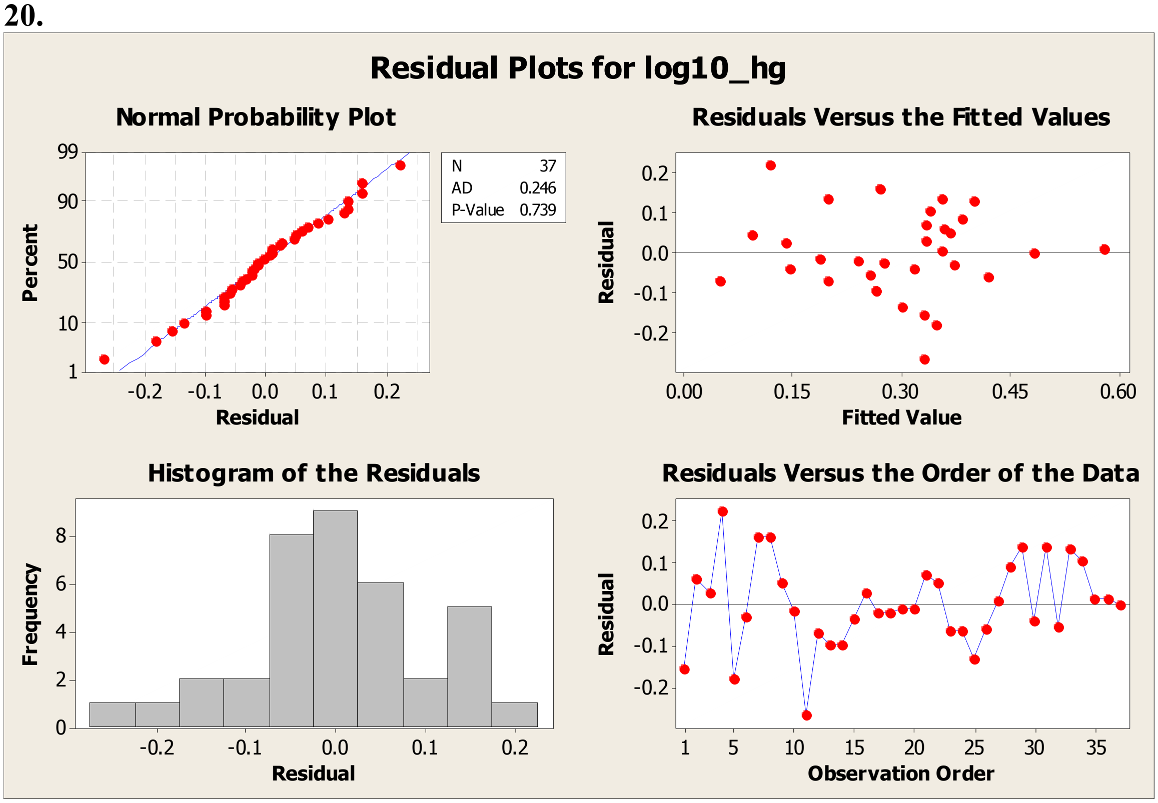
Residual Plots for log10_hg
Normal Probability Plot
Percent
Residual
N 37
AD 0.246
P-Value 0.739
Residuals Versus the Fitted Values
Residual
Fitted Value
Histogram of the Residuals
Frequency
Residual
Residuals Versus the Order of the Data
Residual
Observation Order

21.

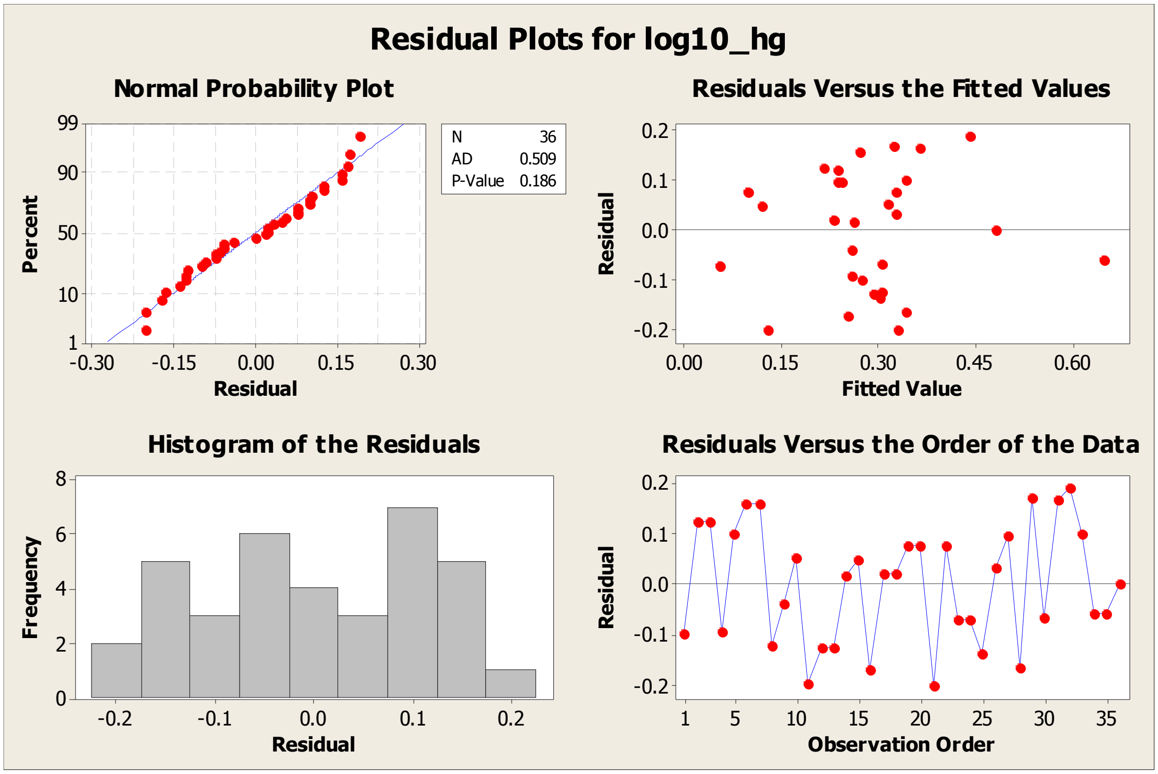

Residual Plots for log10_hg
Normal Probability Plot
N 36
AD 0.509
P-Value 0.186
Percent
Residual
Residuals Versus the Fitted Values
Residual
Fitted Value
Histogram of the Residuals
Frequency
Residual
Residuals Versus the Order of the Data
Residual
Observation Order

22.

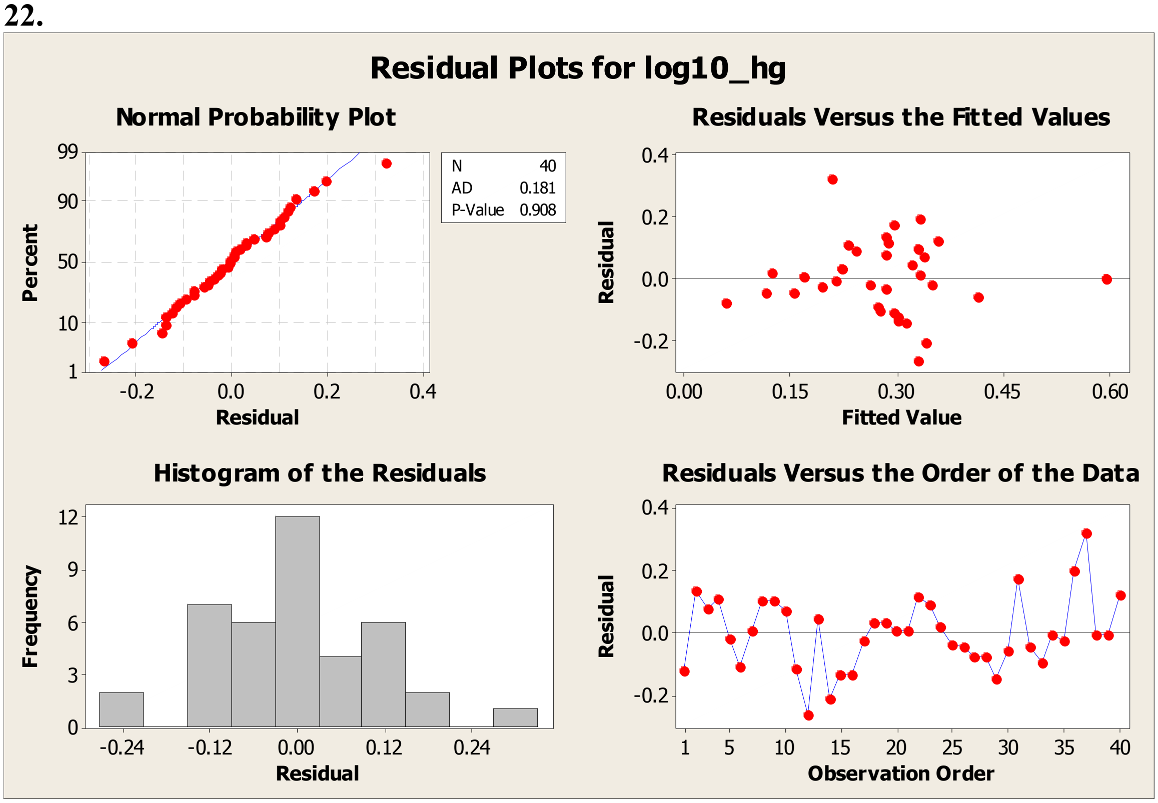

Residual Plots for log10_hg
Normal Probability Plot
N 40
AD 0.181
P-Value 0.908
Percent
Residual
Residuals Versus the Fitted Values
Residual
Fitted Value
Histogram of the Residuals
Frequency
Residual
Residuals Versus the Order of the Data
Residual
Observation Order

23.

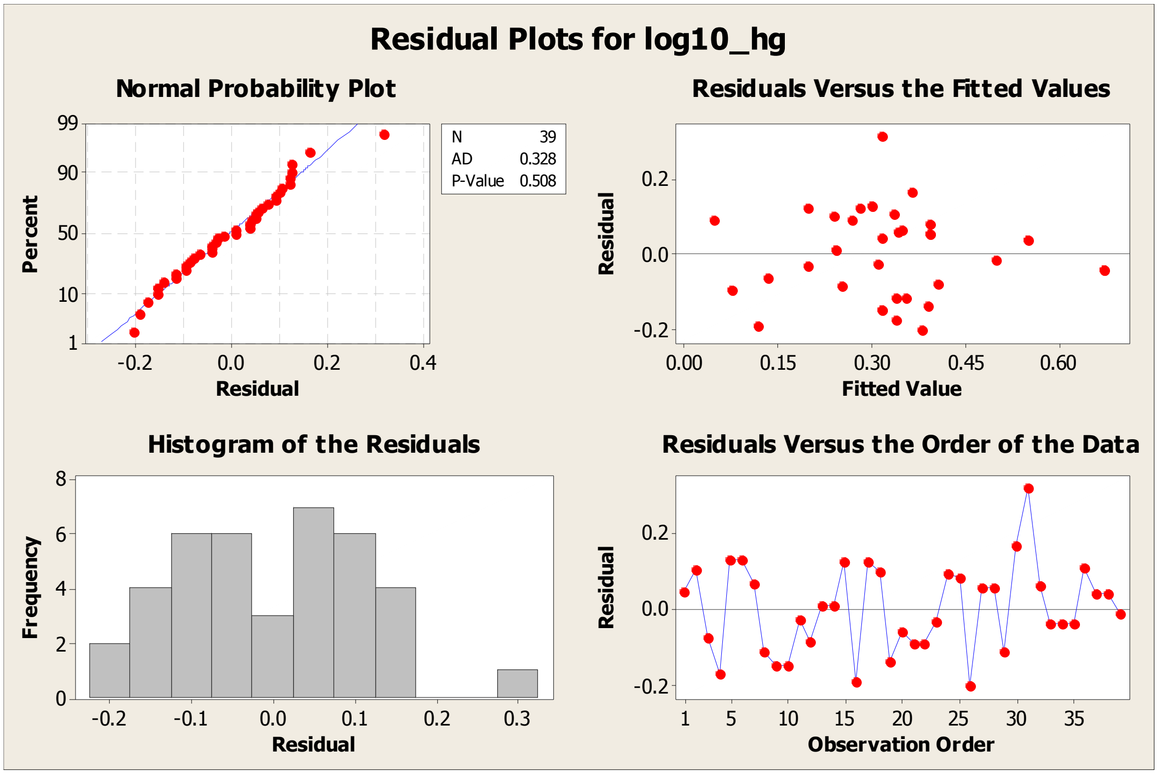
Residual Plots for log10_hg
Normal Probability Plot
Percent
Residual
N 39
AD 0.328
P-Value 0.508
Residuals Versus the Fitted Values
Residual
Fitted Value
Histogram of the Residuals
Frequency
Residual
Residuals Versus the Order of the Data
Residual
Observation Order

24.

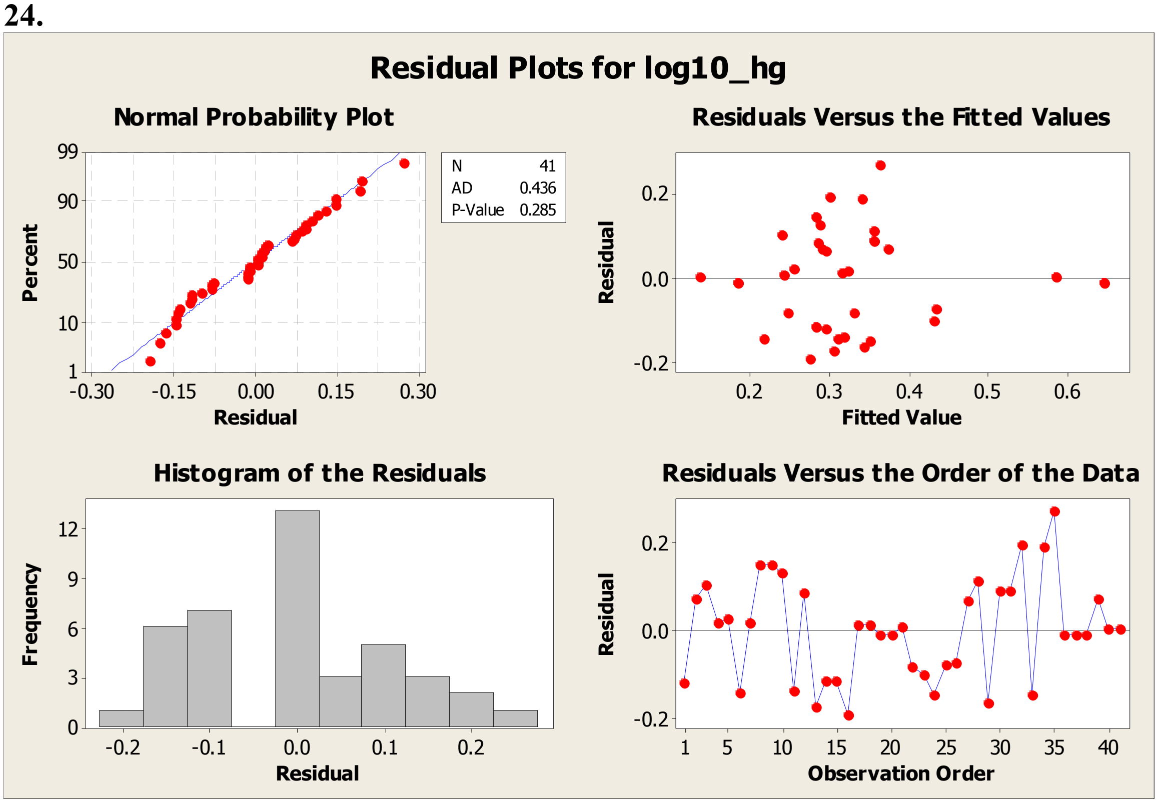
Residual Plots for log10_hg
Normal Probability Plot
Percent
Residual
N 41
AD 0.436
P-Value 0.285
Residuals Versus the Fitted Values
Residual
Fitted Value
Histogram of the Residuals
Frequency
Residual
Residuals Versus the Order of the Data
Residual
Observation Order

25.

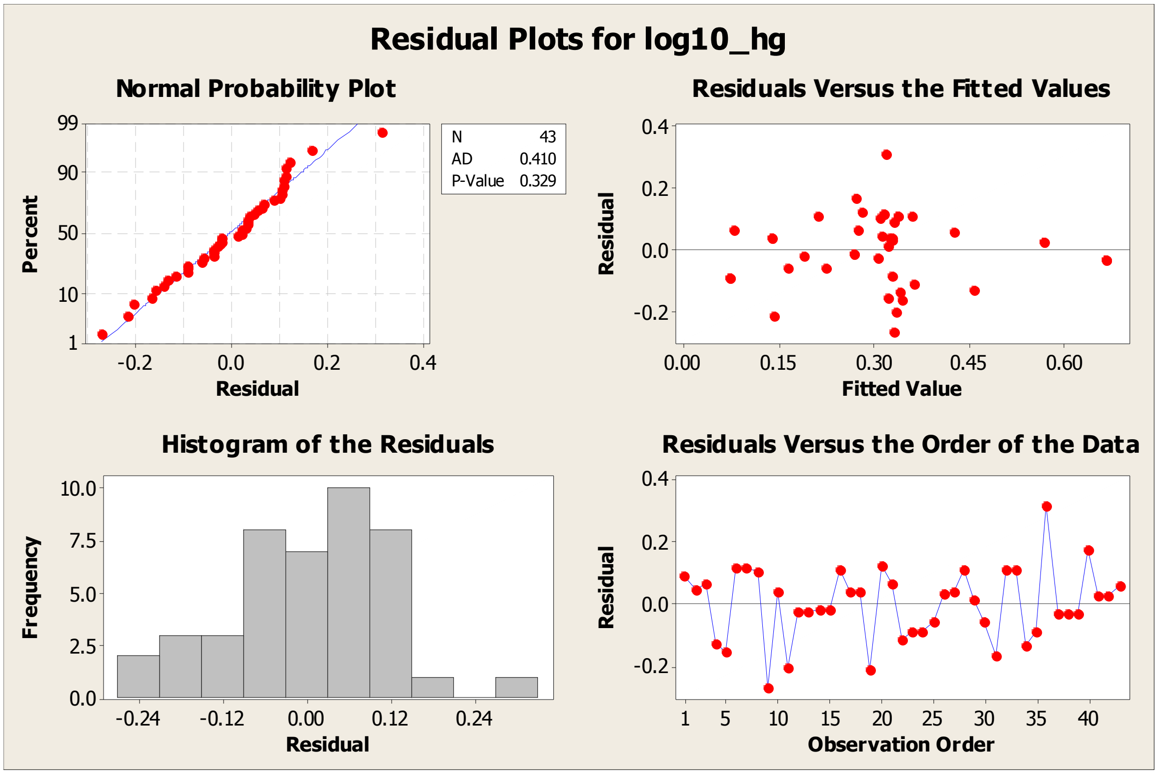

Residual Plots for log10_hg
Normal Probability Plot
Percent
Residual
N 43
AD 0.410
P-Value 0.329
Residuals Versus the Fitted Values
Residual
Fitted Value
Histogram of the Residuals
Frequency
Residual
Residuals Versus the Order of the Data
Residual
Observation Order

26.

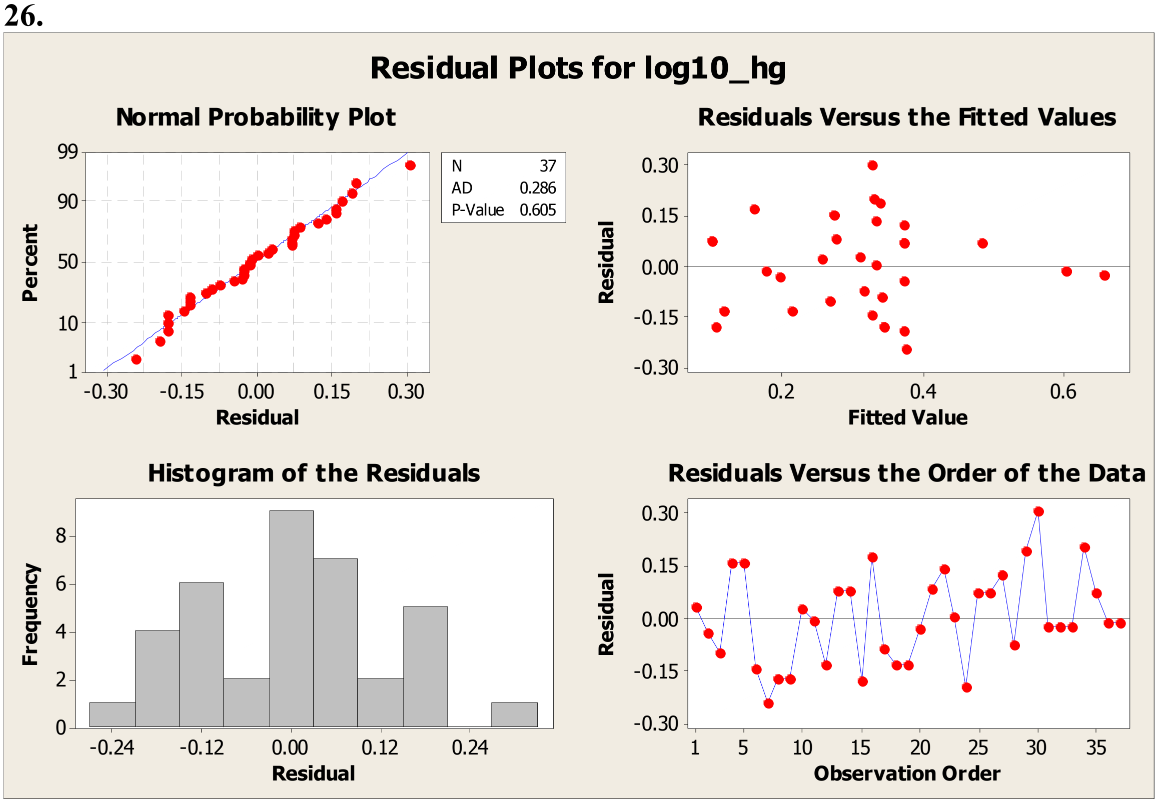

Residual Plots for log10_hg
Normal Probability Plot
Percent
Residual
N 37
AD 0.286
P-Value 0.605
Residuals Versus the Fitted Values
Residual
Fitted Value
Histogram of the Residuals
Frequency
Residual
Residuals Versus the Order of the Data
Residual
Observation Order

27.

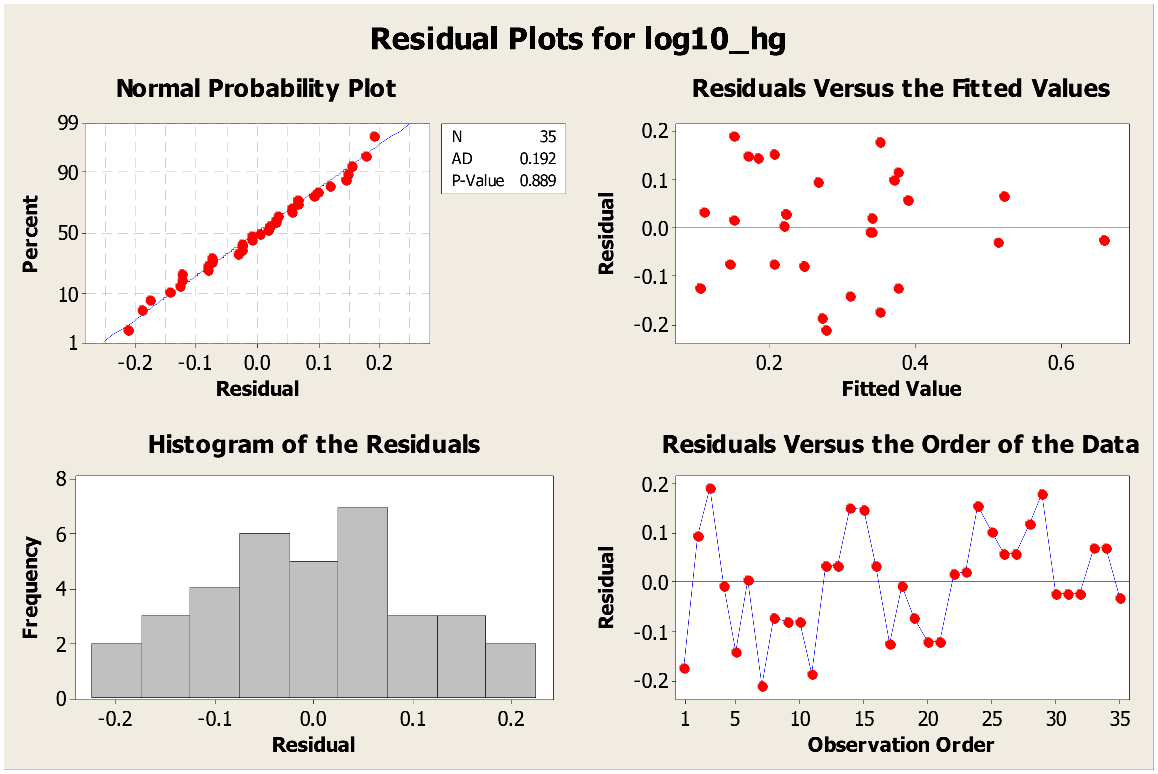
Residual Plots for log10_hg
Normal Probability Plot
Percent
Residual
N 35
AD 0.192
P-Value 0.889
Residuals Versus the Fitted Values
Residual
Fitted Value
Histogram of the Residuals
Frequency
Residual
Residuals Versus the Order of the Data
Residual
Observation Order

28.

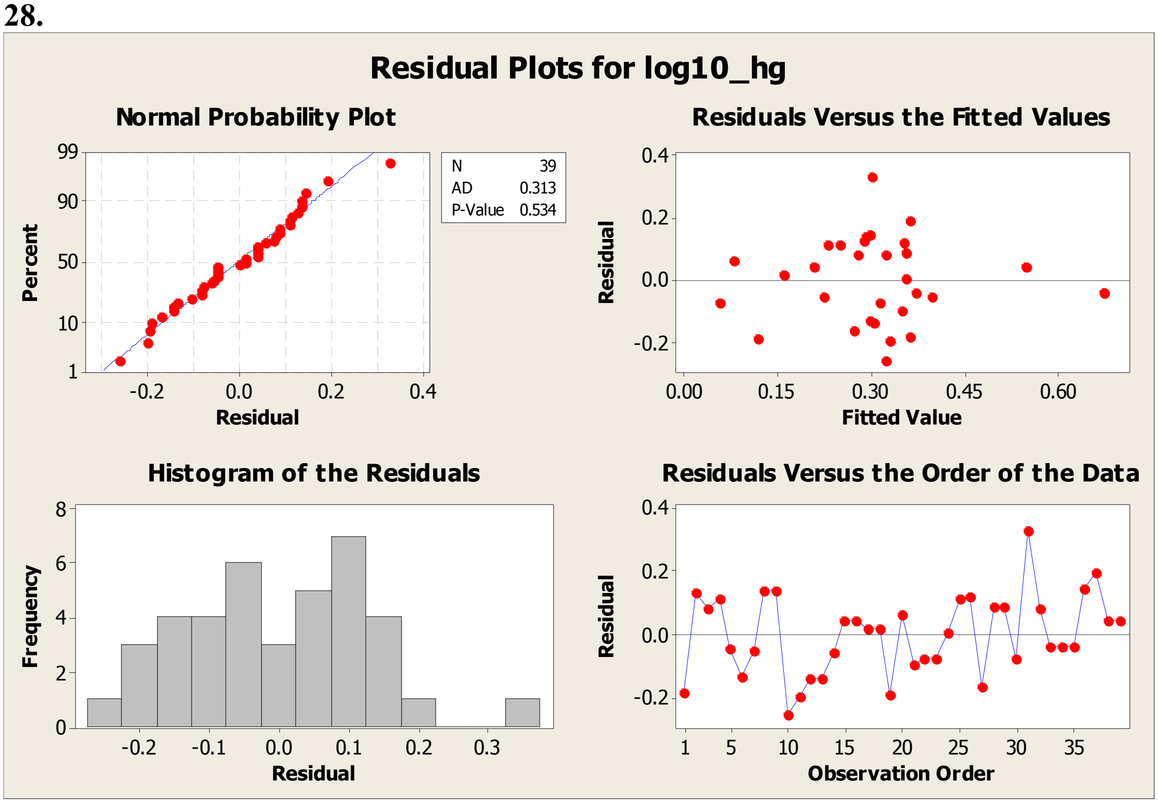
Residual Plots for log10_hg
Normal Probability Plot
Percent
Residual
N 39
AD 0.313
P-Value 0.534
Residuals Versus the Fitted Values
Residual
Fitted Value
Histogram of the Residuals
Frequency
Residual
Residuals Versus the Order of the Data
Residual
Observation Order

29.

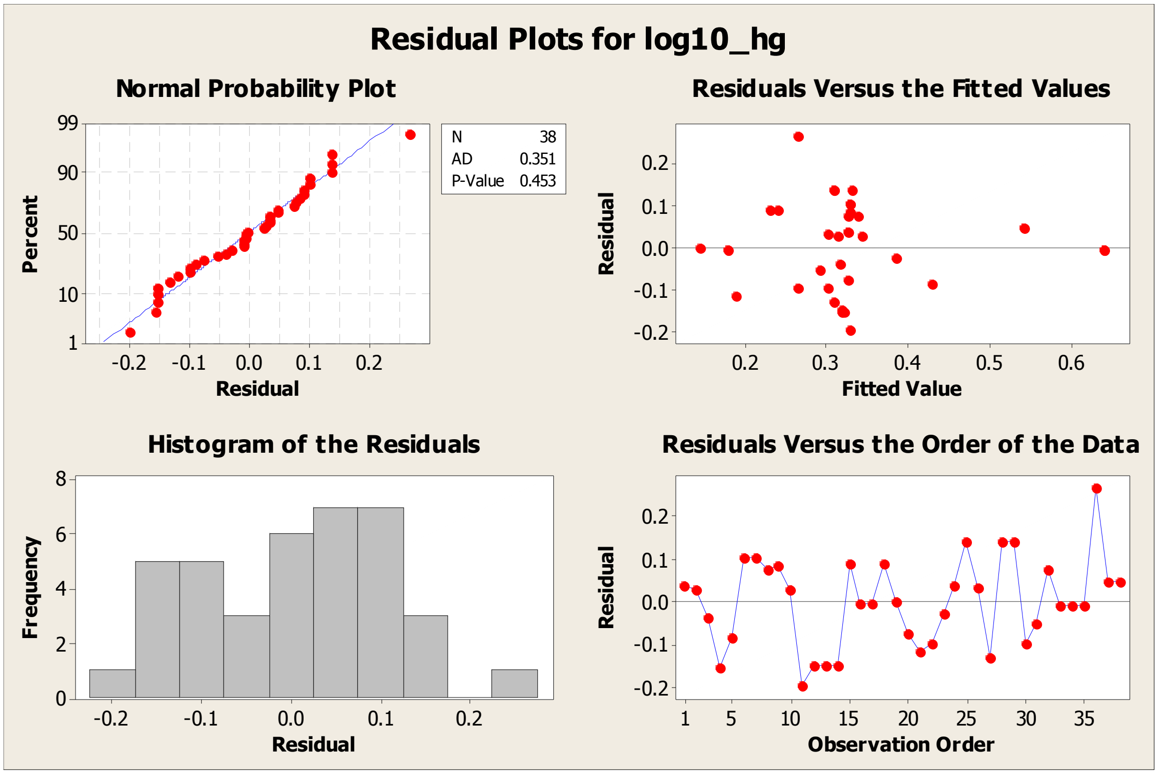
Residual Plots for log10_hg
Normal Probability Plot
Percent
Residual
N 38
AD 0.351
P-Value 0.453
Residuals Versus the Fitted Values
Residual
Fitted Value
Histogram of the Residuals
Frequency
Residual
Residuals Versus the Order of the Data
Residual
Observation Order

30.

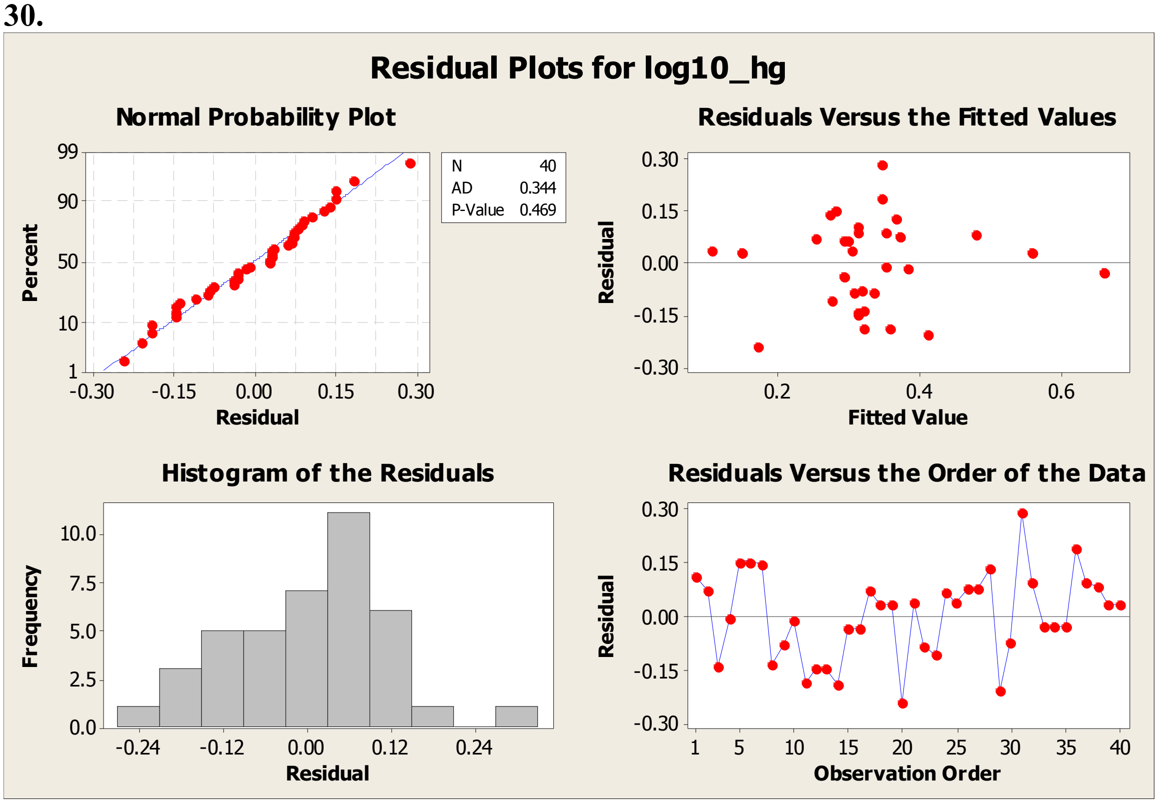
Residual Plots for log10_hg
Normal Probability Plot
Percent
Residual
N 40
AD 0.344
P-Value 0.469
Residuals Versus the Fitted Values
Residual
Fitted Value
Histogram of the Residuals
Frequency
Residual
Residuals Versus the Order of the Data
Residual
Observation Order

Appendix B. Residual Plots from Sensitivity Analysis (300m)

1.

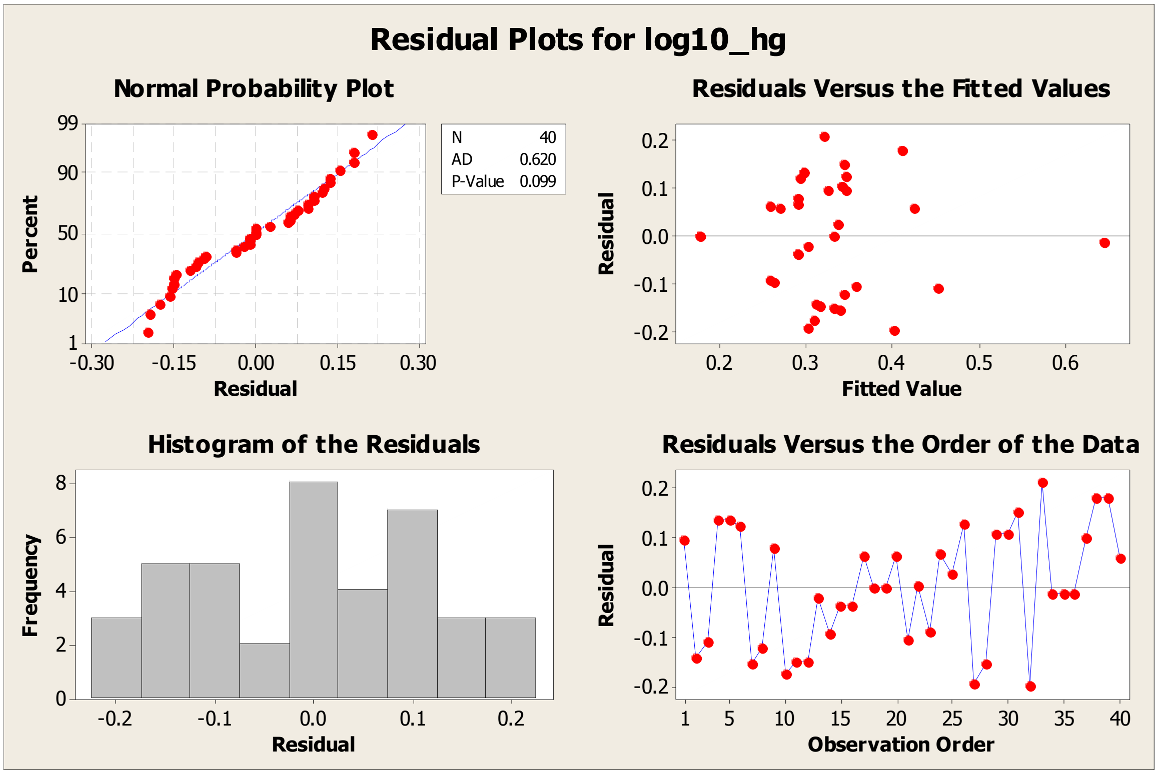

2.

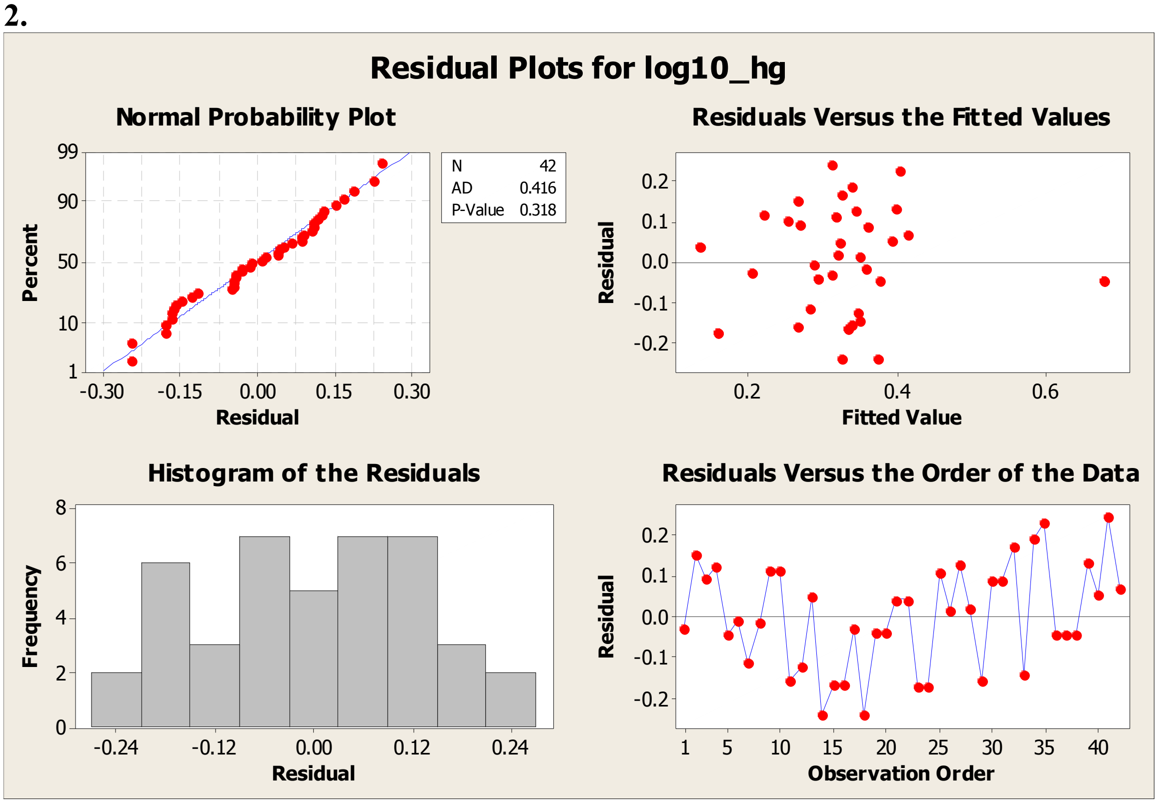

3.

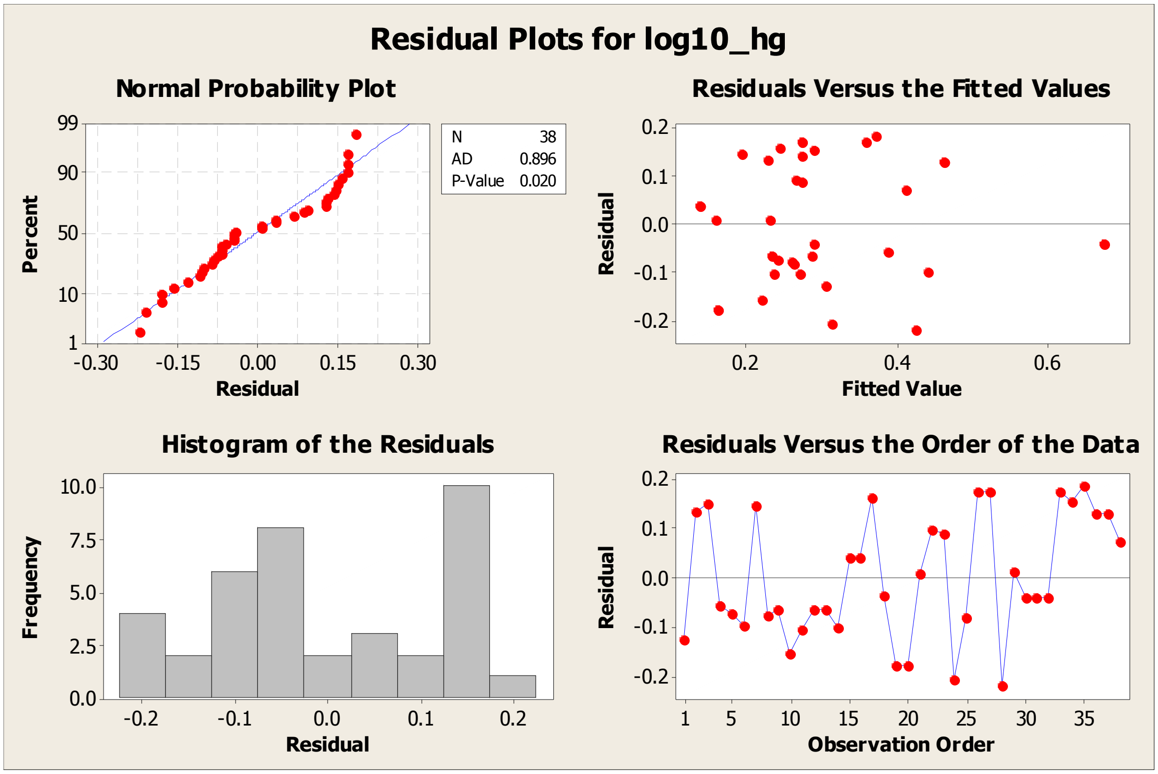
Residual Plots for log10_hg
Normal Probability Plot
Percent
Residual
N 38
AD 0.896
P-Value 0.020
Residuals Versus the Fitted Values
Residual
Fitted Value
Histogram of the Residuals
Frequency
Residual
Residuals Versus the Order of the Data
Residual
Observation Order

4.

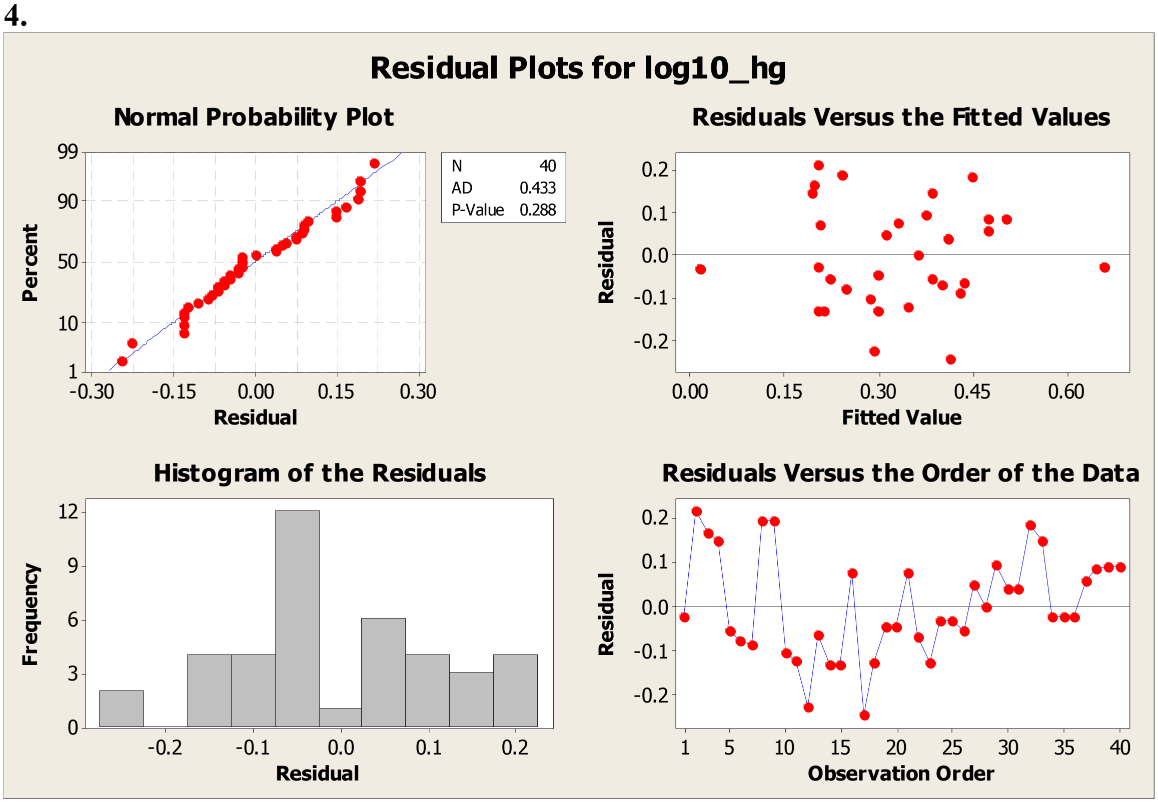
Residual Plots for log10_hg
Normal Probability Plot
Percent
Residual
N 40
AD 0.433
P-Value 0.288
Residuals Versus the Fitted Values
Residual
Fitted Value
Histogram of the Residuals
Frequency
Residual
Residuals Versus the Order of the Data
Residual
Observation Order

5.

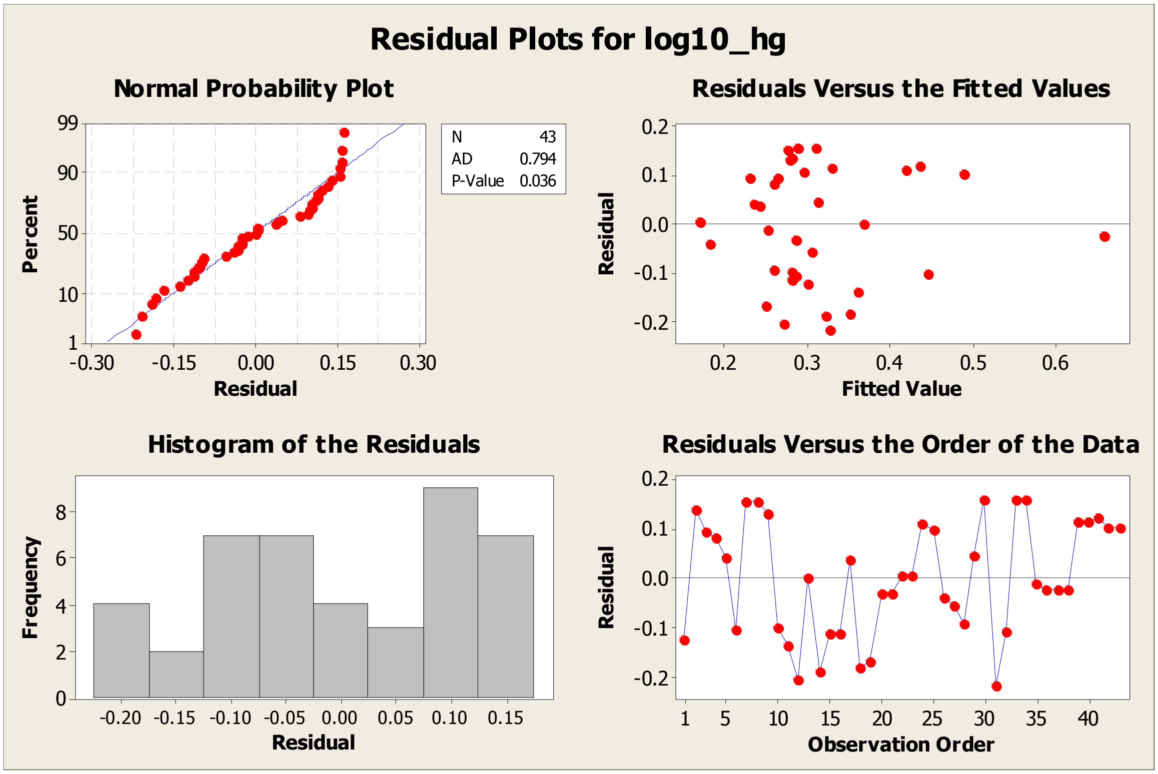
Residual Plots for log10_hg
Normal Probability Plot
N 43
AD 0.794
P-Value 0.036
Percent
Residual
Residuals Versus the Fitted Values
Residual
Fitted Value
Histogram of the Residuals
Frequency
Residual
Residuals Versus the Order of the Data
Residual
Observation Order

6.

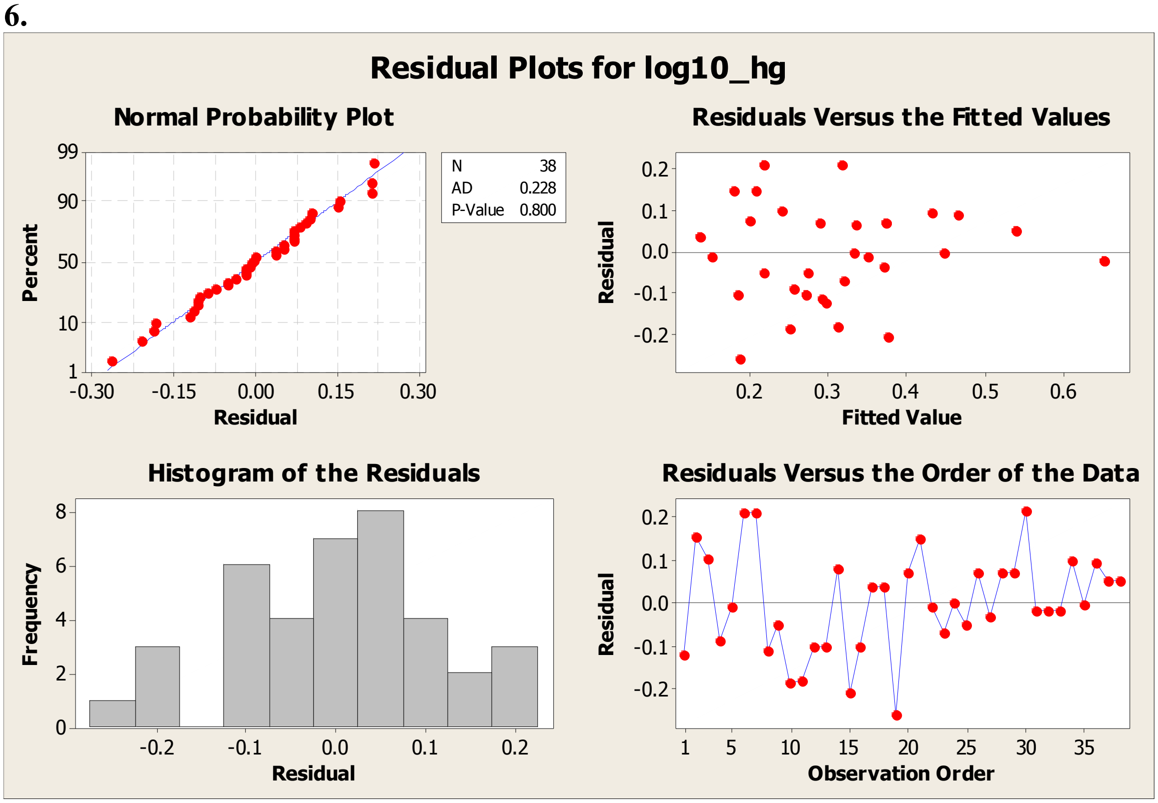
Residual Plots for log10_hg
Normal Probability Plot
N 38
AD 0.228
P-Value 0.800
Percent
Residual
Residuals Versus the Fitted Values
Residual
Fitted Value
Histogram of the Residuals
Frequency
Residual
Residuals Versus the Order of the Data
Residual
Observation Order

7.

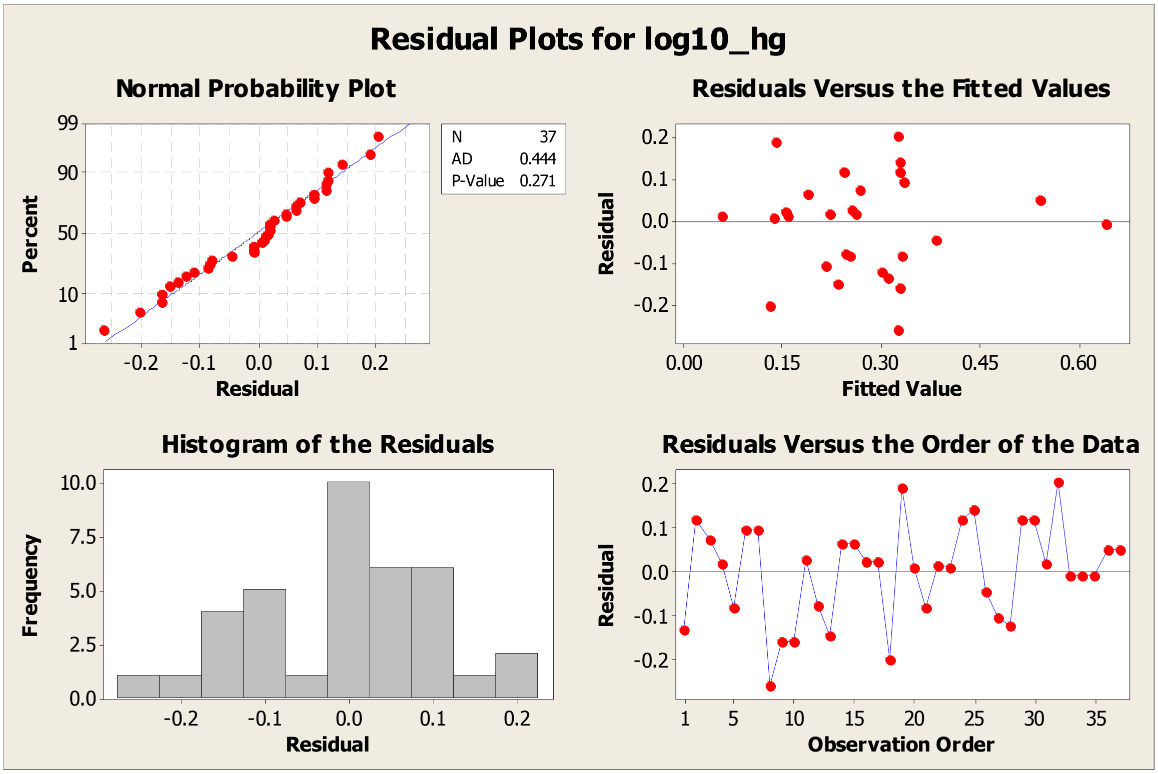

Residual Plots for log10_hg
Normal Probability Plot
Residuals Versus the Fitted Values
N 37
AD 0.444
P-Value 0.271
Percent
Residual
Fitted Value
Histogram of the Residuals
Residuals Versus the Order of the Data
Frequency
Observation Order

8.

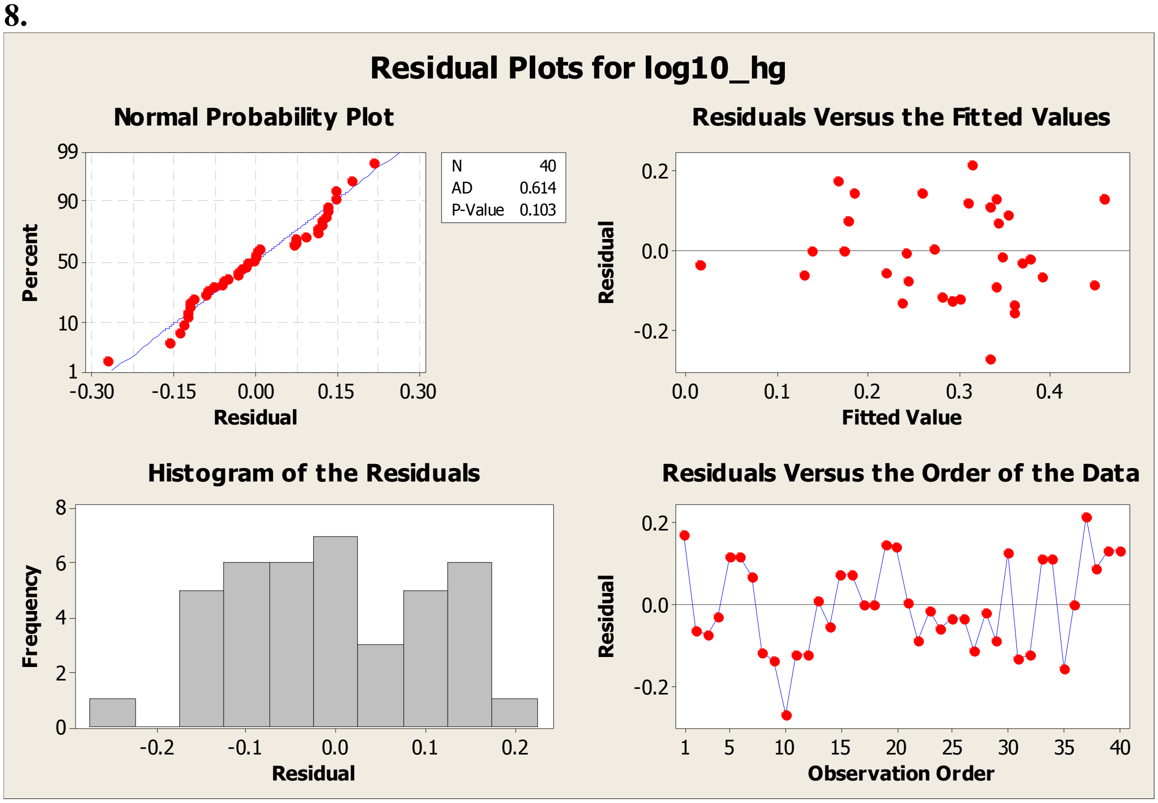

Residual Plots for log10_hg
Normal Probability Plot
Residuals Versus the Fitted Values
N 40
AD 0.614
P-Value 0.103
Percent
Residual
Fitted Value
Histogram of the Residuals
Residuals Versus the Order of the Data
Frequency
Observation Order

9.

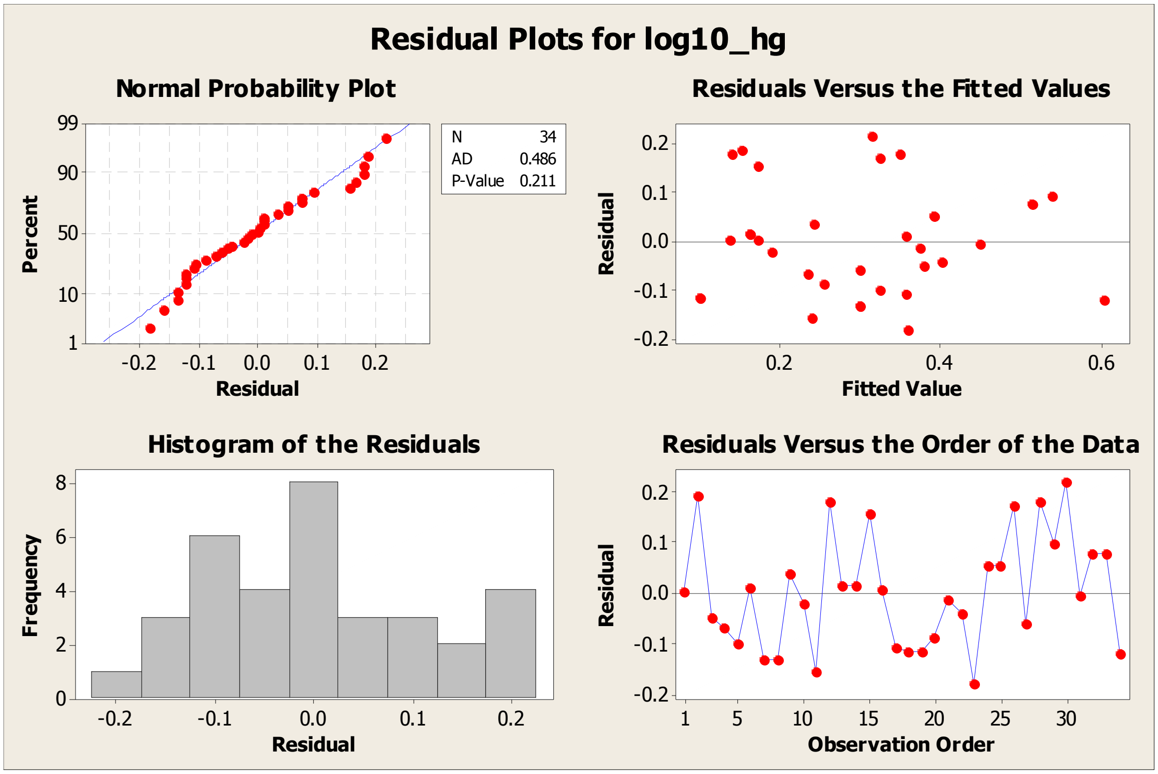
Residual Plots for log10_hg
Normal Probability Plot
Percent
Residual
N 34
AD 0.486
P-Value 0.211
Residuals Versus the Fitted Values
Residual
Fitted Value
Histogram of the Residuals
Frequency
Residual
Residuals Versus the Order of the Data
Residual
Observation Order

10.

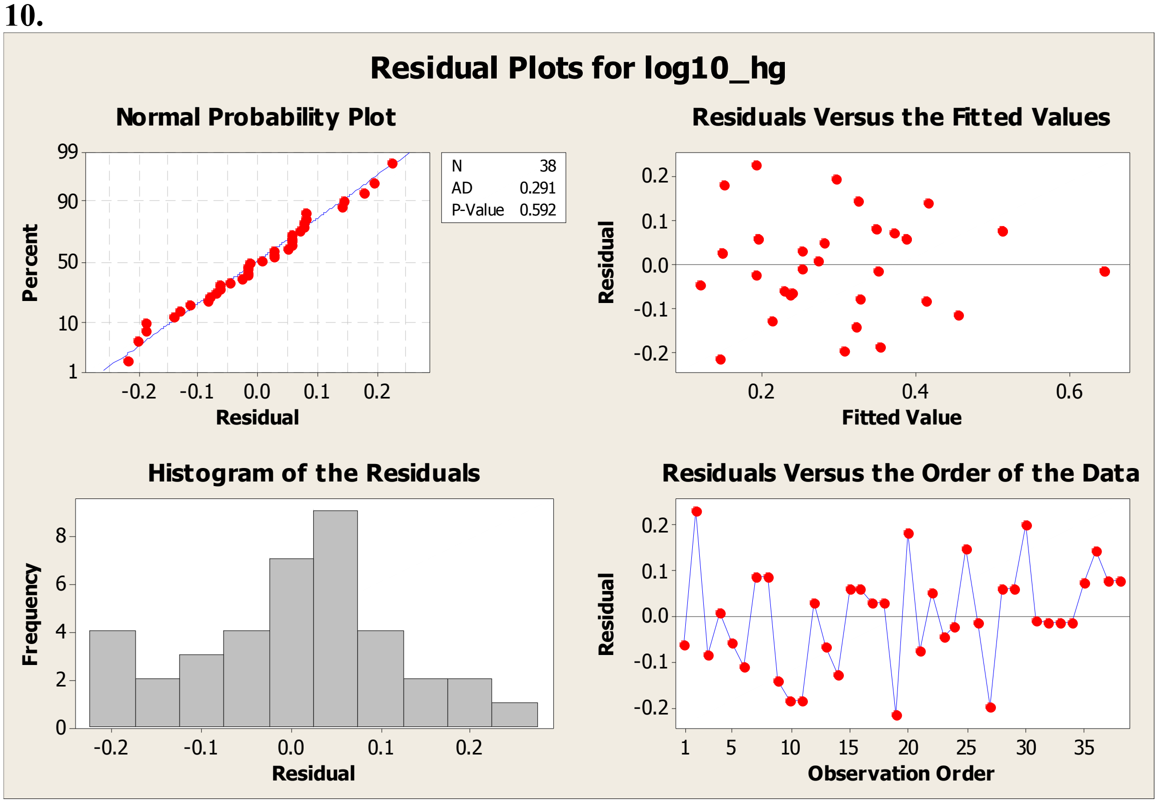
Residual Plots for log10_hg
Normal Probability Plot
Percent
Residual
N 38
AD 0.291
P-Value 0.592
Residuals Versus the Fitted Values
Residual
Fitted Value
Histogram of the Residuals
Frequency
Residual
Residuals Versus the Order of the Data
Residual
Observation Order

11.

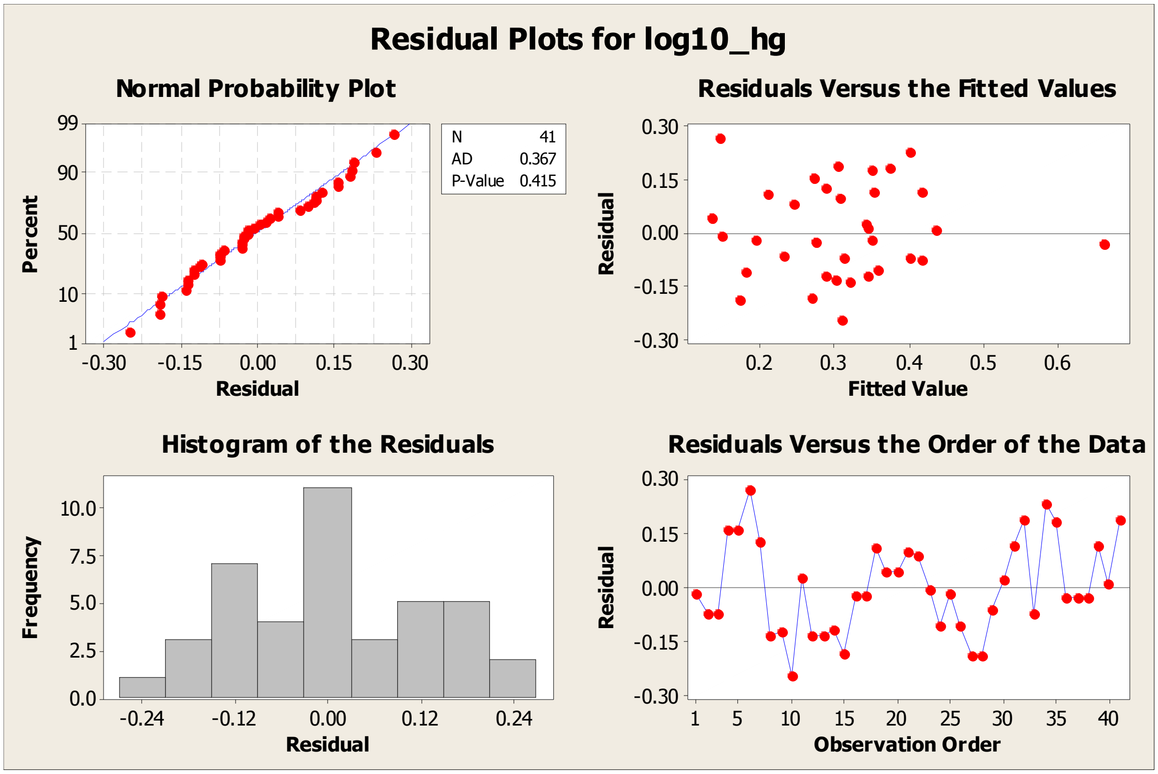
Residual Plots for log10_hg
Normal Probability Plot
N 41
AD 0.367
P-Value 0.415
Percent
Residual
Residuals Versus the Fitted Values
Residual
Fitted Value
Histogram of the Residuals
Frequency
Residual
Residuals Versus the Order of the Data
Residual
Observation Order

12.

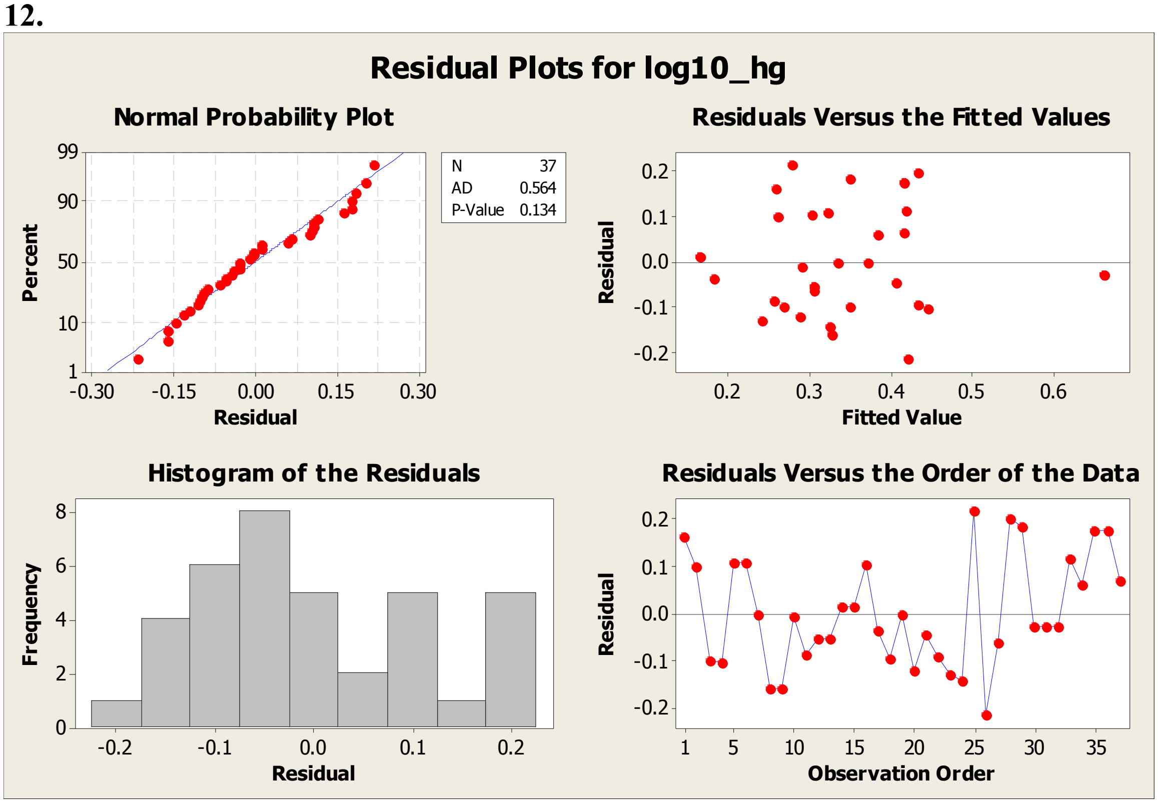
Residual Plots for log10_hg
Normal Probability Plot
N 37
AD 0.564
P-Value 0.134
Percent
Residual
Residuals Versus the Fitted Values
Residual
Fitted Value
Histogram of the Residuals
Frequency
Residual
Residuals Versus the Order of the Data
Residual
Observation Order

13.

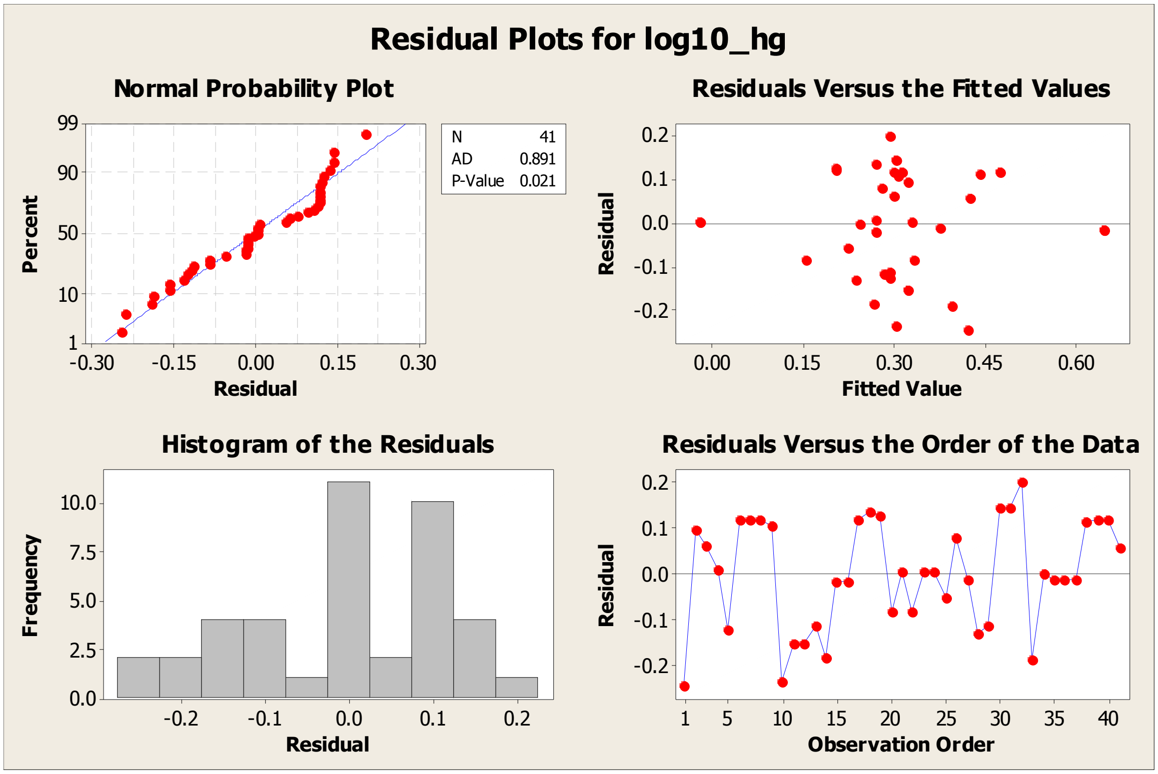
Residual Plots for log10_hg
Normal Probability Plot
Residuals Versus the Fitted Values
Histogram of the Residuals
Residuals Versus the Order of the Data
N 41
AD 0.891
P-Value 0.021
Percent
Residual
Fitted Value
Frequency
Observation Order

14.

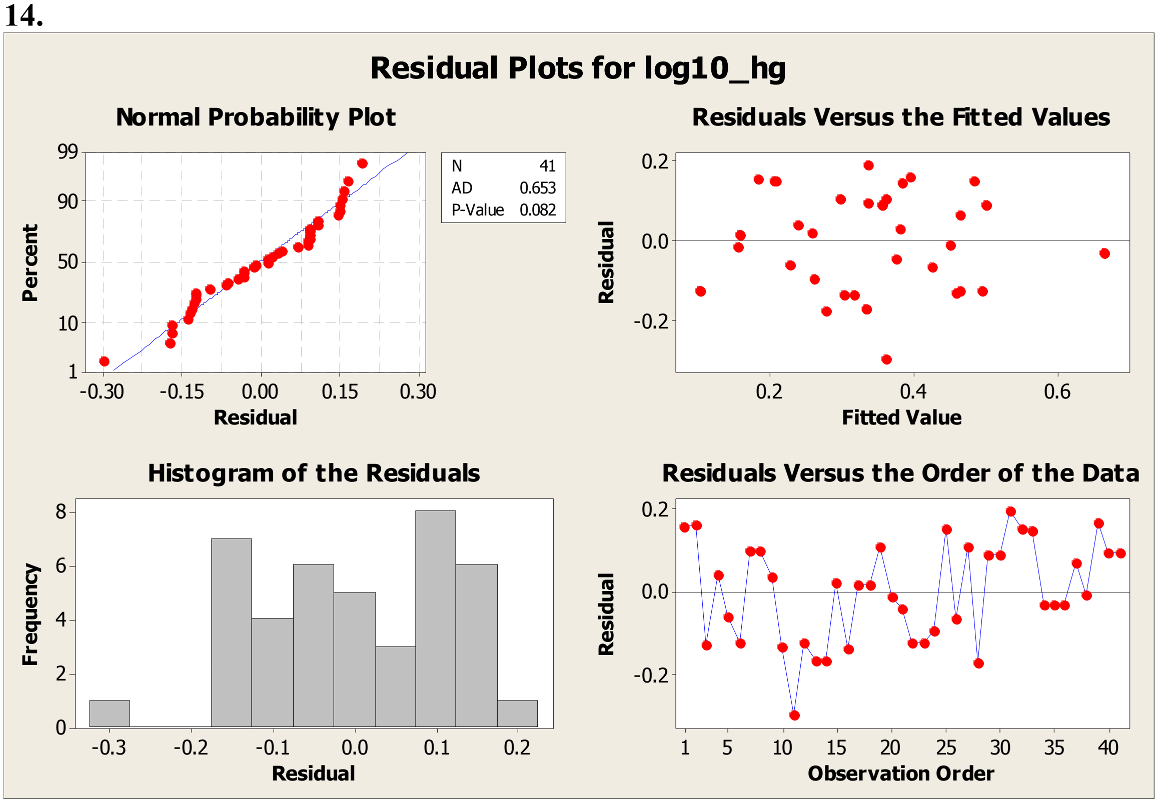
Residual Plots for log10_hg
Normal Probability Plot
Residuals Versus the Fitted Values
Histogram of the Residuals
Residuals Versus the Order of the Data
N 41
AD 0.653
P-Value 0.082
Percent
Residual
Fitted Value
Frequency
Observation Order

15.

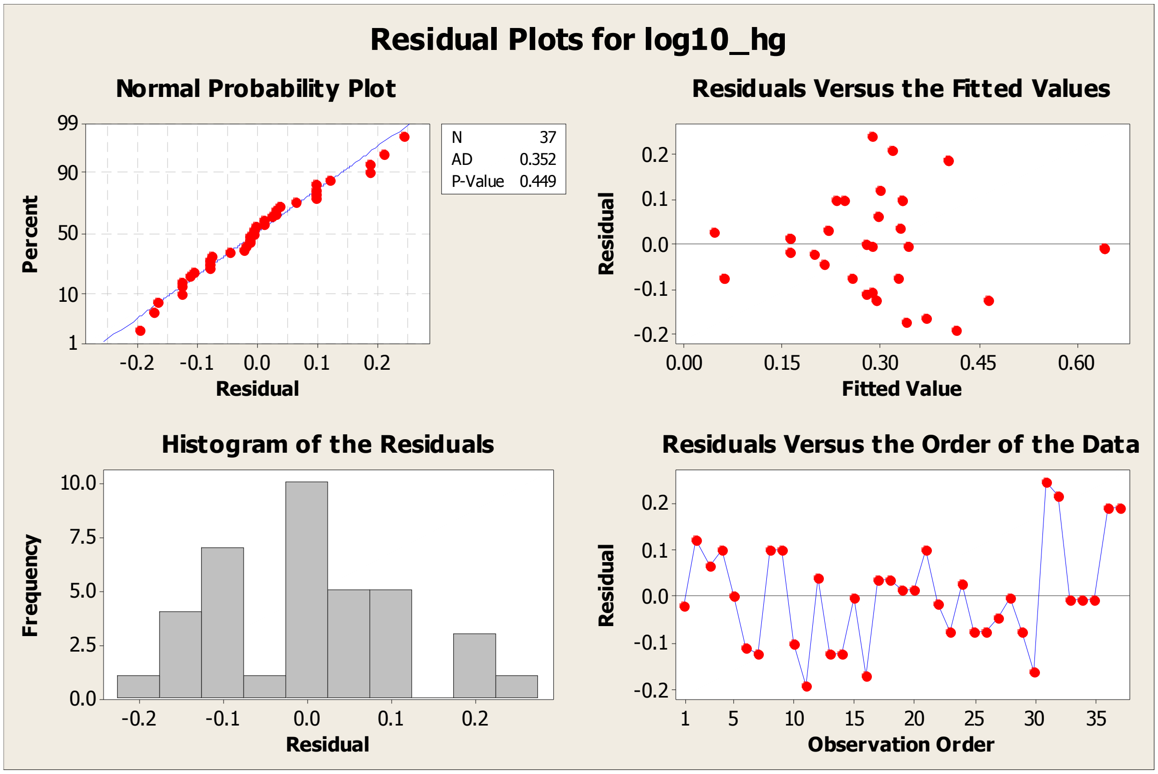
Residual Plots for log10_hg
Normal Probability Plot
Residuals Versus the Fitted Values
N 37
AD 0.352
P-Value 0.449
Percent
Residual
Fitted Value
Histogram of the Residuals
Residuals Versus the Order of the Data
Frequency
Observation Order

16.

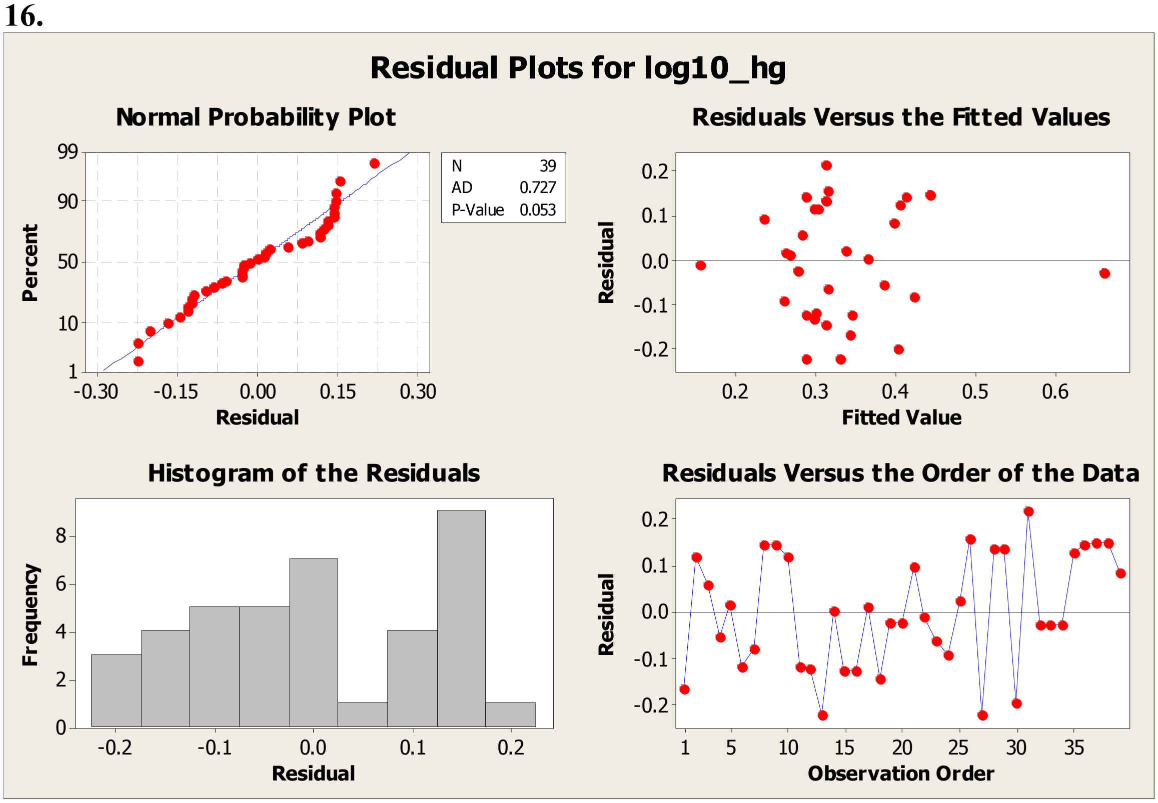
Residual Plots for log10_hg
Normal Probability Plot
Residuals Versus the Fitted Values
N 39
AD 0.727
P-Value 0.053
Percent
Residual
Fitted Value
Histogram of the Residuals
Residuals Versus the Order of the Data
Frequency
Observation Order

17.

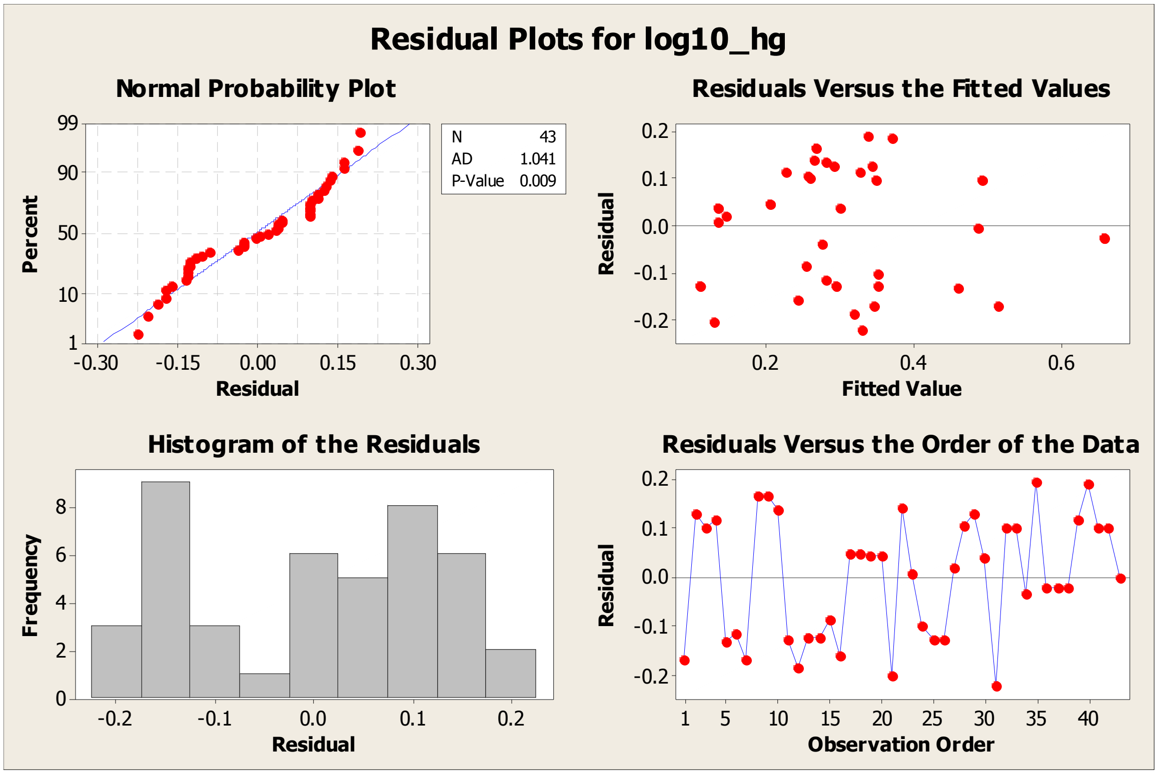
Residual Plots for log10_hg
Normal Probability Plot
N 43
AD 1.041
P-Value 0.009
Percent
Residual
Residuals Versus the Fitted Values
Residual
Fitted Value
Histogram of the Residuals
Frequency
Residual
Residuals Versus the Order of the Data
Residual
Observation Order

18.

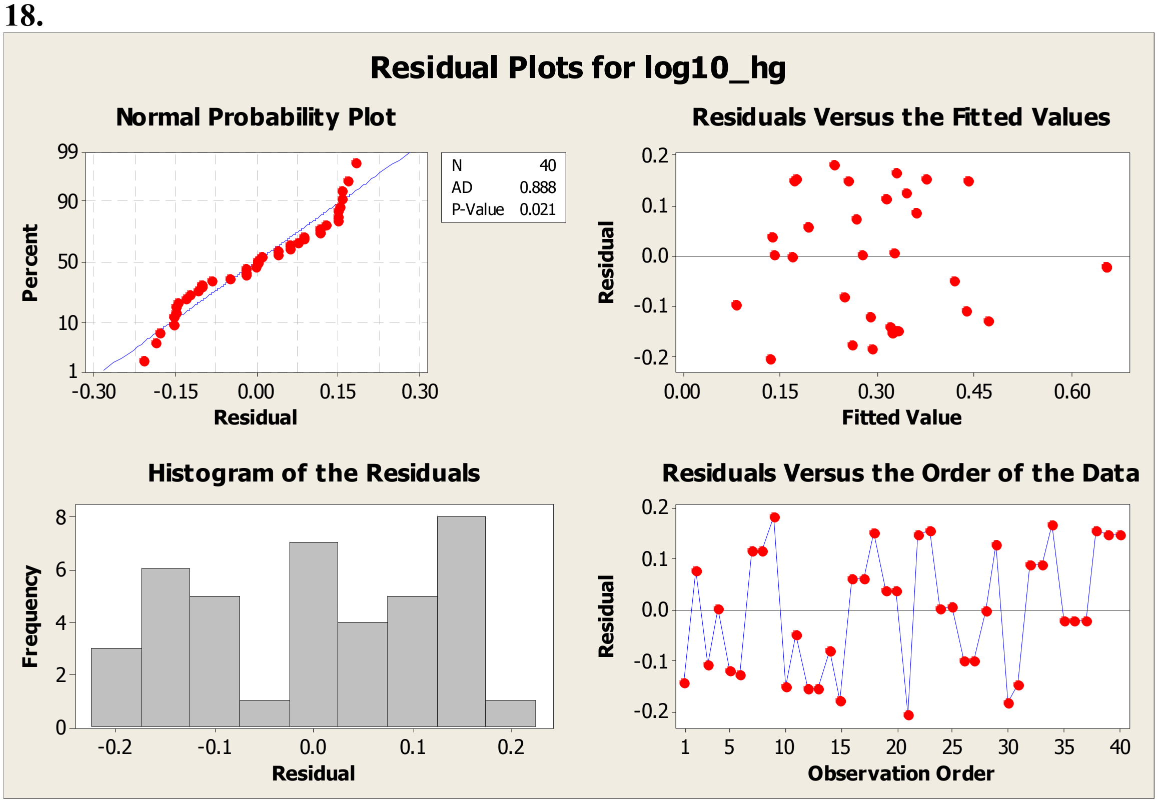
Residual Plots for log10_hg
Normal Probability Plot
N 40
AD 0.888
P-Value 0.021
Percent
Residual
Residuals Versus the Fitted Values
Residual
Fitted Value
Histogram of the Residuals
Frequency
Residual
Residuals Versus the Order of the Data
Residual
Observation Order

19.

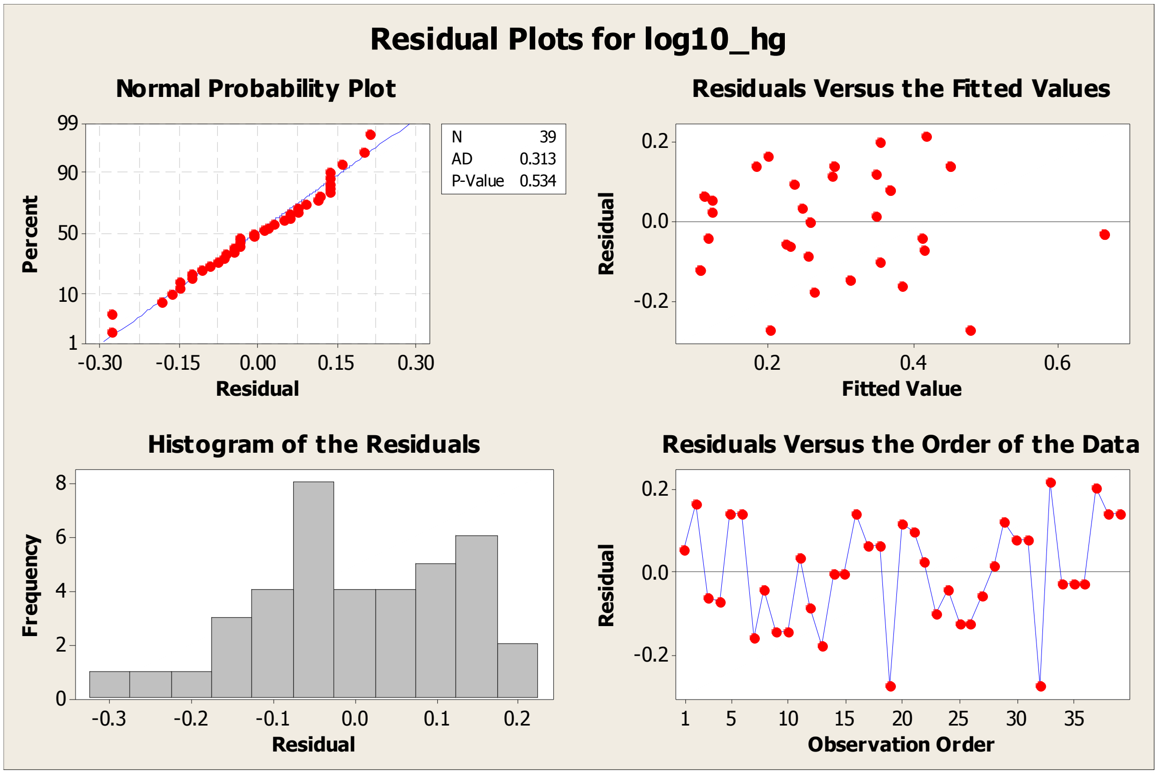
Residual Plots for log10_hg
Normal Probability Plot
Percent
99
90
50
10
1
-0.30
-0.15
0.00
0.15
0.30
Residual
N 39
AD 0.313
P-Value 0.534
Residuals Versus the Fitted Values
Residual
0.2
0.0
-0.2
0.2
0.4
0.6
Fitted Value
Histogram of the Residuals
Frequency
8
6
4
2
0
-0.3
-0.2
-0.1
0.0
0.1
0.2
Residual
Residuals Versus the Order of the Data
Residual
0.2
0.0
-0.2
1
5
10
15
20
25
30
35
Observation Order

20.

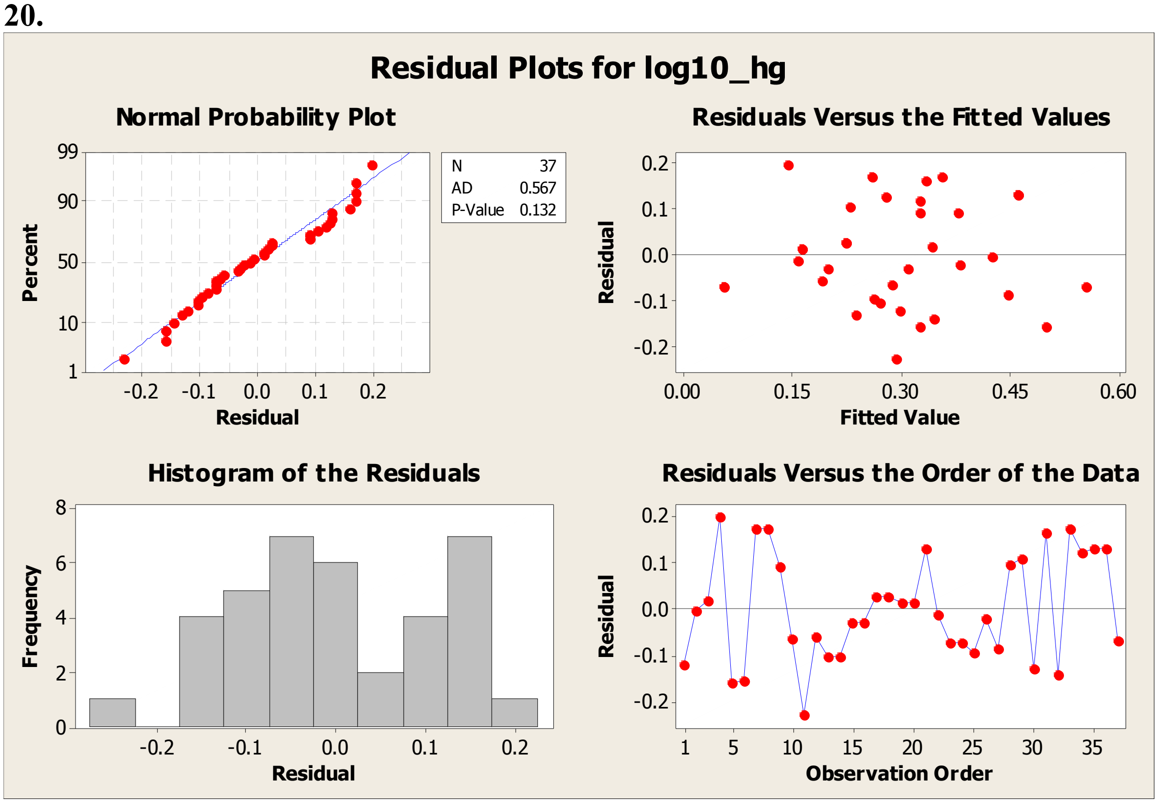
Residual Plots for log10_hg
Normal Probability Plot
Percent
99
90
50
10
1
-0.2
-0.1
0.0
0.1
0.2
Residual
N 37
AD 0.567
P-Value 0.132
Residuals Versus the Fitted Values
Residual
0.2
0.1
0.0
-0.1
-0.2
0.00
0.15
0.30
0.45
0.60
Fitted Value
Histogram of the Residuals
Frequency
8
6
4
2
0
-0.2
-0.1
0.0
0.1
0.2
Residual
Residuals Versus the Order of the Data
Residual
0.2
0.1
0.0
-0.1
-0.2
1
5
10
15
20
25
30
35
Observation Order

21.

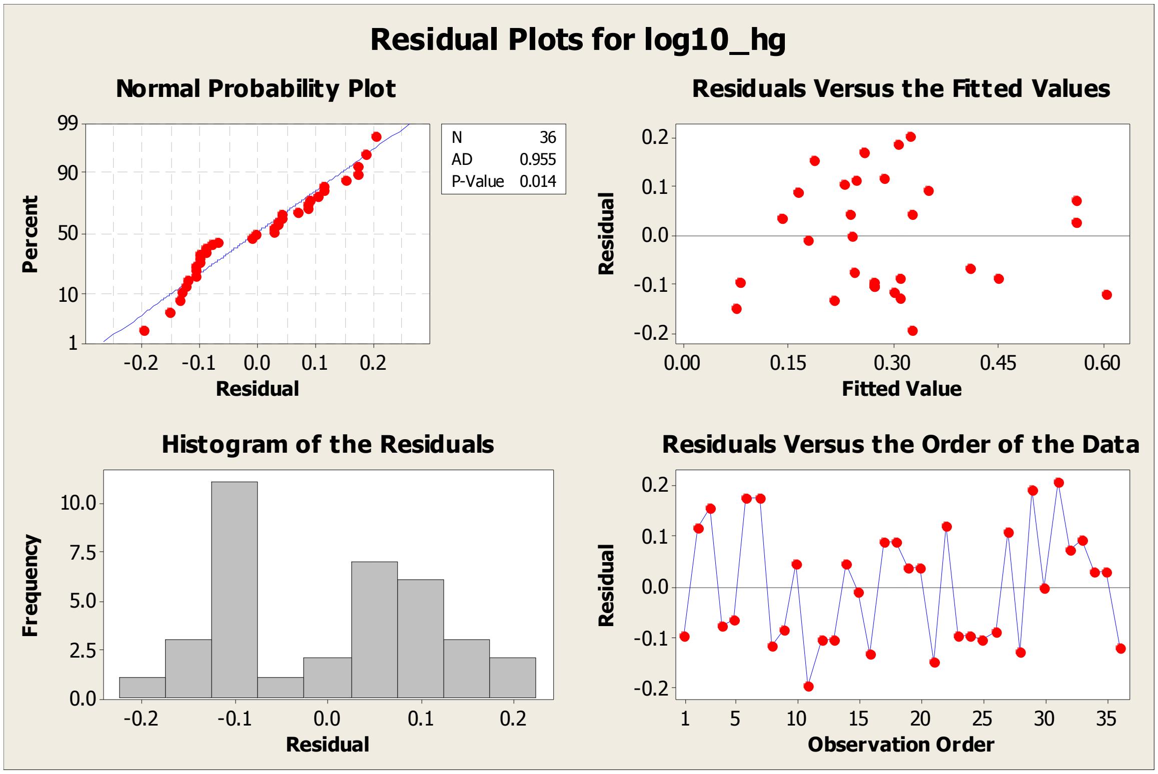

Residual Plots for log10_hg
Normal Probability Plot
Percent
Residual
N 36
AD 0.955
P-Value 0.014
Residuals Versus the Fitted Values
Residual
Fitted Value
Histogram of the Residuals
Frequency
Residual
Residuals Versus the Order of the Data
Residual
Observation Order

22.

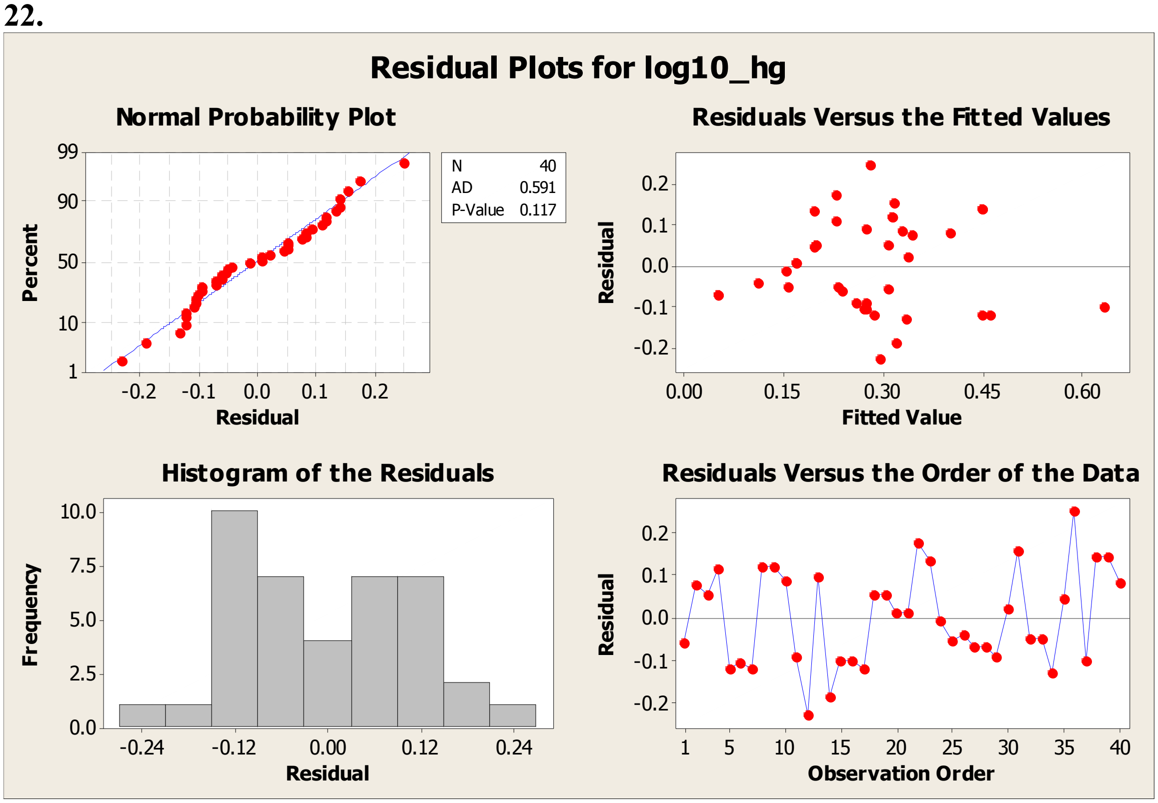

Residual Plots for log10_hg
Normal Probability Plot
Percent
Residual
N 40
AD 0.591
P-Value 0.117
Residuals Versus the Fitted Values
Residual
Fitted Value
Histogram of the Residuals
Frequency
Residual
Residuals Versus the Order of the Data
Residual
Observation Order

23.

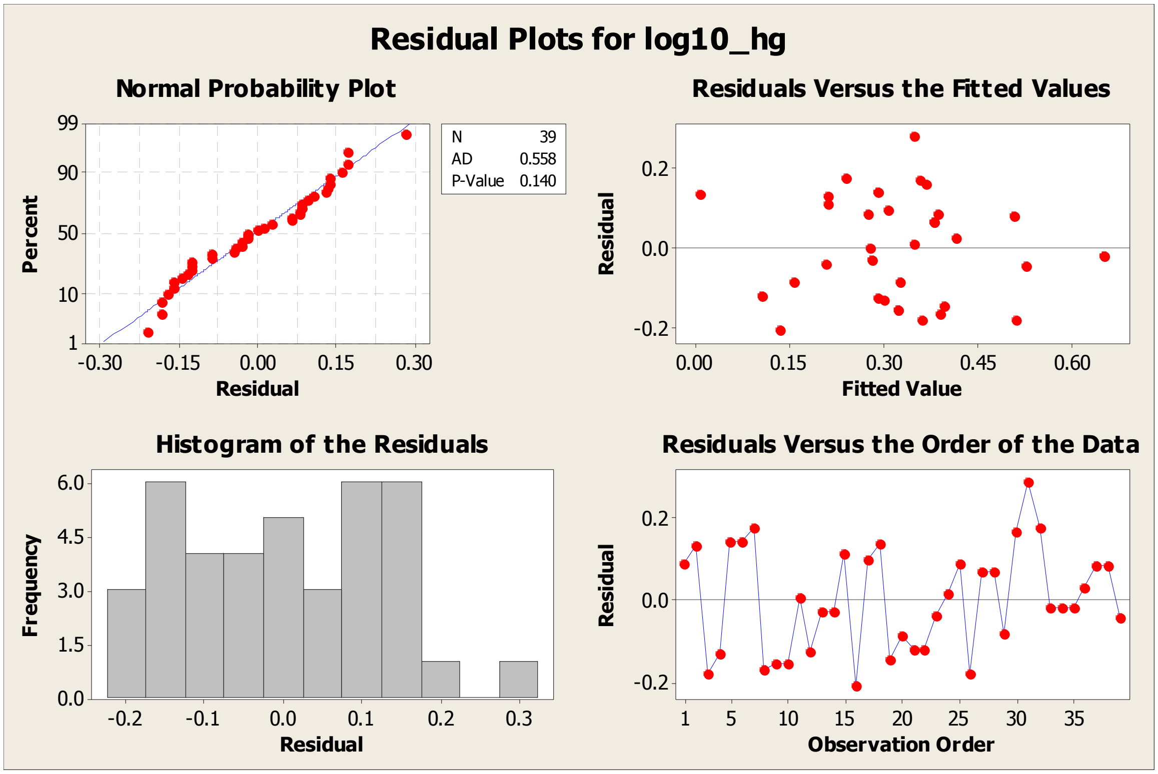
Residual Plots for log10_hg
Normal Probability Plot
Percent
99
90
50
10
1
-0.30
-0.15
0.00
0.15
0.30
Residual
N 39
AD 0.558
P-Value 0.140
Residuals Versus the Fitted Values
Residual
0.2
0.0
-0.2
0.00
0.15
0.30
0.45
0.60
Fitted Value
Histogram of the Residuals
Frequency
6.0
4.5
3.0
1.5
0.0
-0.2
-0.1
0.0
0.1
0.2
0.3
Residual
Residuals Versus the Order of the Data
Residual
0.2
0.0
-0.2
1
5
10
15
20
25
30
35
Observation Order

24.

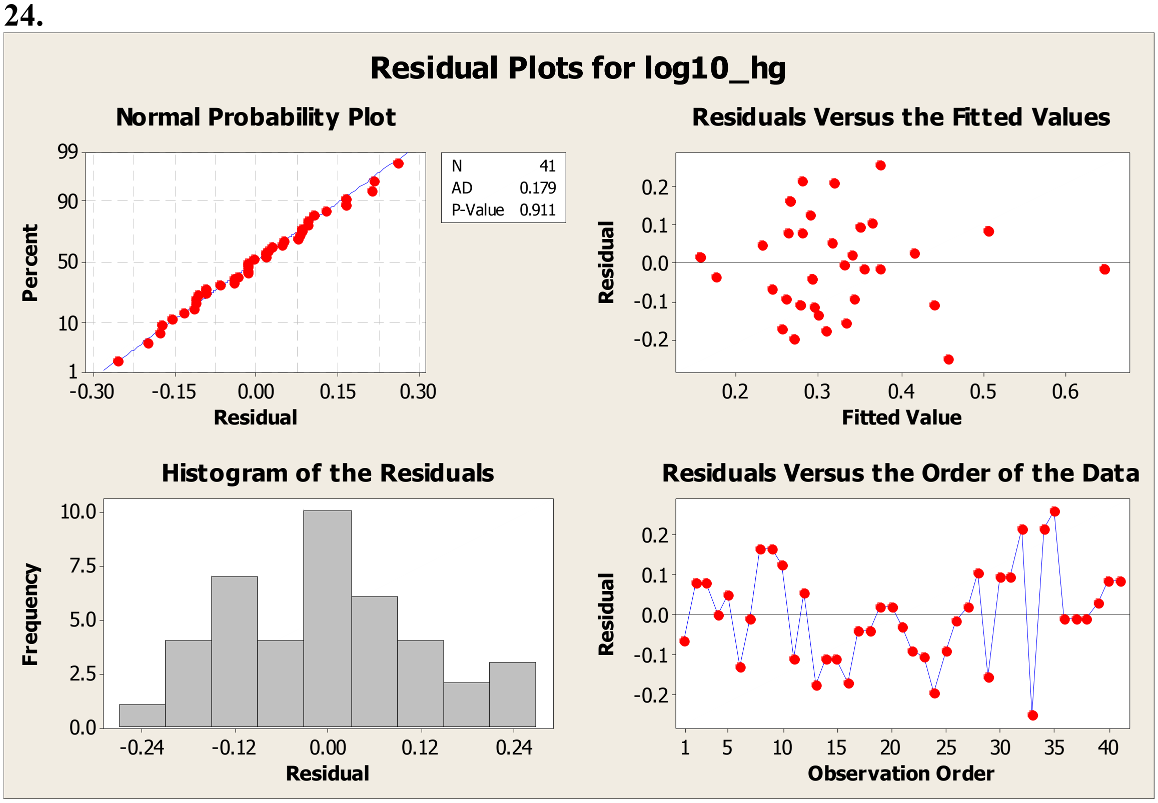
Residual Plots for log10_hg
Normal Probability Plot
Percent
99
90
50
10
1
-0.30
-0.15
0.00
0.15
0.30
Residual
N 41
AD 0.179
P-Value 0.911
Residuals Versus the Fitted Values
Residual
0.2
0.1
0.0
-0.1
-0.2
0.2
0.3
0.4
0.5
0.6
Fitted Value
Histogram of the Residuals
Frequency
10.0
7.5
5.0
2.5
0.0
-0.24
-0.12
0.00
0.12
0.24
Residual
Residuals Versus the Order of the Data
Residual
0.2
0.1
0.0
-0.1
-0.2
1
5
10
15
20
25
30
35
40
Observation Order

25.

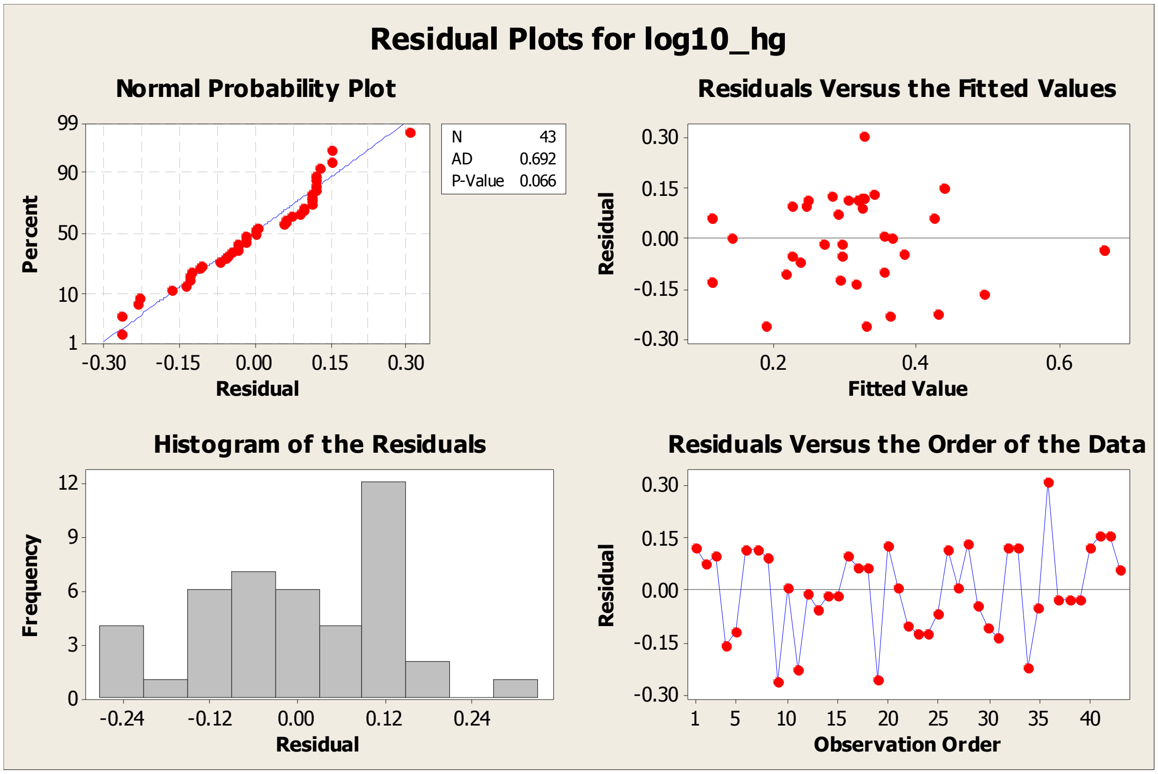

Residual Plots for log10_hg
Normal Probability Plot
Percent
Residual
N 43
AD 0.692
P-Value 0.066
Residuals Versus the Fitted Values
Residual
Fitted Value
Histogram of the Residuals
Frequency
Residual
Residuals Versus the Order of the Data
Residual
Observation Order

26.

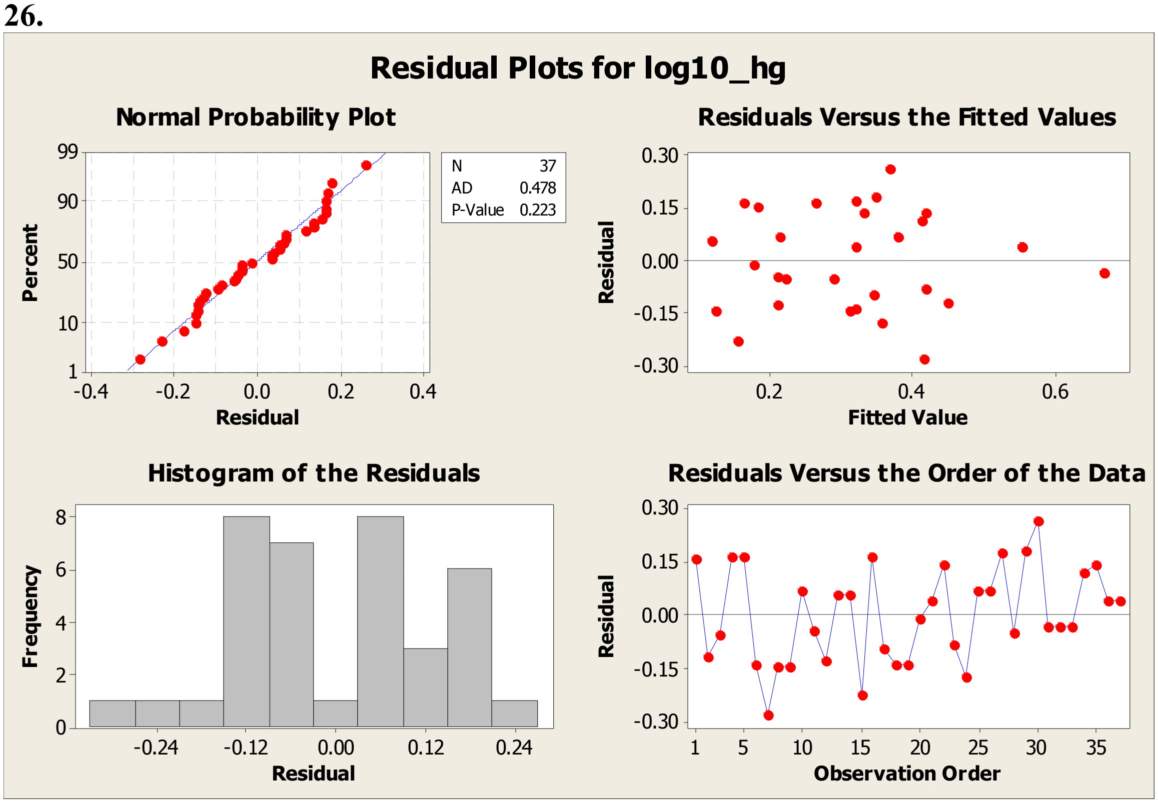

Residual Plots for log10_hg
Normal Probability Plot
Percent
Residual
N 37
AD 0.478
P-Value 0.223
Residuals Versus the Fitted Values
Residual
Fitted Value
Histogram of the Residuals
Frequency
Residual
Residuals Versus the Order of the Data
Residual
Observation Order

27.

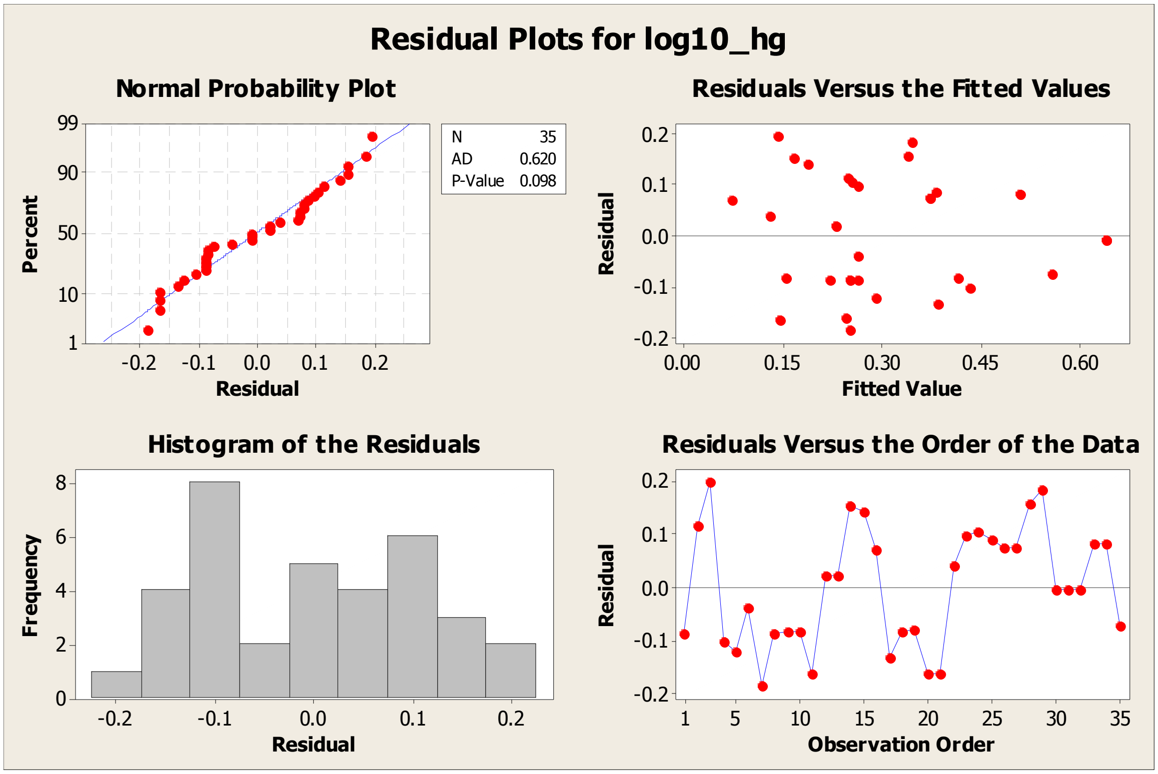
Residual Plots for log10_hg
Normal Probability Plot
Percent
Residual
N 35
AD 0.620
P-Value 0.098
Residuals Versus the Fitted Values
Residual
Fitted Value
Histogram of the Residuals
Frequency
Residual
Residuals Versus the Order of the Data
Residual
Observation Order

28.

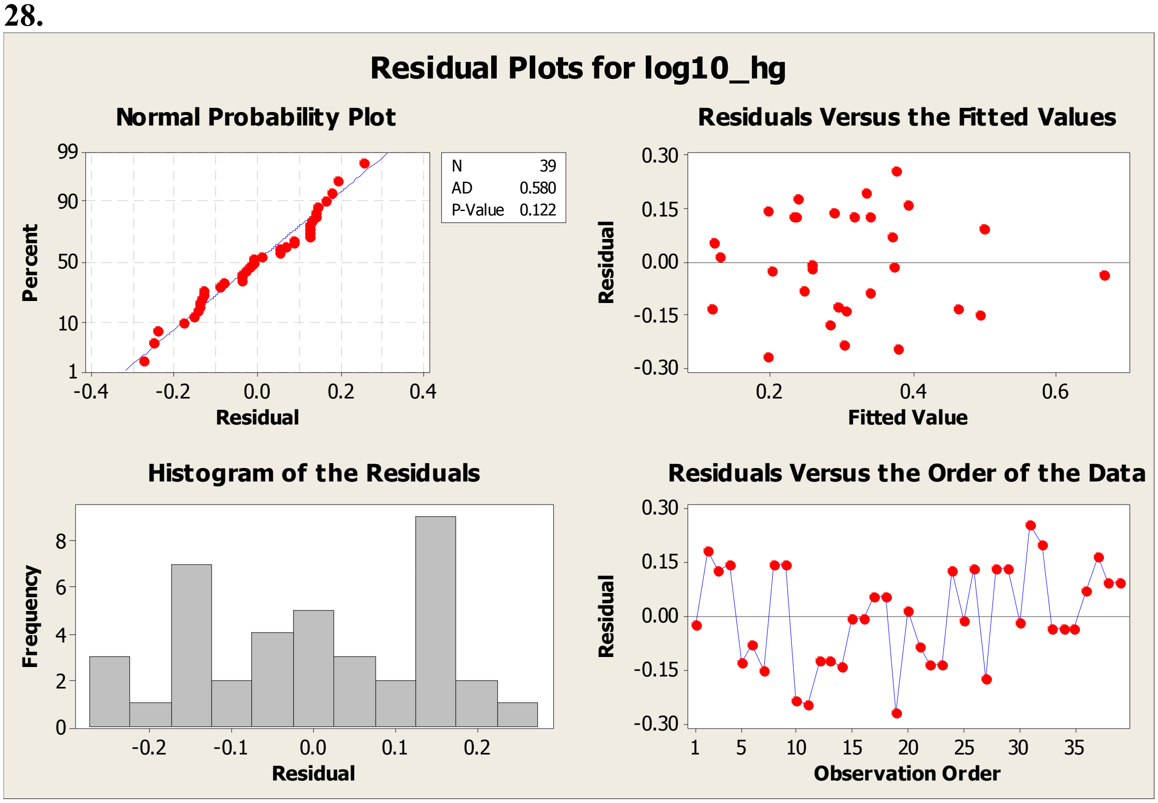
Residual Plots for log10_hg
Normal Probability Plot
Percent
Residual
N 39
AD 0.580
P-Value 0.122
Residuals Versus the Fitted Values
Residual
Fitted Value
Histogram of the Residuals
Frequency
Residual
Residuals Versus the Order of the Data
Residual
Observation Order

29.

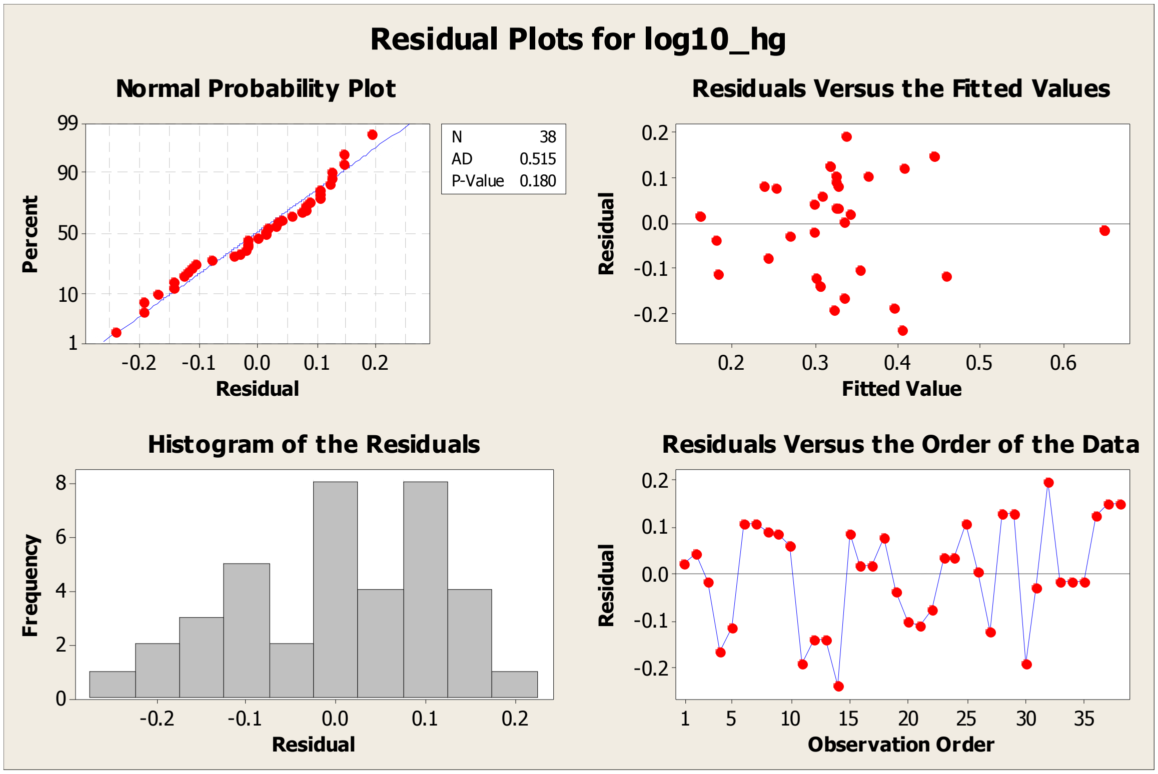
Residual Plots for log10_hg
Normal Probability Plot
Percent
Residual
N 38
AD 0.515
P-Value 0.180
Residuals Versus the Fitted Values
Residual
Fitted Value
Histogram of the Residuals
Frequency
Residual
Residuals Versus the Order of the Data
Residual
Observation Order

30.

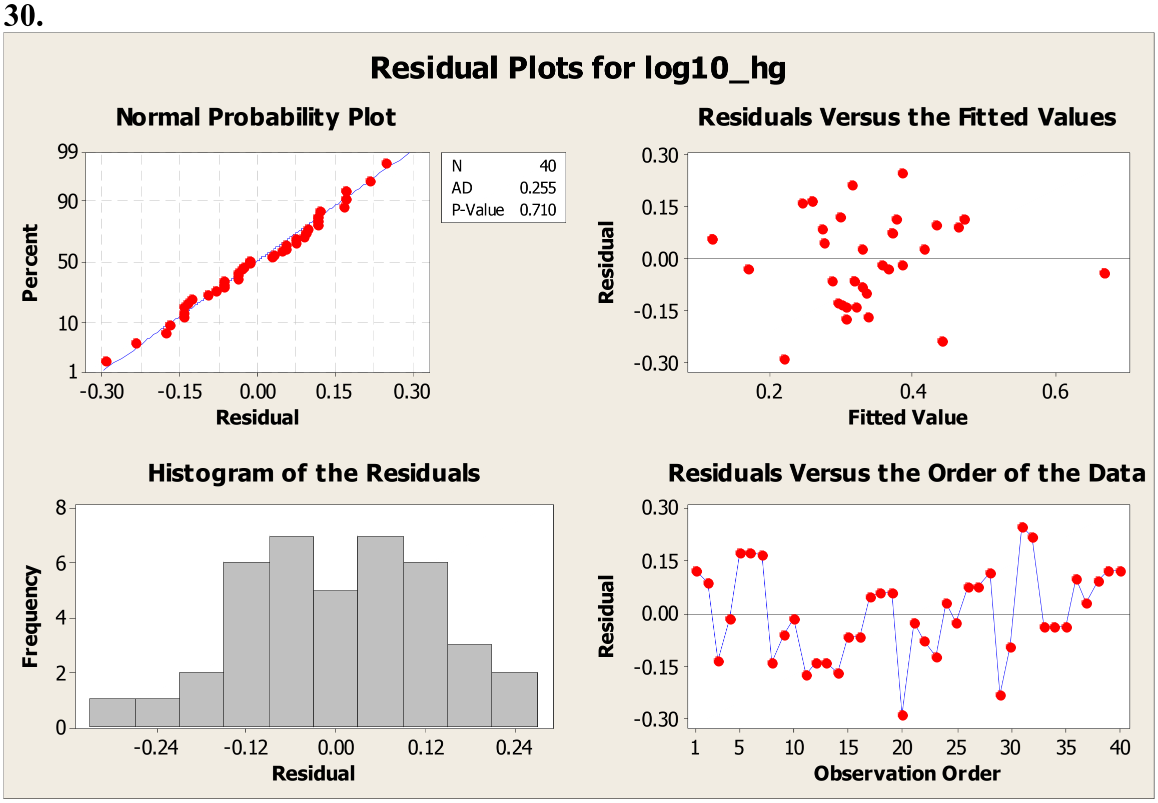
Residual Plots for log10_hg
Normal Probability Plot
Percent
Residual
N 40
AD 0.255
P-Value 0.710
Residuals Versus the Fitted Values
Residual
Fitted Value
Histogram of the Residuals
Frequency
Residual
Residuals Versus the Order of the Data
Residual
Observation Order

Appendix C. Residual Plots from Sensitivity Analysis (600m)

1.

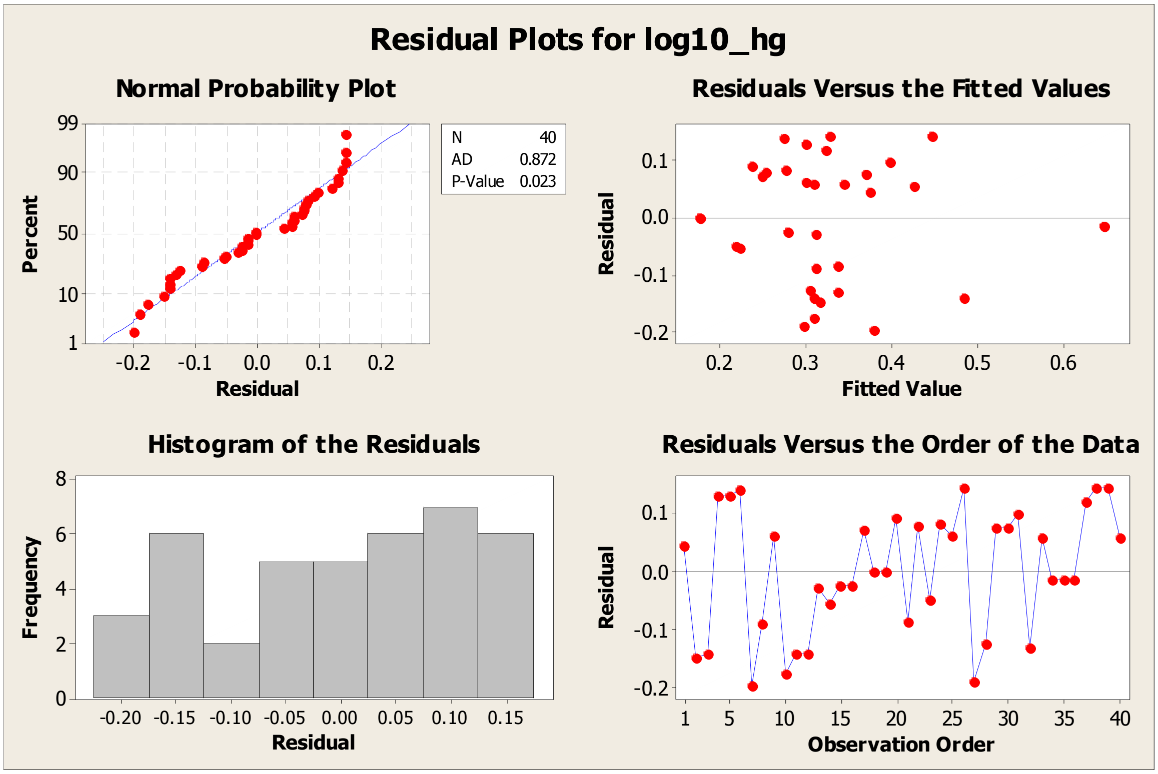

2.

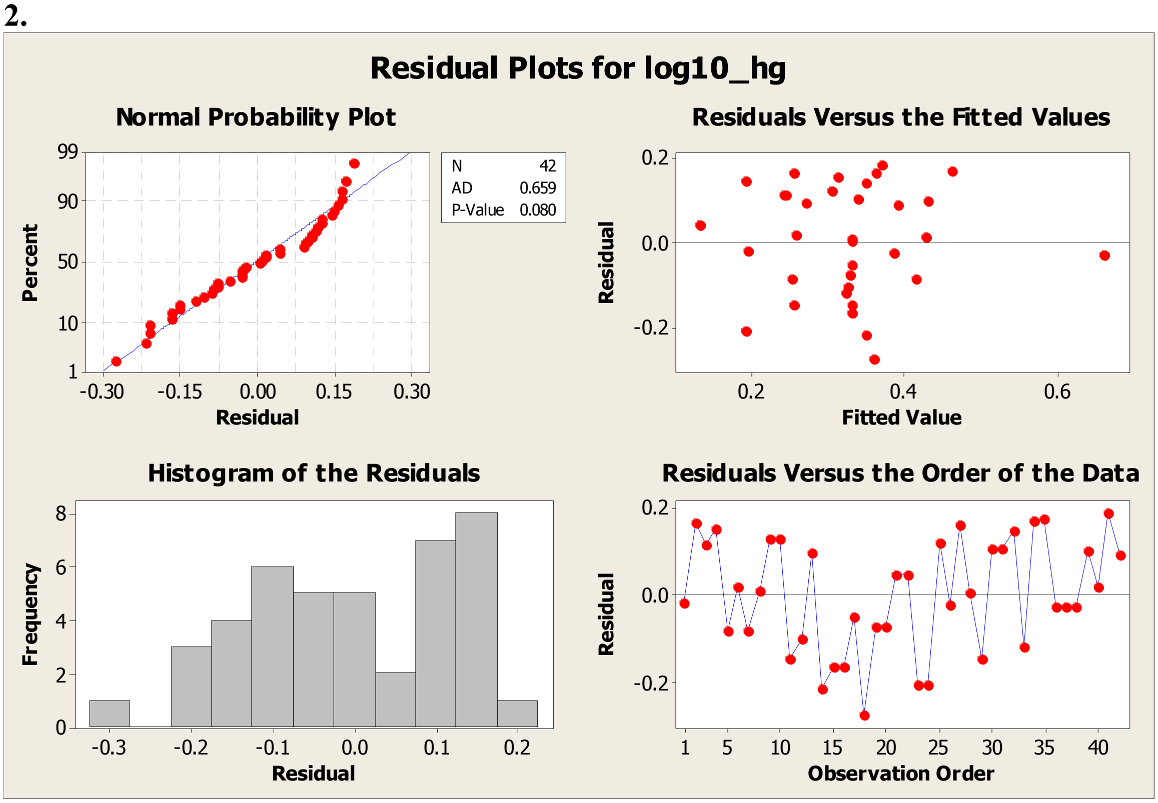

3.

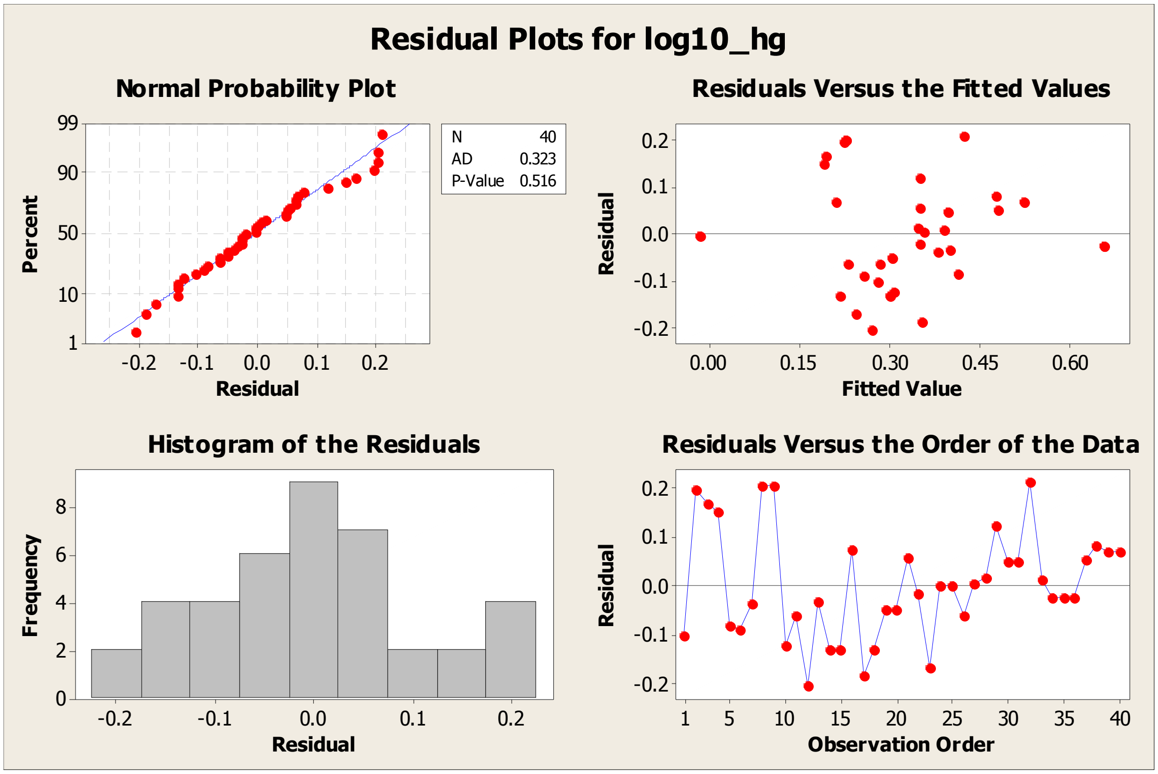
Residual Plots for log10_hg
Normal Probability Plot
Residuals Versus the Fitted Values
N 40
AD 0.323
P-Value 0.516
Percent
Residual
Fitted Value
Histogram of the Residuals
Residuals Versus the Order of the Data
Frequency
Observation Order

4.

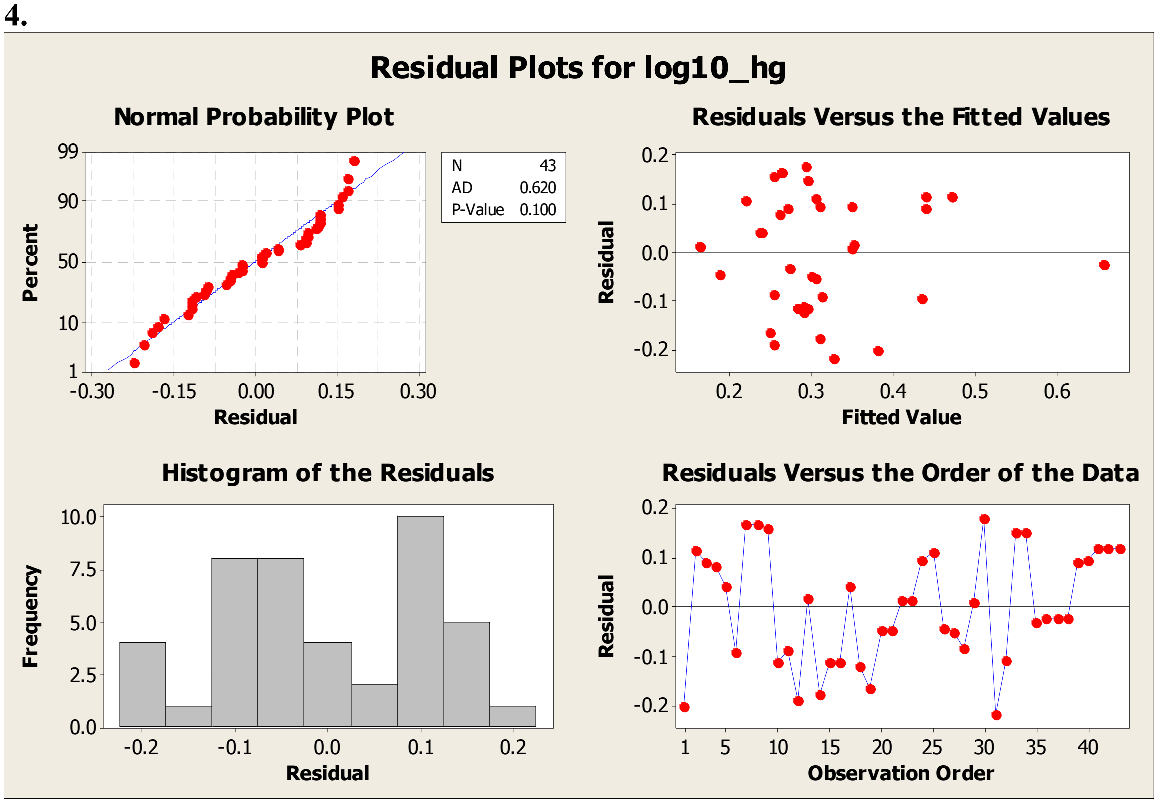
Residual Plots for log10_hg
Normal Probability Plot
Residuals Versus the Fitted Values
N 43
AD 0.620
P-Value 0.100
Percent
Residual
Fitted Value
Histogram of the Residuals
Residuals Versus the Order of the Data
Frequency
Observation Order

5.

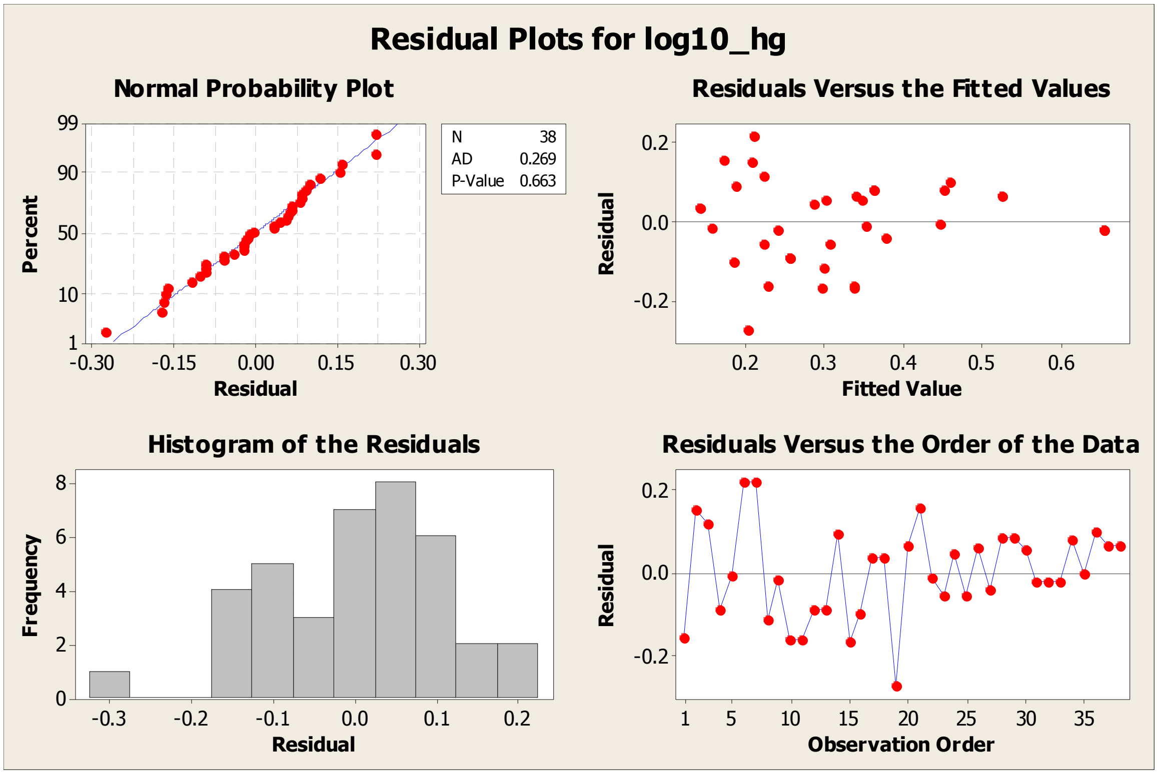
Residual Plots for log10_hg
Normal Probability Plot
Percent
99
90
50
10
1
-0.30
-0.15
0.00
0.15
0.30
Residual
N 38
AD 0.269
P-Value 0.663
Residuals Versus the Fitted Values
Residual
0.2
0.0
-0.2
0.2
0.3
0.4
0.5
0.6
Fitted Value
Histogram of the Residuals
Frequency
8
6
4
2
0
-0.3
-0.2
-0.1
0.0
0.1
0.2
Residual
Residuals Versus the Order of the Data
Residual
0.2
0.0
-0.2
1
5
10
15
20
25
30
35
Observation Order

6.

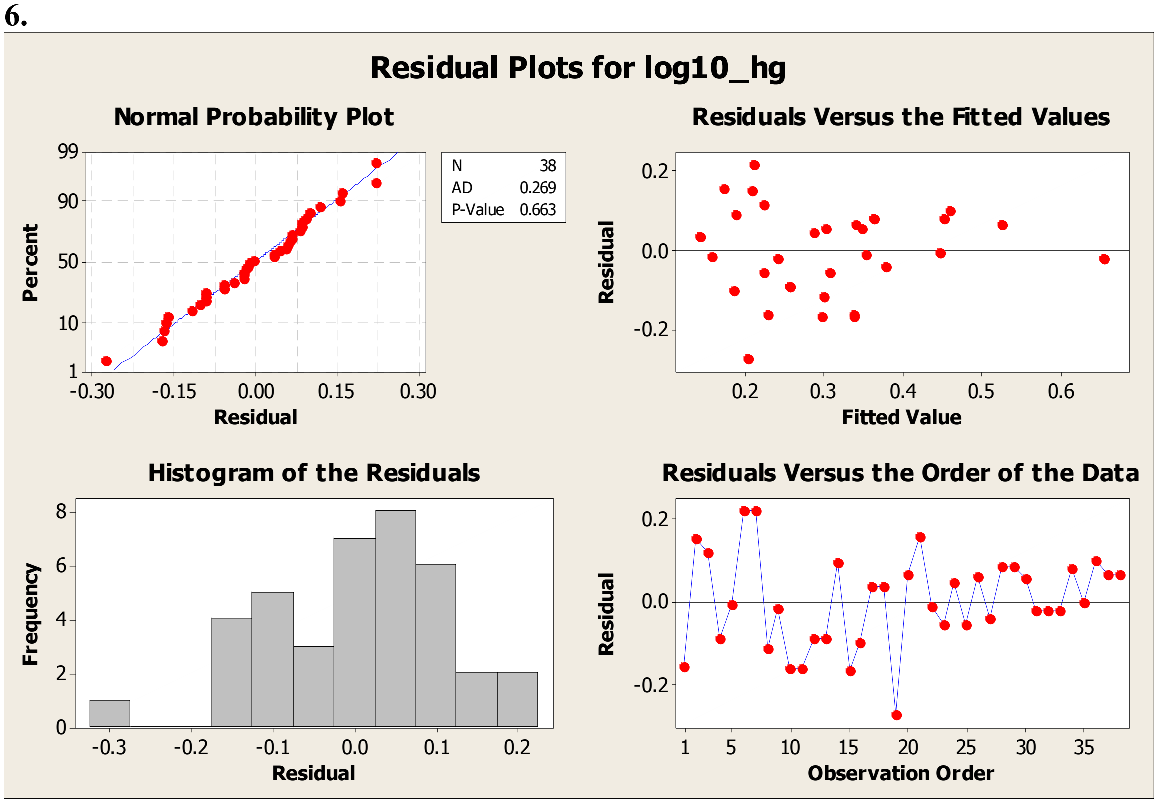
Residual Plots for log10_hg
Normal Probability Plot
Percent
99
90
50
10
1
-0.30
-0.15
0.00
0.15
0.30
Residual
N 38
AD 0.269
P-Value 0.663
Residuals Versus the Fitted Values
Residual
0.2
0.0
-0.2
0.2
0.3
0.4
0.5
0.6
Fitted Value
Histogram of the Residuals
Frequency
8
6
4
2
0
-0.3
-0.2
-0.1
0.0
0.1
0.2
Residual
Residuals Versus the Order of the Data
Residual
0.2
0.0
-0.2
1
5
10
15
20
25
30
35
Observation Order

7.

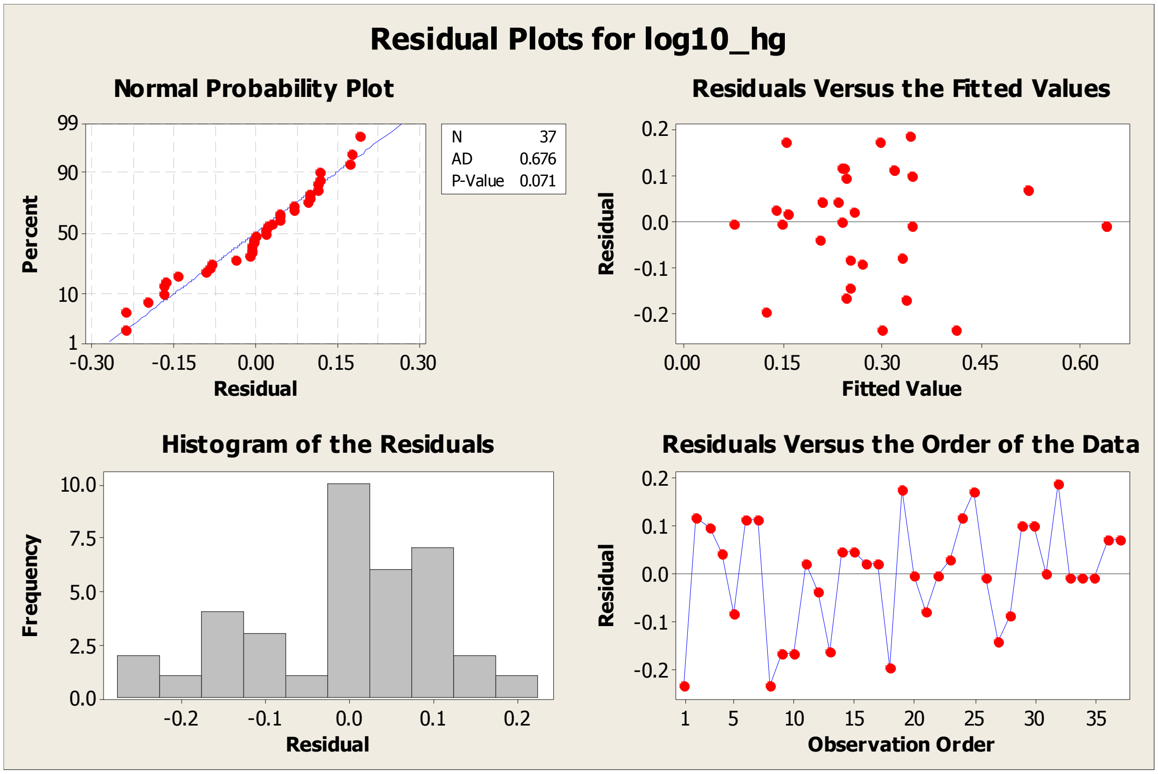

Residual Plots for log10_hg
Normal Probability Plot
Percent
Residual
N 37
AD 0.676
P-Value 0.071
Residuals Versus the Fitted Values
Residual
Fitted Value
Histogram of the Residuals
Frequency
Residual
Residuals Versus the Order of the Data
Residual
Observation Order

8.

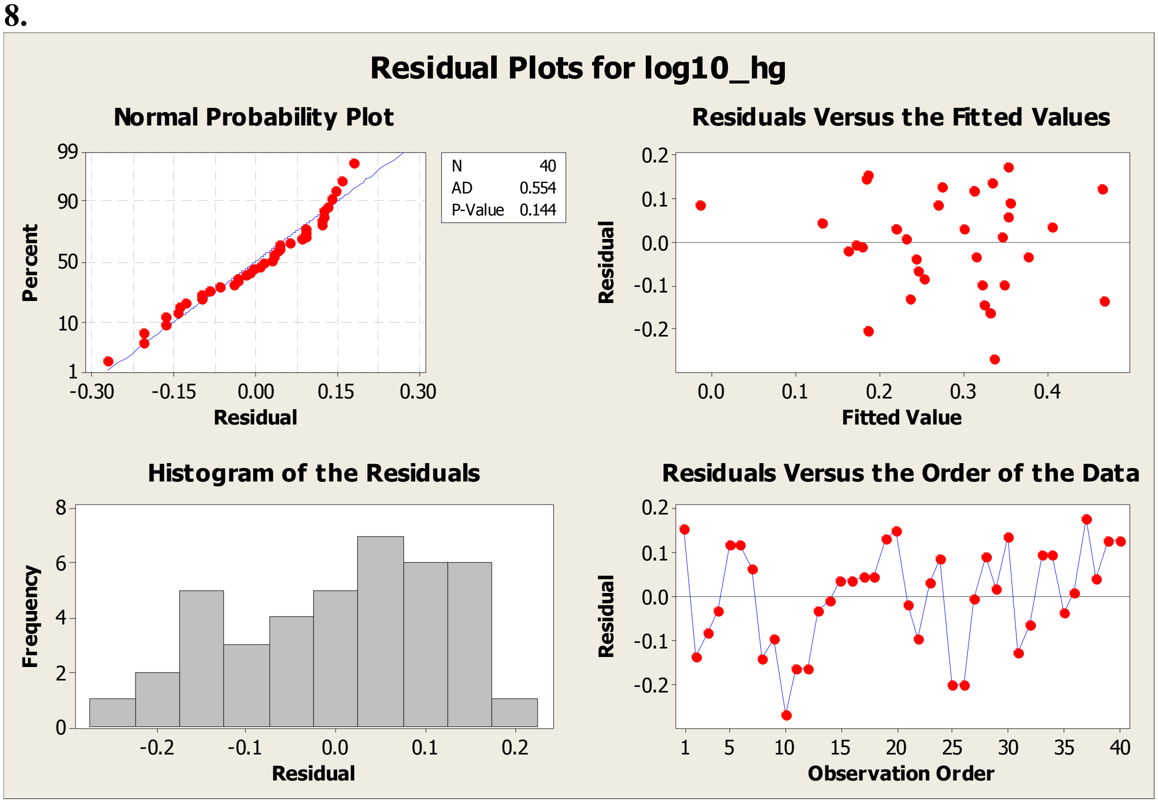

Residual Plots for log10_hg
Normal Probability Plot
Percent
Residual
N 40
AD 0.554
P-Value 0.144
Residuals Versus the Fitted Values
Residual
Fitted Value
Histogram of the Residuals
Frequency
Residual
Residuals Versus the Order of the Data
Residual
Observation Order

9.

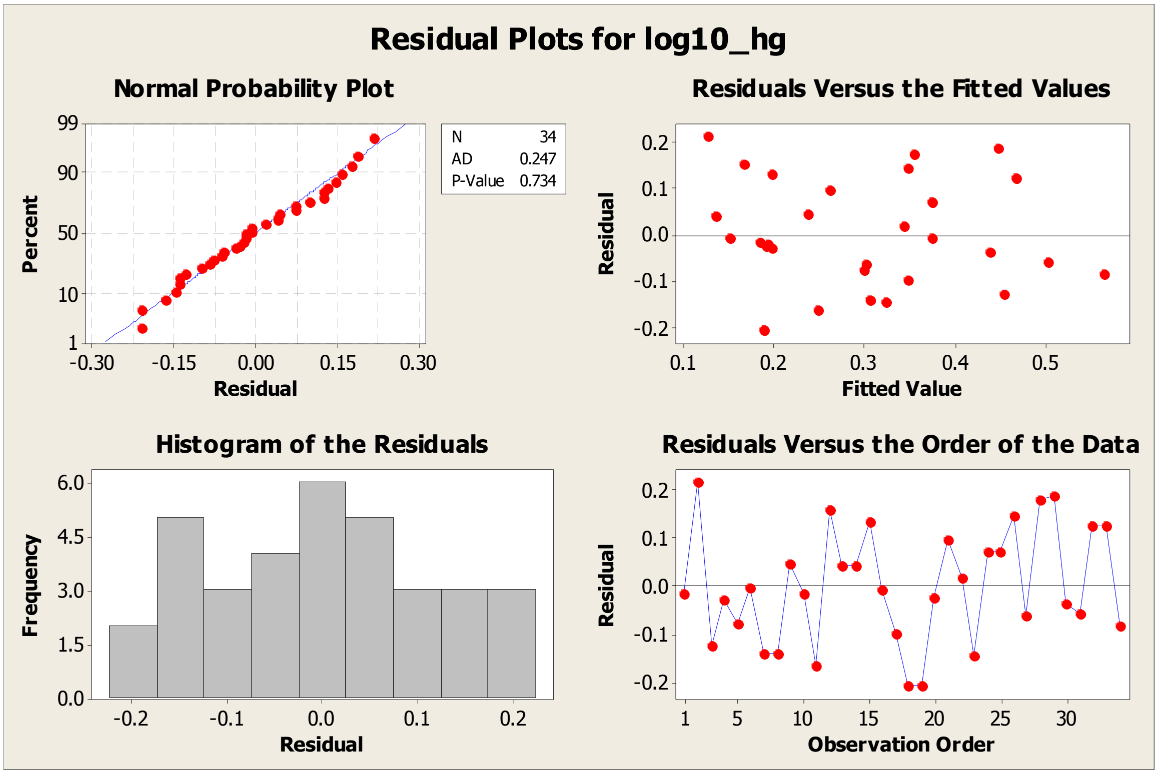

Residual Plots for log10_hg
Normal Probability Plot
N 34
AD 0.247
P-Value 0.734
Percent
Residual
Residuals Versus the Fitted Values
Residual
Fitted Value
Histogram of the Residuals
Frequency
Residual
Residuals Versus the Order of the Data
Residual
Observation Order

10.

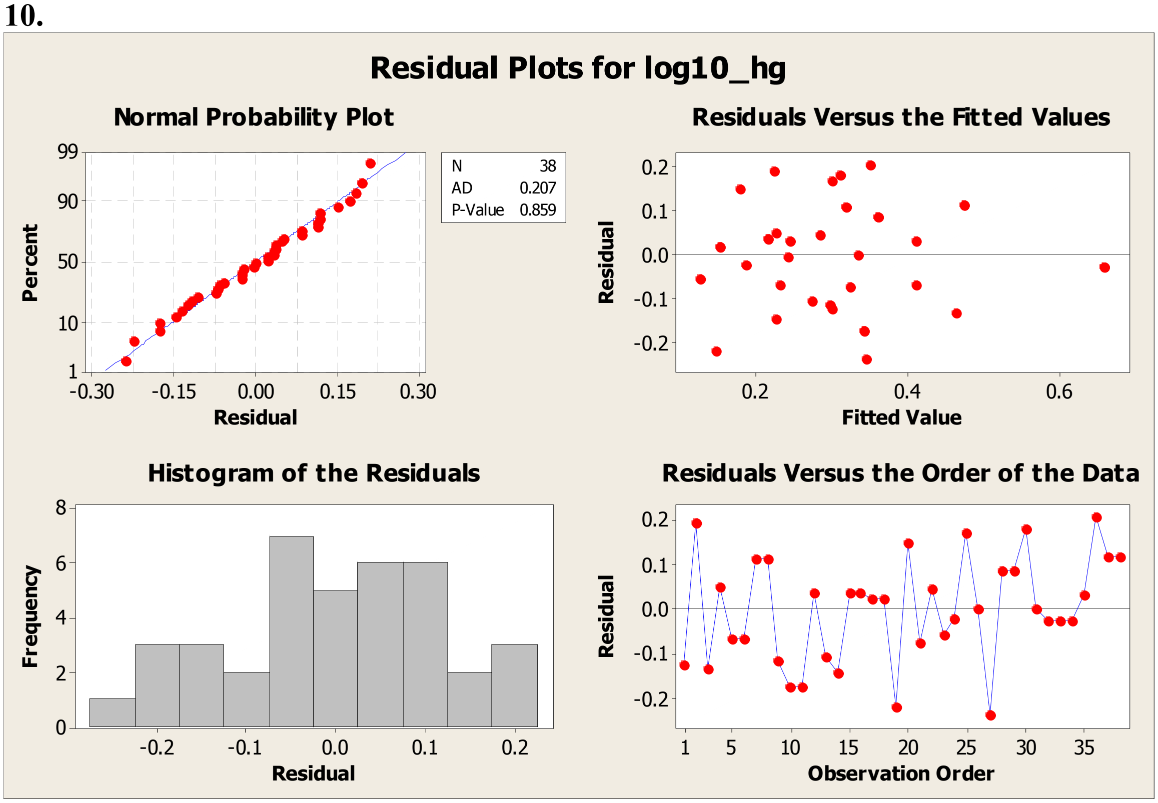

Residual Plots for log10_hg
Normal Probability Plot
N 38
AD 0.207
P-Value 0.859
Percent
Residual
Residuals Versus the Fitted Values
Residual
Fitted Value
Histogram of the Residuals
Frequency
Residual
Residuals Versus the Order of the Data
Residual
Observation Order

11.

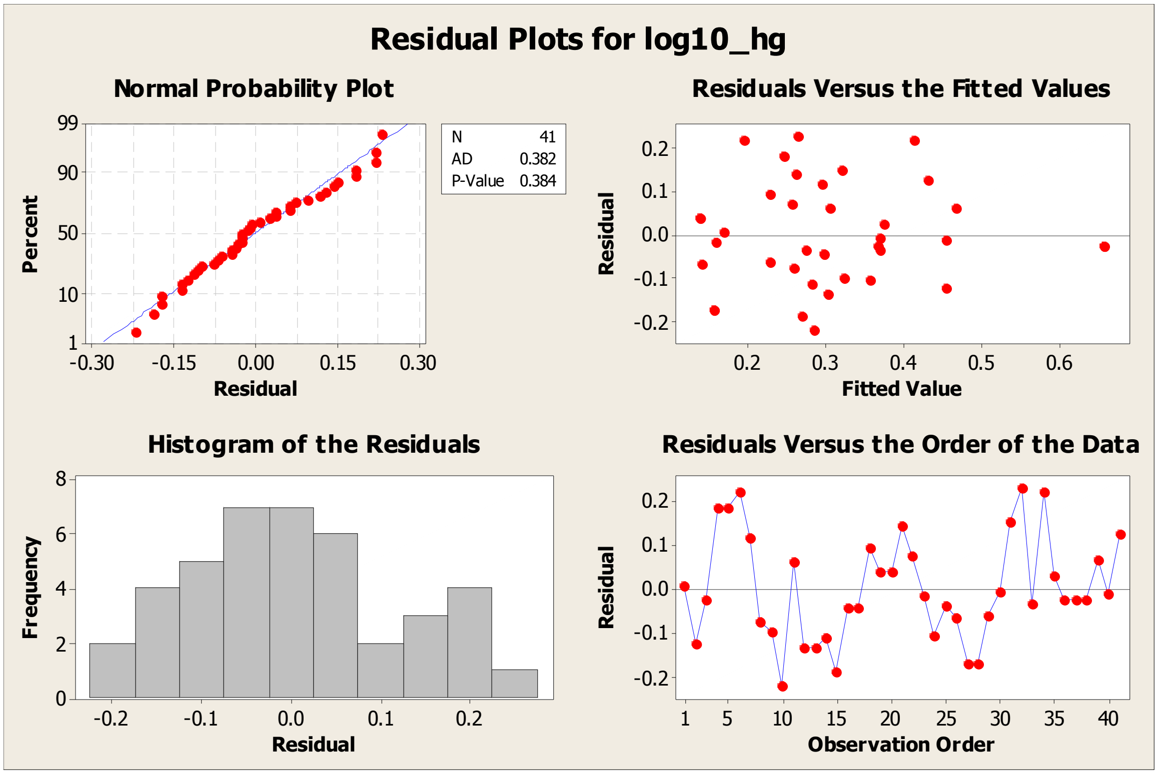
Residual Plots for log10_hg
Normal Probability Plot
N 41
AD 0.382
P-Value 0.384
Percent
Residual
Residuals Versus the Fitted Values
Residual
Fitted Value
Histogram of the Residuals
Frequency
Residual
Residuals Versus the Order of the Data
Residual
Observation Order

12.

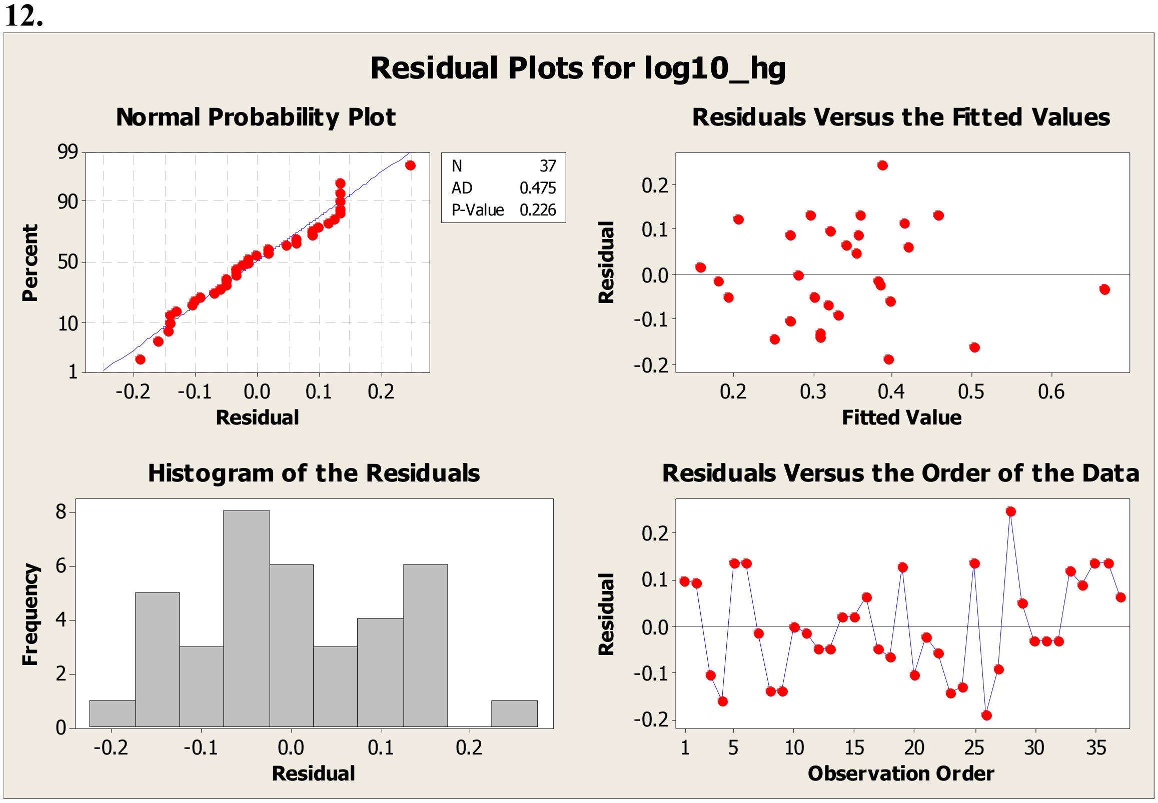
Residual Plots for log10_hg
Normal Probability Plot
N 37
AD 0.475
P-Value 0.226
Percent
Residual
Residuals Versus the Fitted Values
Residual
Fitted Value
Histogram of the Residuals
Frequency
Residual
Residuals Versus the Order of the Data
Residual
Observation Order

13.

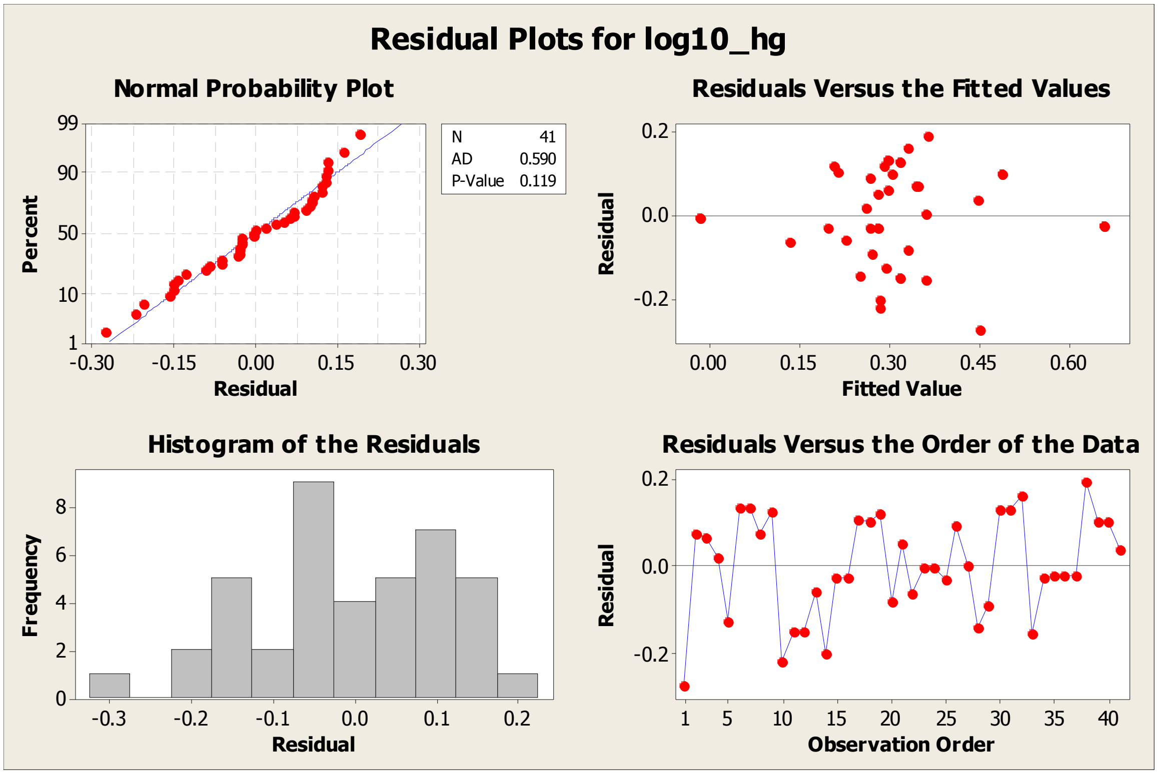

Residual Plots for log10_hg
Normal Probability Plot
Residuals Versus the Fitted Values
Histogram of the Residuals
Residuals Versus the Order of the Data
N 41
AD 0.590
P-Value 0.119
Percent
Residual
Fitted Value
Frequency
Observation Order

14.

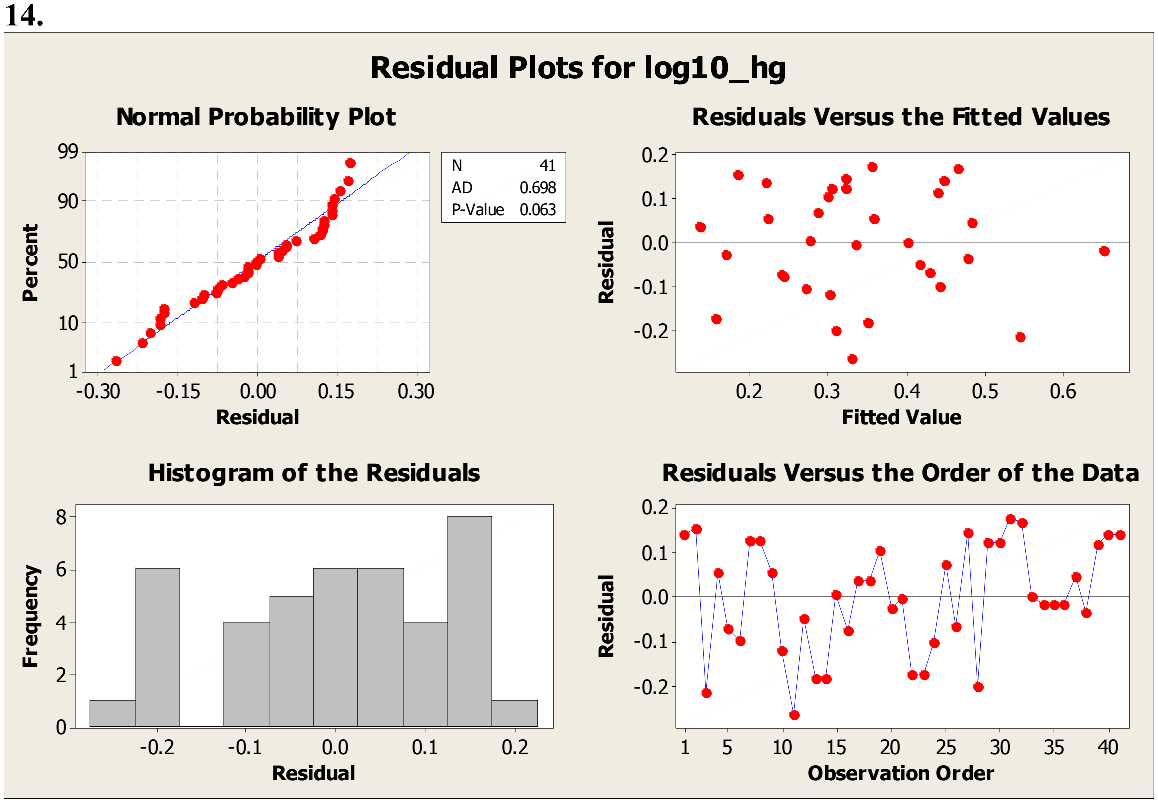

Residual Plots for log10_hg
Normal Probability Plot
Residuals Versus the Fitted Values
Histogram of the Residuals
Residuals Versus the Order of the Data
N 41
AD 0.698
P-Value 0.063
Percent
Residual
Fitted Value
Frequency
Observation Order

15.

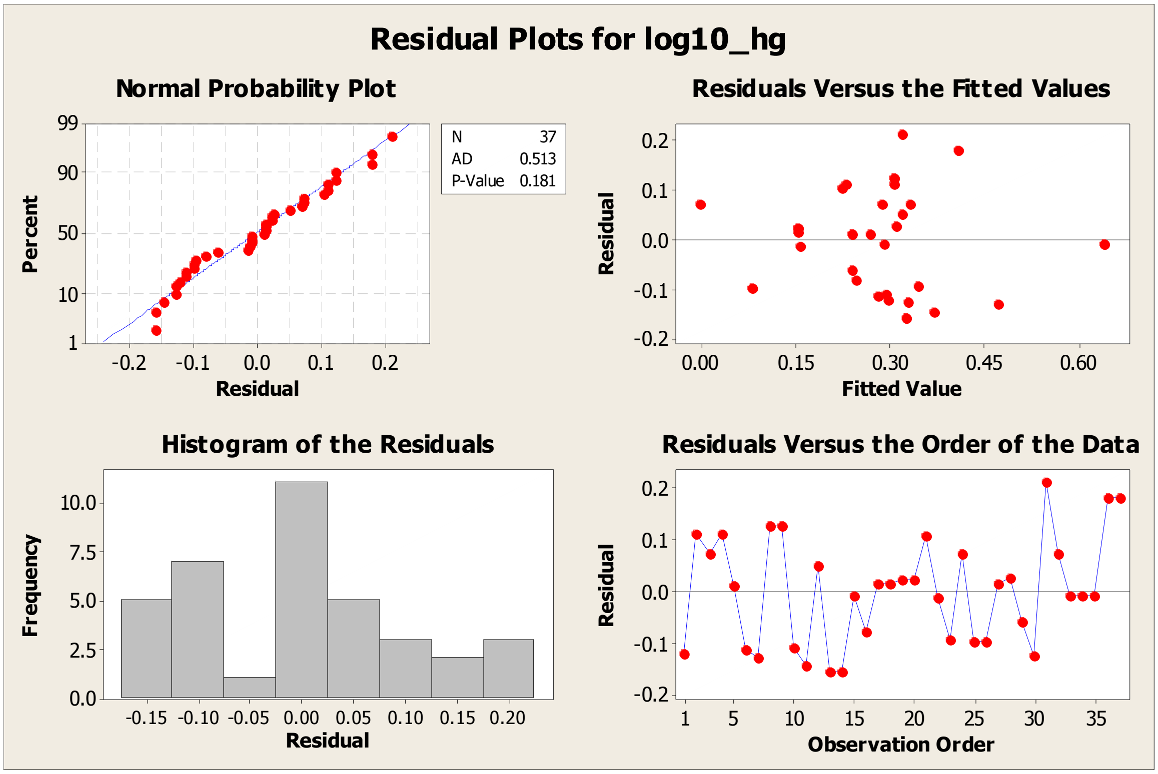
Residual Plots for log10_hg
Normal Probability Plot
N 37
AD 0.513
P-Value 0.181
Percent
Residual
Residuals Versus the Fitted Values
Residual
Fitted Value
Histogram of the Residuals
Frequency
Residual
Residuals Versus the Order of the Data
Residual
Observation Order

16.

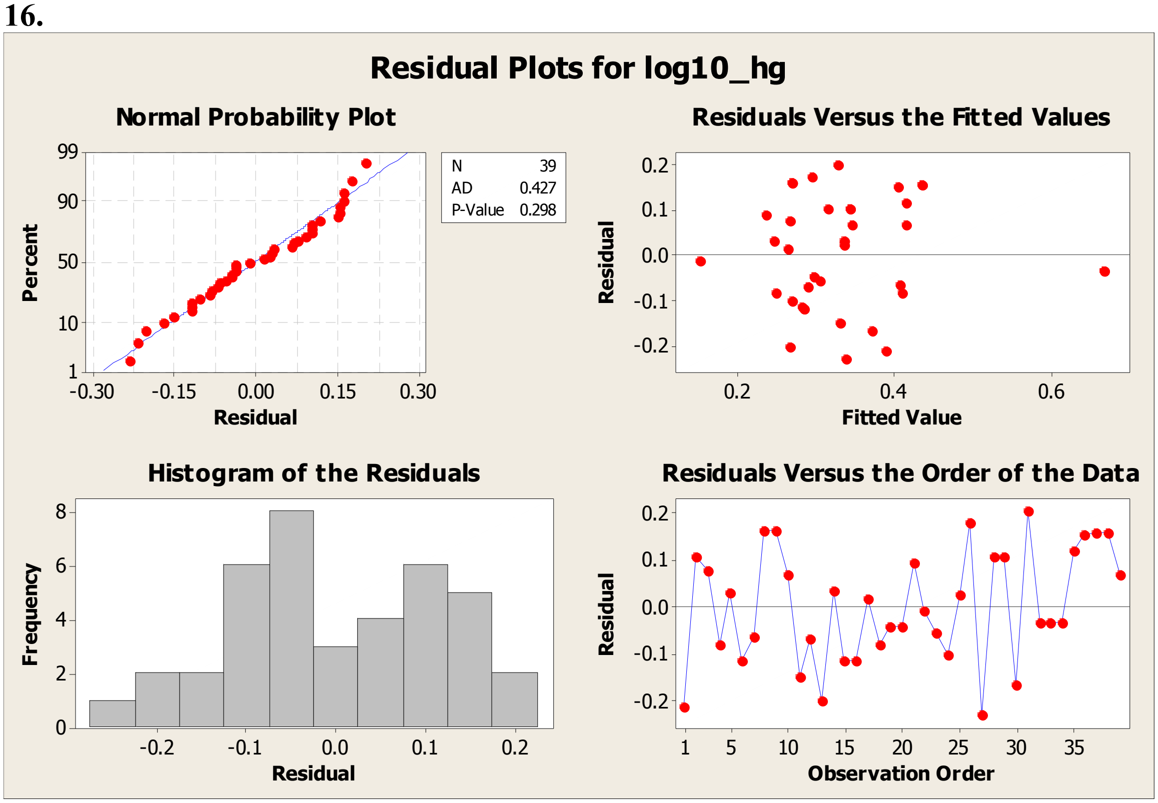
Residual Plots for log10_hg
Normal Probability Plot
N 39
AD 0.427
P-Value 0.298
Percent
Residual
Residuals Versus the Fitted Values
Residual
Fitted Value
Histogram of the Residuals
Frequency
Residual
Residuals Versus the Order of the Data
Residual
Observation Order

17.

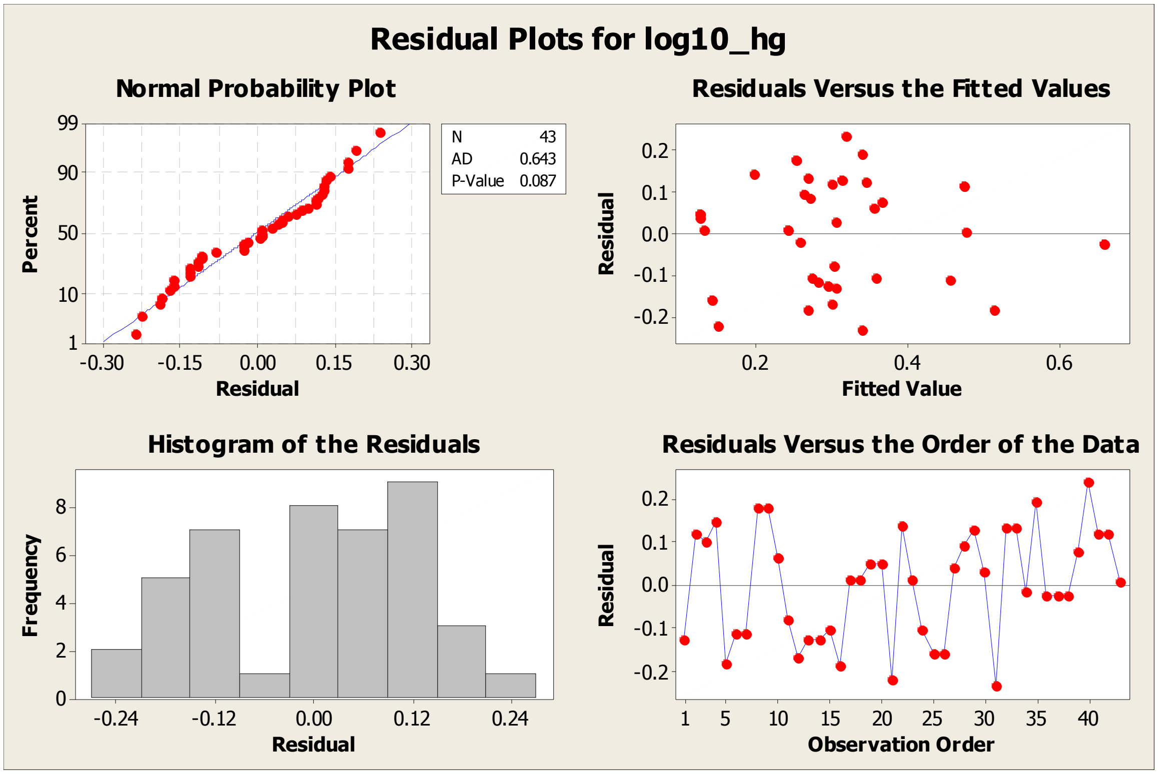
Residual Plots for log10_hg
Normal Probability Plot
Residuals Versus the Fitted Values
N 43
AD 0.643
P-Value 0.087
Percent
Residual
Fitted Value
Histogram of the Residuals
Residuals Versus the Order of the Data
Frequency
Observation Order

18.

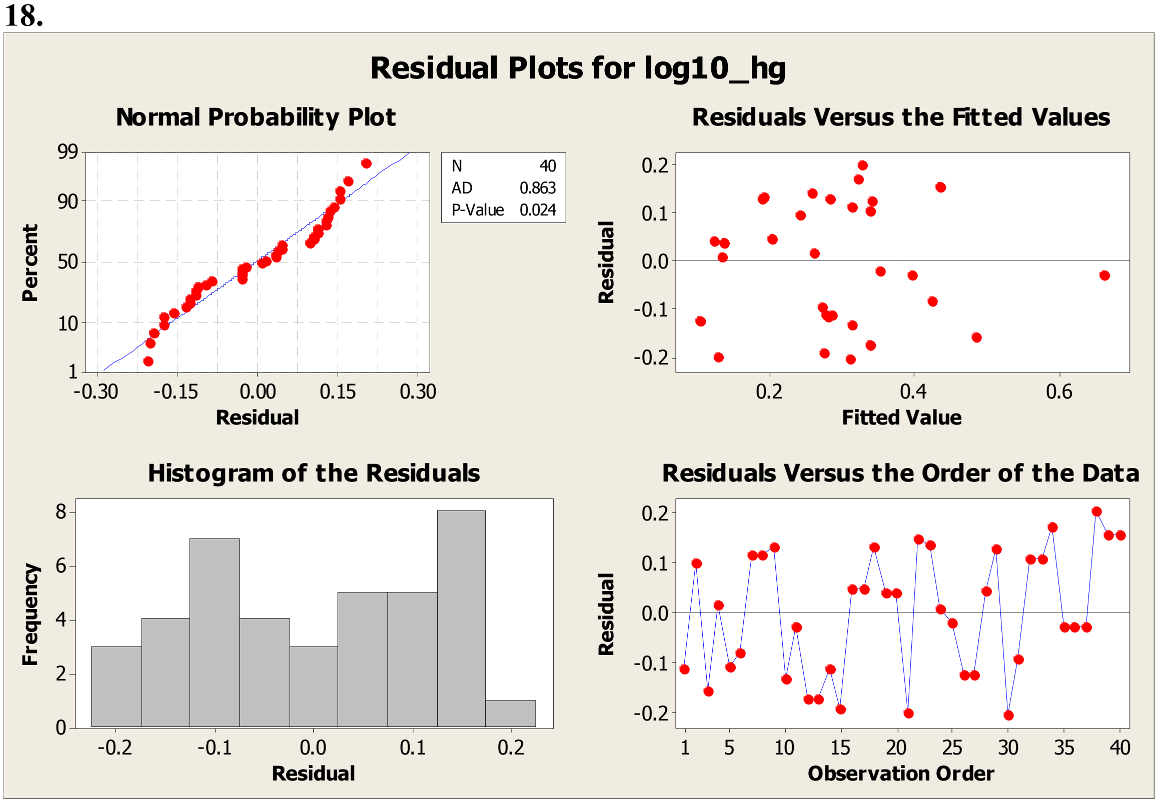
Residual Plots for log10_hg
Normal Probability Plot
Residuals Versus the Fitted Values
N 40
AD 0.863
P-Value 0.024
Percent
Residual
Fitted Value
Histogram of the Residuals
Residuals Versus the Order of the Data
Frequency
Observation Order

19.

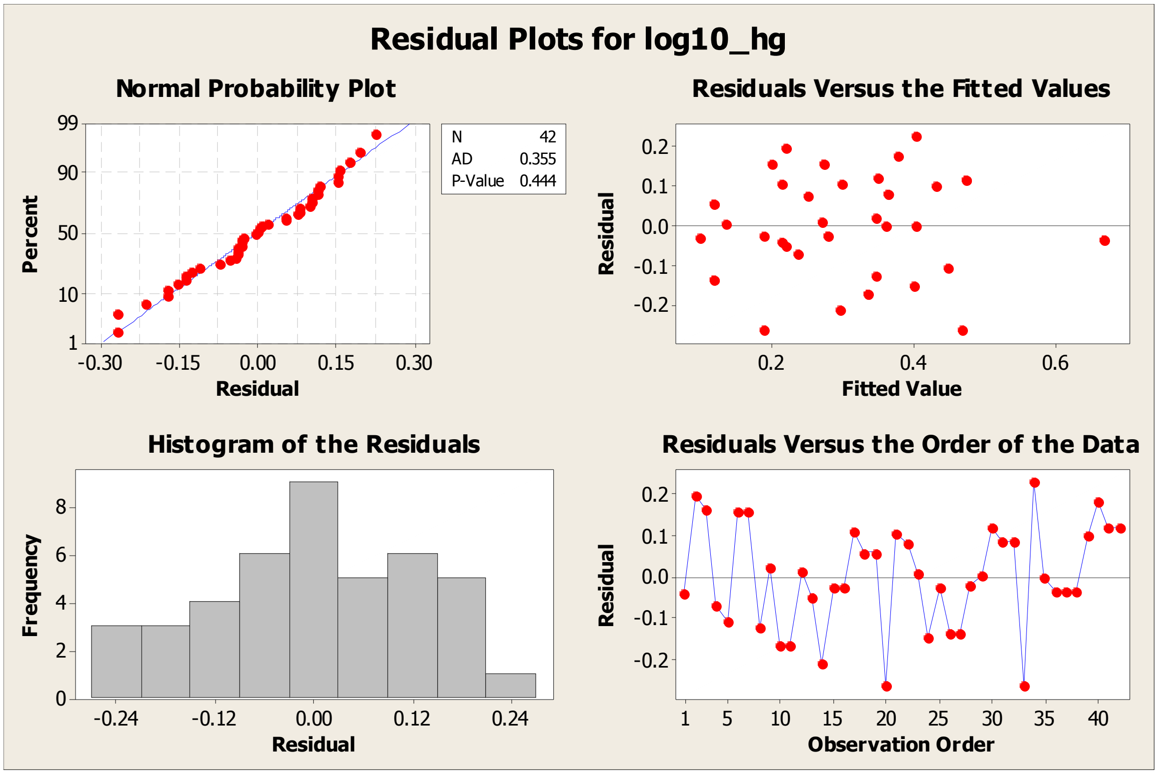
Residual Plots for log10_hg
Normal Probability Plot
Percent
Residual
N 42
AD 0.355
P-Value 0.444
Residuals Versus the Fitted Values
Residual
Fitted Value
Histogram of the Residuals
Frequency
Residual
Residuals Versus the Order of the Data
Residual
Observation Order

20.

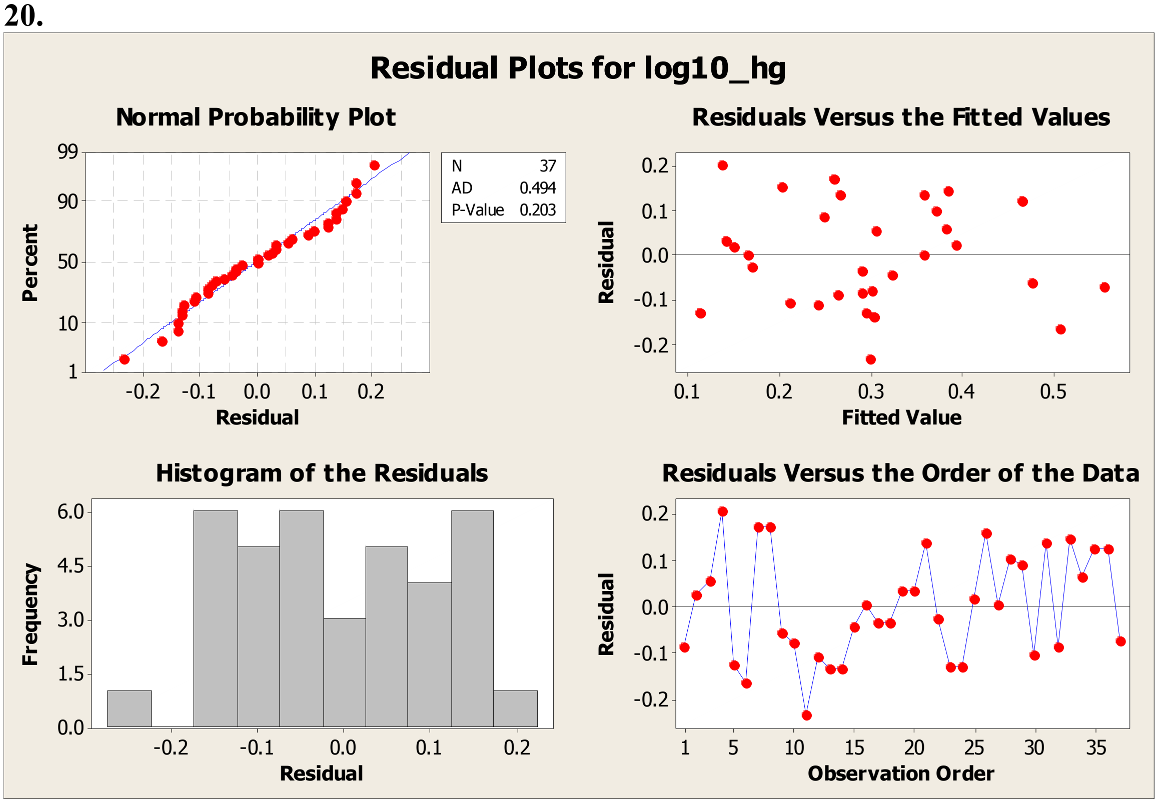
Residual Plots for log10_hg
Normal Probability Plot
Percent
Residual
N 37
AD 0.494
P-Value 0.203
Residuals Versus the Fitted Values
Residual
Fitted Value
Histogram of the Residuals
Frequency
Residual
Residuals Versus the Order of the Data
Residual
Observation Order

21.

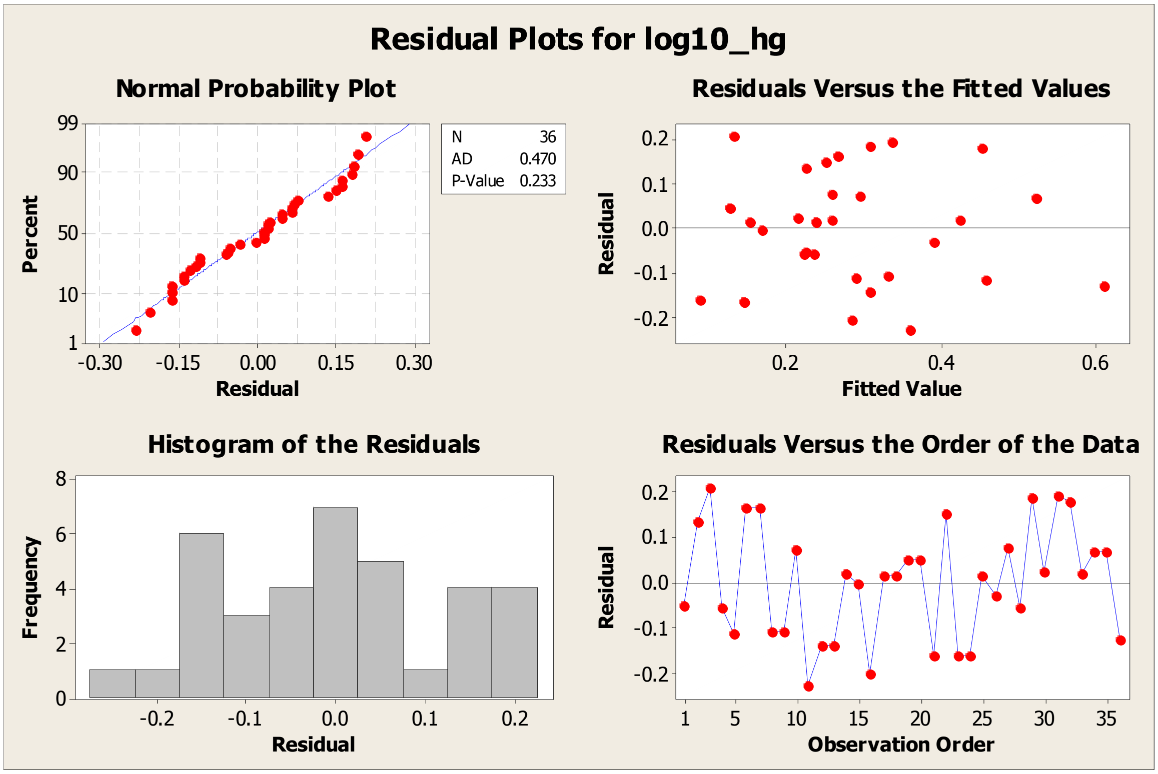
Residual Plots for log10_hg
Normal Probability Plot
Percent
Residual
N 36
AD 0.470
P-Value 0.233
Residuals Versus the Fitted Values
Residual
Fitted Value
Histogram of the Residuals
Frequency
Residual
Residuals Versus the Order of the Data
Residual
Observation Order

22.

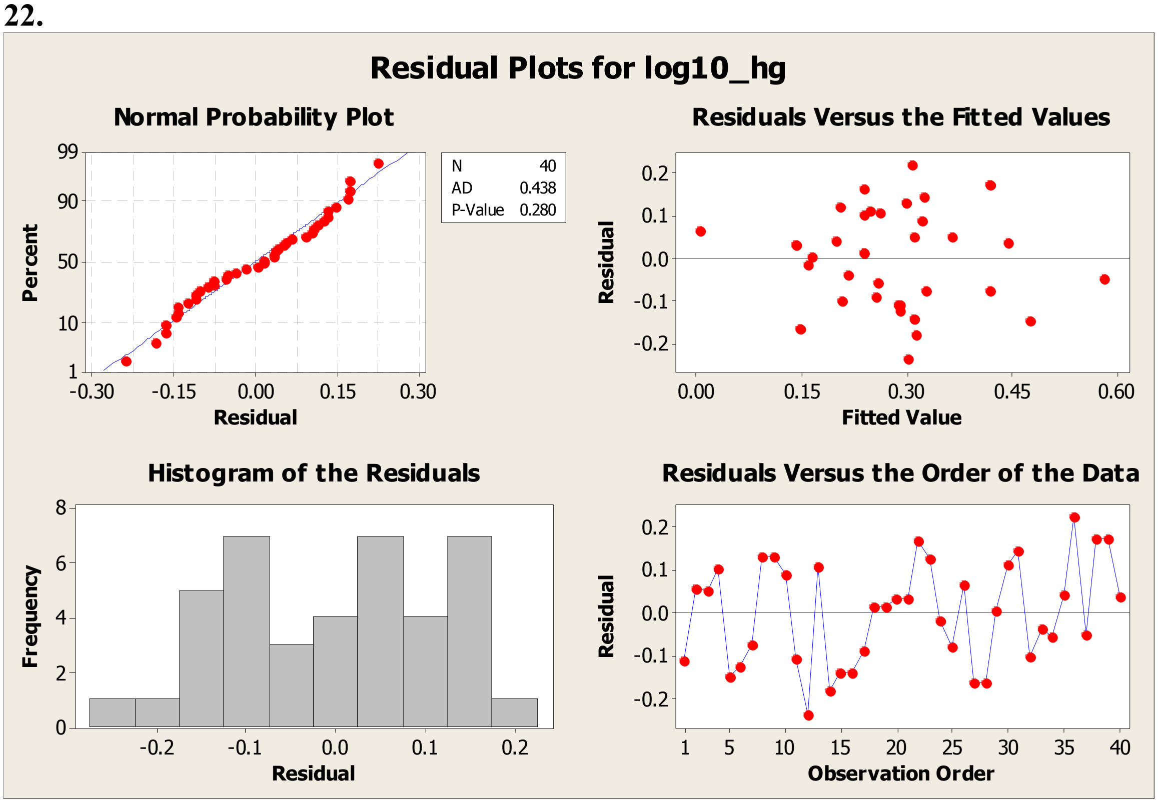
Residual Plots for log10_hg
Normal Probability Plot
Percent
Residual
N 40
AD 0.438
P-Value 0.280
Residuals Versus the Fitted Values
Residual
Fitted Value
Histogram of the Residuals
Frequency
Residual
Residuals Versus the Order of the Data
Residual
Observation Order

23.

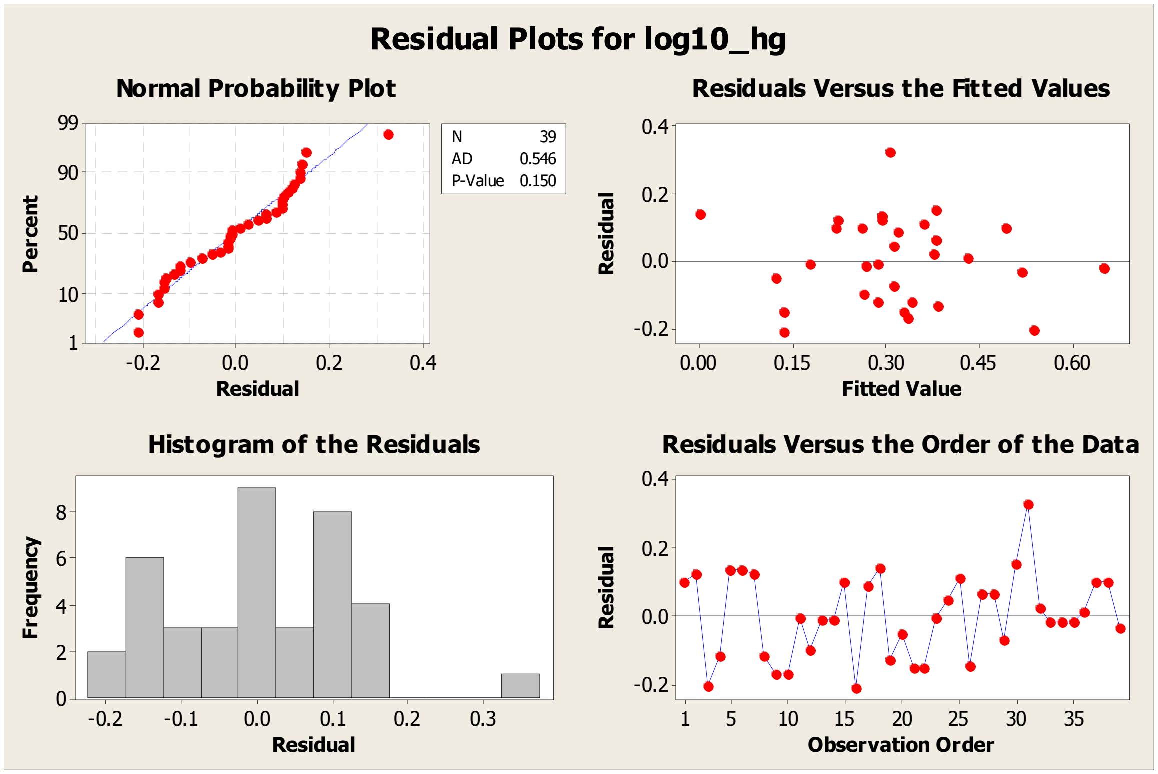

Residual Plots for log10_hg
Normal Probability Plot
Percent
Residual
N 39
AD 0.546
P-Value 0.150
Residuals Versus the Fitted Values
Residual
Fitted Value
Histogram of the Residuals
Frequency
Residual
Residuals Versus the Order of the Data
Residual
Observation Order

24.

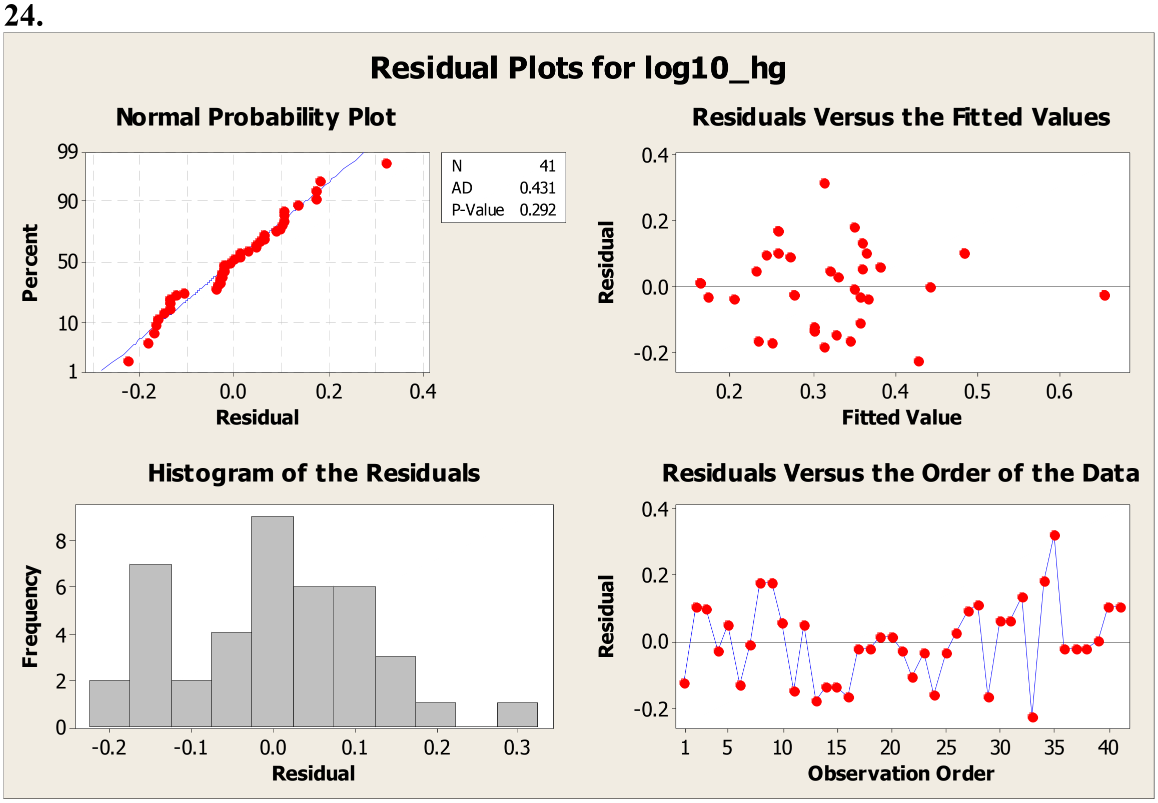

Residual Plots for log10_hg
Normal Probability Plot
Percent
Residual
N 41
AD 0.431
P-Value 0.292
Residuals Versus the Fitted Values
Residual
Fitted Value
Histogram of the Residuals
Frequency
Residual
Residuals Versus the Order of the Data
Residual
Observation Order

25.

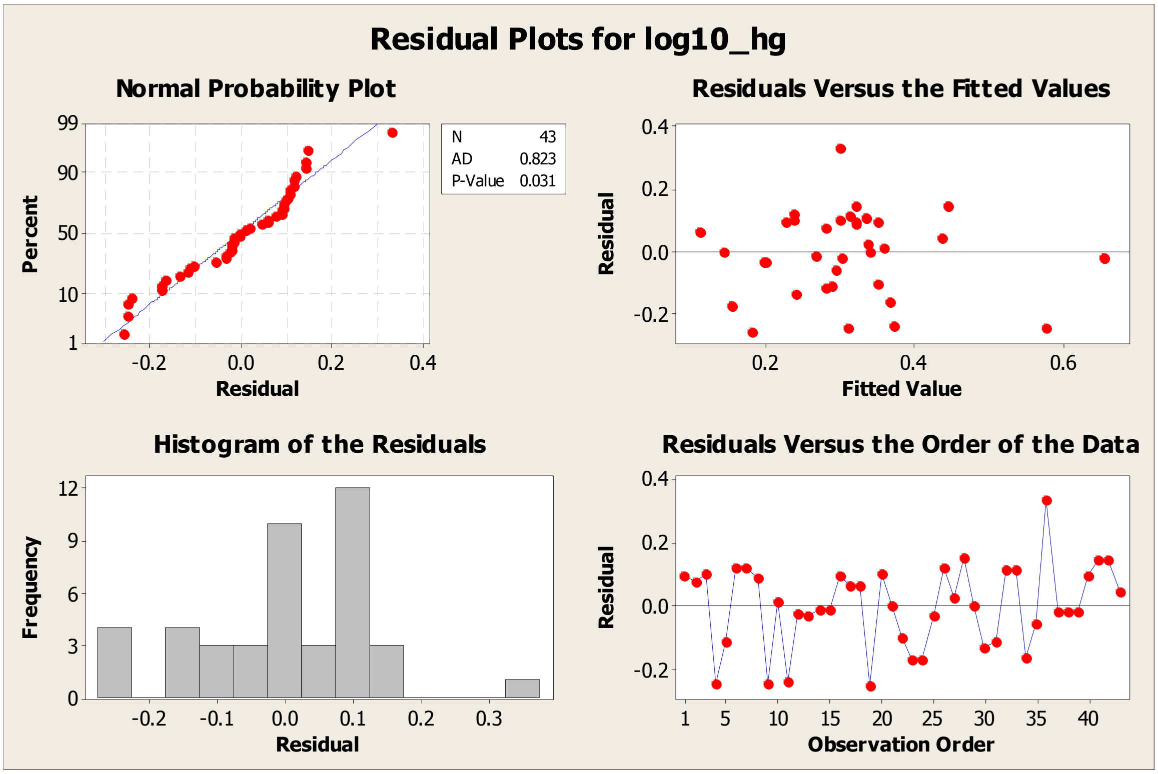
Residual Plots for log10_hg
Normal Probability Plot
N 43
AD 0.823
P-Value 0.031
Percent
Residual
Residuals Versus the Fitted Values
Residual
Fitted Value
Histogram of the Residuals
Frequency
Residual
Residuals Versus the Order of the Data
Residual
Observation Order

26.

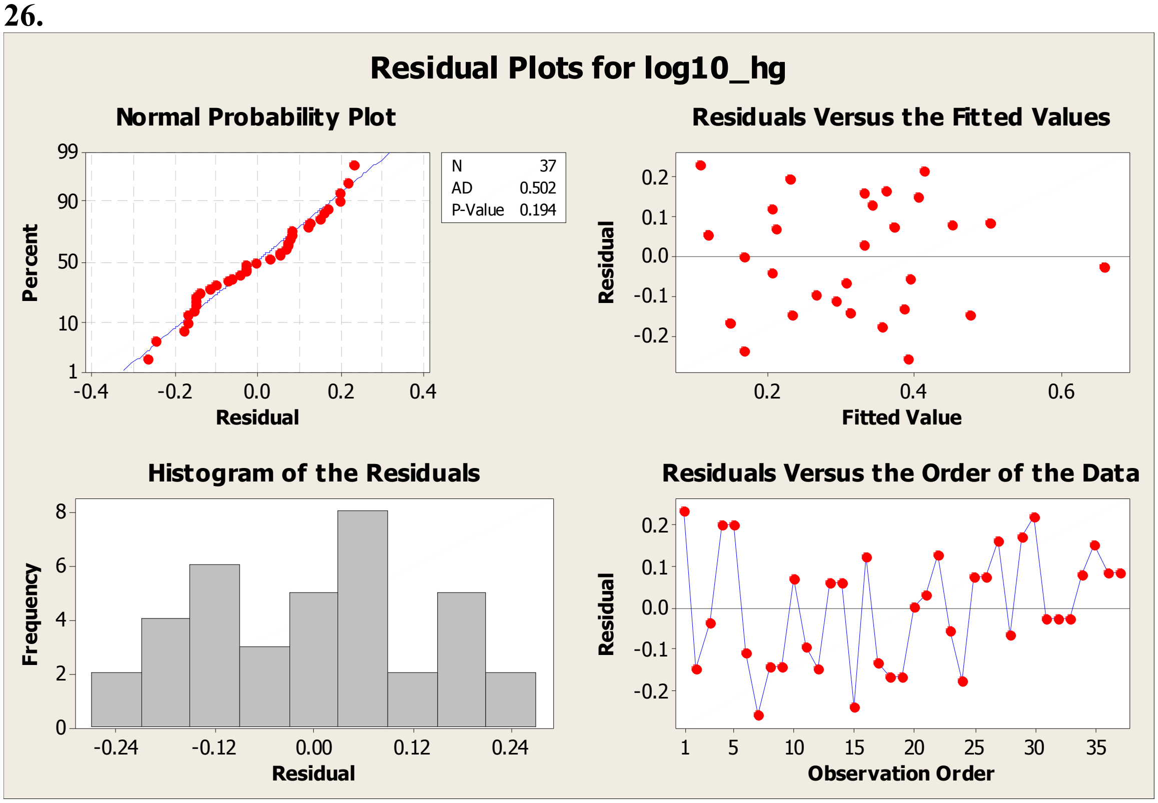
Residual Plots for log10_hg
Normal Probability Plot
N 37
AD 0.502
P-Value 0.194
Percent
Residual
Residuals Versus the Fitted Values
Residual
Fitted Value
Histogram of the Residuals
Frequency
Residual
Residuals Versus the Order of the Data
Residual
Observation Order

27.

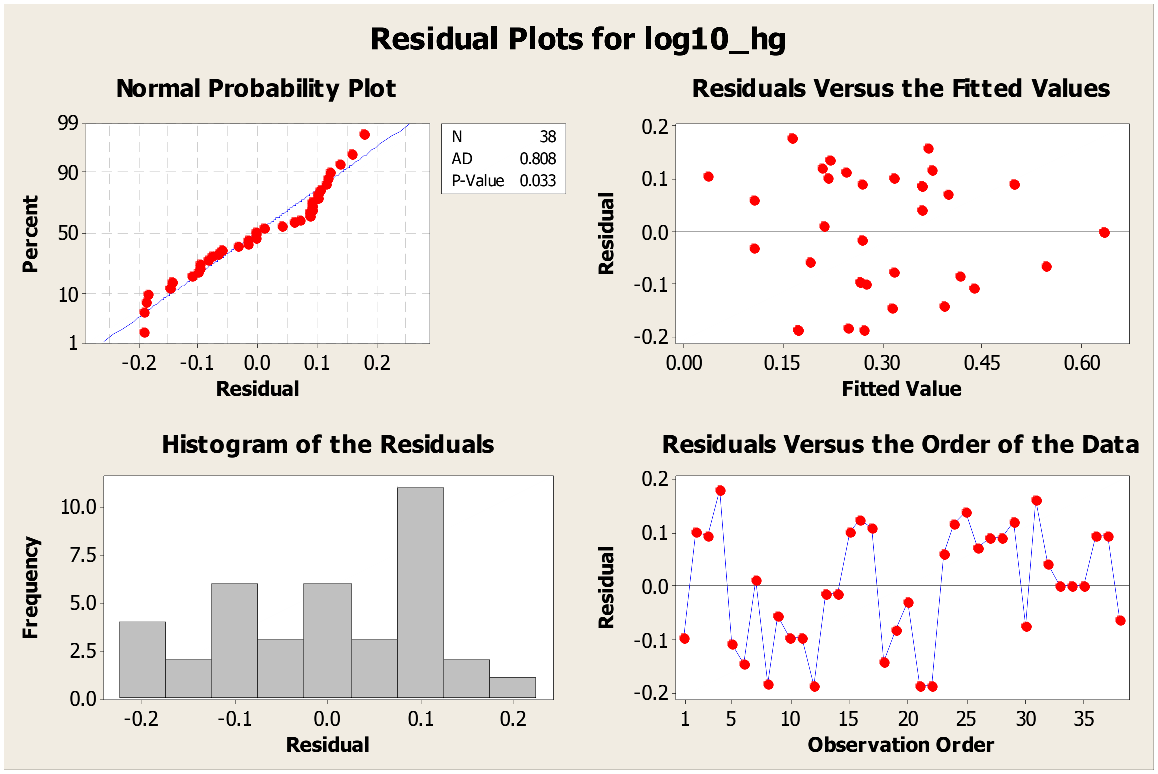
Residual Plots for log10_hg
Normal Probability Plot
Percent
Residual
N 38
AD 0.808
P-Value 0.033
Residuals Versus the Fitted Values
Residual
Fitted Value
Histogram of the Residuals
Frequency
Residual
Residuals Versus the Order of the Data
Residual
Observation Order

28.

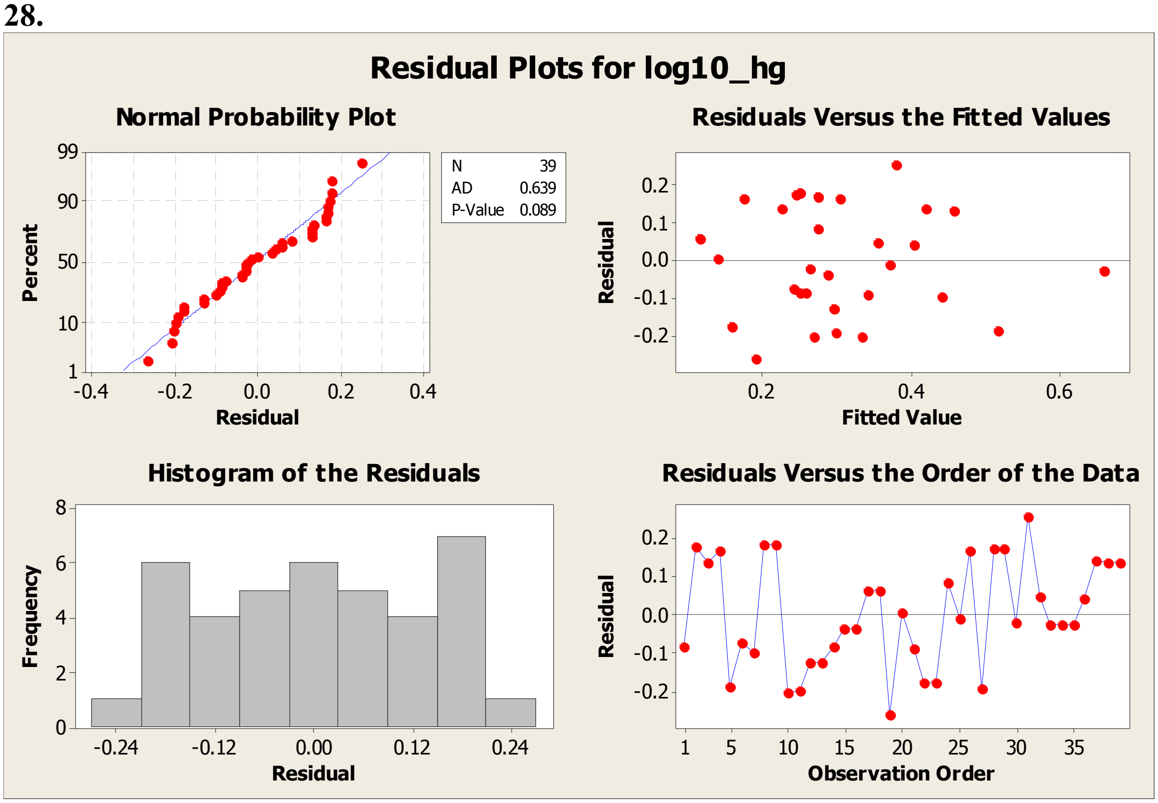
Residual Plots for log10_hg
Normal Probability Plot
Percent
Residual
N 39
AD 0.639
P-Value 0.089
Residuals Versus the Fitted Values
Residual
Fitted Value
Histogram of the Residuals
Frequency
Residual
Residuals Versus the Order of the Data
Residual
Observation Order

29.

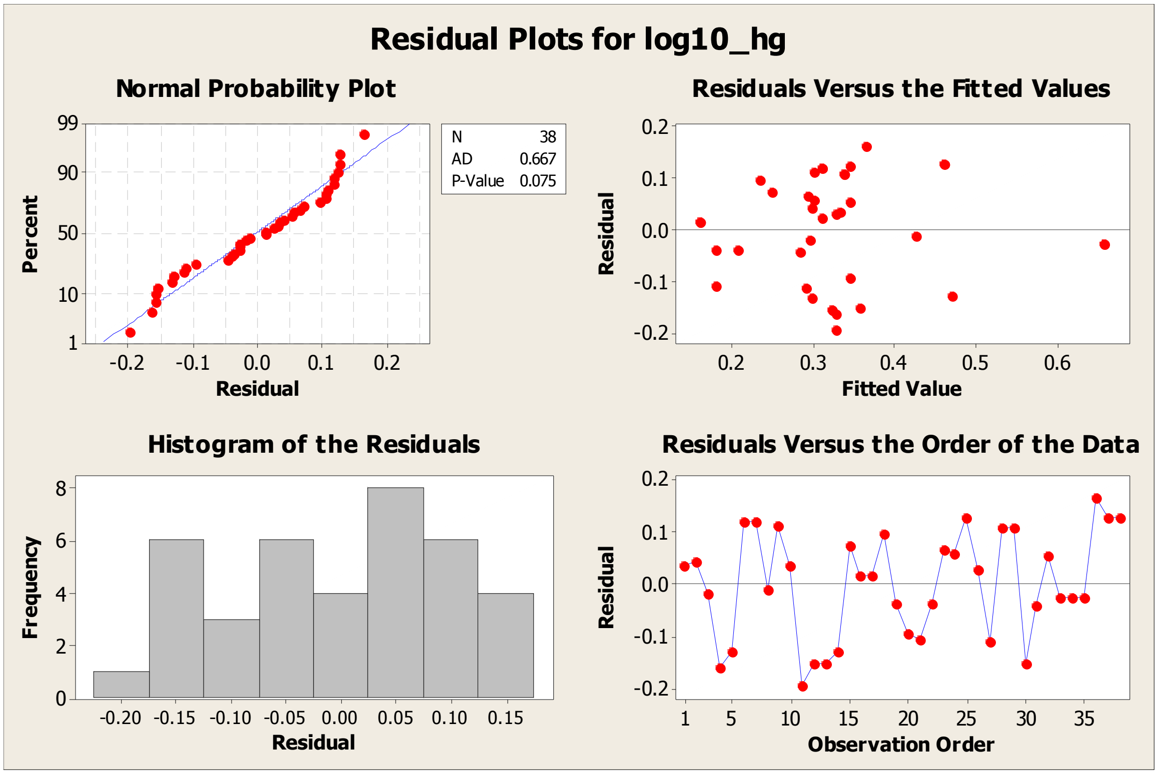
Residual Plots for log10_hg
Normal Probability Plot
Percent
Residual
N 38
AD 0.667
P-Value 0.075
Residuals Versus the Fitted Values
Residual
Fitted Value
Histogram of the Residuals
Frequency
Residual
Residuals Versus the Order of the Data
Residual
Observation Order

30.

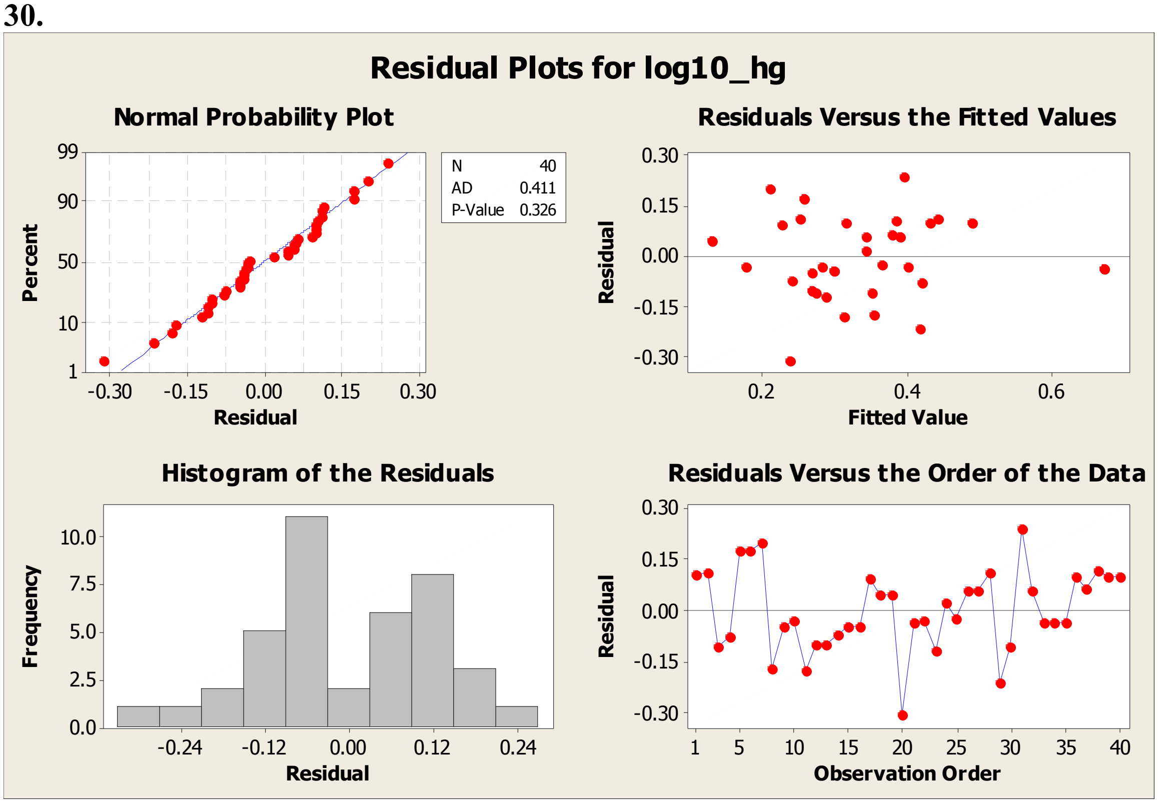
Residual Plots for log10_hg
Normal Probability Plot
Percent
Residual
N 40
AD 0.411
P-Value 0.326
Residuals Versus the Fitted Values
Residual
Fitted Value
Histogram of the Residuals
Frequency
Residual
Residuals Versus the Order of the Data
Residual
Observation Order